Stony Brook University

Nucleocytoplasmic Transport of the Transcription Factor STAT6

A dissertation presented

By

Hui-Chen Chen

To

The Graduate School

in Partial Fulfillment of the

Requirements

for the Degree of

Doctor in Philosophy

in

Molecular and Cellular Biology

Stony Brook University

December 2010

Stony Brook University

The Graduate School

Hui-Chen Chen

We, the dissertation committee for the above candidate for the Doctor of Philosophy Degree hereby recommend acceptance of this dissertation

Nancy C. Reich Marshall, Ph.D., Dissertation Advisor

Professor, Department of Molecular Genetics and Microbiology

Michael J. Hayman, Ph.D., Chairperson of Defense

Professor, Department of Molecular Genetics and Microbiology

Nicholas Carpino, Ph.D.

Assistant Professor, Department of Molecular Genetics and Microbiology

Patrick Hearing, Ph.D.

Professor, Department of Molecular Genetics and Microbiology

Hsien-yu Wang, Ph.D.

Research Associate Professor, Department of Physiology and Biophysics

Janet Hearing, Ph.D.

Associate Professor, Department of Molecular Genetics and Microbiology

This dissertation is accepted by the Graduate School

Lawrence Martin
Dean of the Graduate school

ABSTRACT OF THE DISSERTATION

Nucleocytoplasmic Transport of the Transcription Factor STAT6

By

Hui-Chen Chen

Doctor of Philosophy

in

Molecular and Cellular Biology

Stony Brook University

2010

Signal Transducer and Activator of Transcription 6 (STAT6) is a member of the STAT family of transcription factors that regulate cytokine signaling pathways. STATs are activated by tyrosine phosphorylation by receptor-associated Janus kinases (JAKs) and gain the ability to bind DNA. In this manner they transmit signals from the cell membrane to the nucleus to induce expression of genes involved in many biological functions. STAT6 needs to enter the nucleus for its function as a transcription factor. Therefore, regulation of STAT6 nuclear trafficking provides a mechanism to control specific gene expression.

STAT6 is primarily activated by interleukin-4 (IL-4) and interleukin-13 (IL-13) and plays an important role in protective immunity including development of T helper 2

(T_H2) lymphocytes and normal B cell functions. To assess the dynamic movement of STAT6, I used live cell imaging with photobleaching techniques. This approach has provided critical insight to the spatial distribution of STAT6. I provide evidence that STAT6 is imported continually into the nucleus and independent of tyrosine phosphorylation. *In vitro* binding assays and importin-β1 siRNA knock down assays indicate that STAT6 uses the importin-α-importin-β1 system for nuclear import. In addition, a region required for nuclear localization was found to map within the coiled-coil domain and is critical for nuclear import and transcriptional function of STAT6.

STAT6 is also continuously exported out of the nucleus in a tyrosine phosphorylation-independent manner. Although nuclear import rates of STAT6 are similar before and after tyrosine phosphorylation, nuclear accumulation occurs after tyrosine phosphorylation. I have shown that this is dependent on the DNA-binding ability of STAT6 which results in the decrease of nuclear export rate. Furthermore, the nuclear export process of STAT6 appears to be both Crm1 dependent and independent. These findings will impact diagnostic approaches and strategies to block the deleterious effects of STAT6 in autoimmunity.

DEDICATION

To my parents, Lung-Chuan Chen and Pai-Ho Yeh

with LOVE

TABLE OF CONTENTS

LIST OF FIGURES

LIST OF TABLES

ABBREVIATIONS

aa	Amino acid
Ab	Antibody
Arm	Armadillo
ATP	Adenosine 5’-triphosphate
BSA	Bovine serum albumin
CAS	Cellular apoptosis susceptibility
cDNA	Complementary deoxyribonucleic acid
cFLIP	Cytoplasmic fluorescent loss in photobleaching
CRM1	Chromosome region maintenance 1
DIC	Differential interference contrast
DMEM	Dulbecco’s modified eagles medium
DNA	Deoxyribonucleic acid
ds	Double strand
DTT	Dithiothreitol
EDTA	Ethylenediaminetetraacetic acid
EGFP	Enhanced green fluorescent protein
EGTA	Ethylene glycol-tetraacetic acid
EMSA	Electrophoretic mobility shift assay
FBS	Fetal bovine serum
GAP	GTPase activating protein
GAS	Interferon-γ activated site
GDP	Guanosine 5’ diphosphate
GEF	Guanine-nucleotide exchange factor
GFP	Green fluorescent protein
GH	Growth hormone
GM-CSF	Granulocyte macrophage colony stimulating factor
GST	Glutathione S-transferase
GTP	Guanosine 5’ triphosphate

HEPES	4-(2-Hydroxyethyl)-1-piperazineethanesulfonic acid
IBB	Importin-β1 binding
IFN	Interferon
Ig	Immunoglobulin
IL	Interleukin
Imp	Importin
IPTG	Isopropyl thio-β-D-galactoside
IRF	Interferon regulatory factor
ISGF3	Interferon stimulated gene factor-3
ISRE	Interferon stimulated response element
JAK	Janus kinase
JH	JAK Homology
KCl	Potassium chloride
kDa	Kilodalton
LB	Luria-bertani
LIF	Leukemia Inhibitory Factor
LMB	Leptomycin B
LMP2	Low molecular mass polypeptide 2
μg	Microgram
μl	Microliter
MBP	maltose binding protein
mg	Milligram
ml	Milliliter
mm	Millimeter
mM	milli molar
NaCl	Sodium chloride
NaF	Sodium fluoride
NES	Nuclear export signal
nFLIP	Nuclear fluorescent loss in photobleaching
nFRAP	Nuclear fluorescent recovery after photobleaching

ng	Nanogram
NLS	Nuclear localization signal
NP-40	Nonidet-P40
NTF2	Nuclear transport factor 2
NPC	Nuclear pore complex
OSM	Oncostatin M
PAGE	Polyacrylamide gel electrophoresis
PBS	Phosphate buffered saline
PCR	Polymerase chain reaction
PMSF	Phenylmethylsulphonyl fluoride
pY	Phosphotyrosine
RNA	Ribonucleic acid
RNAi	RNA interference
RT	Room temperature
PTK	Protein tyrosine kinase
PTP	Protein tyrosine phosphatase
RT-PCR	Reverse transcription polymerase chain reaction
SDS	Sodium dodecylsulfate
SH2	Src homology 2
SHP	Src homology 2 domain-containing phosphatase
siRNA	Short interfering ribonucleic acid
STAT	Signal transducer and activator of transcription
SV40	Simian virus 40
TBS	Tris buffered saline
Tris	tris (hydroxymethyl) aminomethane
Tween 20	Polyoxyethylene-sorbitan-monolaurate
wt	Wild-type

ACKNOWLEDGEMENT

This dissertation could not have been completed without the help and guidance of many people. First, I would like to express my deepest gratitude to my advisor, Dr. Nancy C. Reich for having been supportive, patient and encouraging during my Ph.D dissertation study. I am so fortunate to join her laboratory and to do my Ph.D research under her guidance.

I would like to thank my dissertation committee, Dr. Michael Hayman, Dr. Nicholas Carpino, Dr. Janet Hearing, Dr. Patrick Hearing, Dr. Hsien-yu Wang, for their time, insightful discussion and constructive criticism. I would like to particularly thank Dr. Carpino for suggestions and sharing equipments and reagents.

The former and present members of the Reich laboratory have made it a homey and friendly place to work. It has been a wonderful experience to work with Sarah Van Scoy, Dr. Ling Liu, Dr. Tsu-Fan Cheng, Dr. Janaki Iyer, Dr. Sabrina Brzostek, Dr. Yiwei Gao, Amy Graff, Dr. Velasco Cimica, Dr. Jane Foreman, Marcin Stawowczyk, Hayoun Shin, and Patricio Mena. Thank you all for your help and friendship. I would like to specially thank Dr. Janaki Iyer helped me a lot to start the project.

I am also grateful to my friends who have made the past few years a memorable experience. Last, I would like to dedicate this dissertation to my family, especially to my parents. Their unconditional support and love enable me to complete this work.

Chapter 1

Introduction

Cells sense and respond to changes from their environment to function properly. Multicellular organisms have developed an integrated network of cell-cell communication and humoral interactions to coordinate various physiological responses, such as cell differentiation, proliferation and apoptosis. Cytokines that are small polypeptide hormones produced by single cells or endocrine glands help communication among cells and modulation of cellular processes. Cytokines bind to cell-surface receptors and transmit signals through cytoplasmic proteins to alter the pattern of expressed genes. One family of such cytoplasmic proteins is the Signal Transducer and Activator of Transcription (STAT).

In this dissertation, I have focused on a member of STAT protein family, STAT6. STAT6 is tyrosine phosphorylated following cytokine stimulation and gains the ability to bind to DNA. After translocation into the nucleus, STAT6 can bind to the promoters of target genes and activate transcription. STAT6 has been known to play an important role in T helper 2 (T_H2) cell development and proper function of B lymphocytes. Deregulation of STAT6 leads to certain diseases and cancers, therefore its activity is tightly regulated in cells. Activity of STAT6 is regulated by different mechanisms and my research has been focused on the process of STAT6 nuclear transport.

1. JAK-STAT signaling pathway

Cytokines bind to specific cell surface receptors and control many important biological functions relating to hematopoiesis and immune responses including cell proliferation, differentiation and cell activation. Over the years, cytokine-induced signaling pathways have been extensively studied and one of the important pathways is the Janus kinase (JAK)-STAT pathway. The canonical STAT activation pathway is

depicted in Figure 1. After cytokine binding, the cognate cell surface-bound receptors form dimers or oligomers which leads to JAK apposition, transphosphorylation on tyrosines and activation. JAKs are constitutively associated with specific receptors and four members were found including JAK1, JAK2, JAK3 and TYK2. They are non-receptor tyrosine kinases of approximately 120-130 kDa and share ~40% sequence identity and similar domain structures (1, 2). In contrast to JAK1, JAK2 and TYK2 which are expressed ubiquitously, expression of JAK3 is restricted to myeloid and lymphoid cells (3). Because each JAK associates with various cytokine receptors, different cytokines can activate different JAKs and downstream STAT proteins.

JAK activation is followed by phosphorylation of the receptors on specific tyrosines that provide docking sites for STAT protein recruitment through their Src homology 2 (SH2) domains. After binding, JAKs can phosphorylate a conserved tyrosine at the carboxyl terminus of STATs (4). The tyrosine phosphorylation of STAT induces homodimer or heterodimer formation through reciprocal phosphotyrosine and SH2 domain interaction. Subsequently, STATs gain DNA binding ability for consensus sequences (Interferon Stimulated Response Element (ISRE) or IFNγ-Activated Sequence (GAS)) and activate transcription of specific target genes in the nucleus.

2. Signal transducers and activators of transcription (STAT) family

Studies on how cells respond to interferon-α (IFNα) led to the discovery of a conserved DNA element named the ISRE and the binding complex, IFN-Stimulated Gene Factor-3 (ISGF-3) (5-9). ISGF-3 is composed of three proteins with different molecular weights (48 kDa, 91 kDa and 113 kDa) and this complex is formed minutes after IFNα stimulation (10). Further studies found that the 48 kDa protein belongs to the Interferon Regulatory Factors (IRF) transcription factor family and was named IRF9 (11). The other two proteins shared about 40% sequence homology indicating that they belong to the same protein family. Based on their dual roles in signal transduction in the cytoplasm and inducing gene expression in the nucleus, they were named STAT1 and STAT2 (12, 13). After discovering STAT1 and STAT2, five more STAT proteins were found in mammalian cells including STAT3, STAT4, STAT5a, STAT5b and STAT6 (14-17). In addition to mammalian STATs, homologous STAT proteins were also found in lower

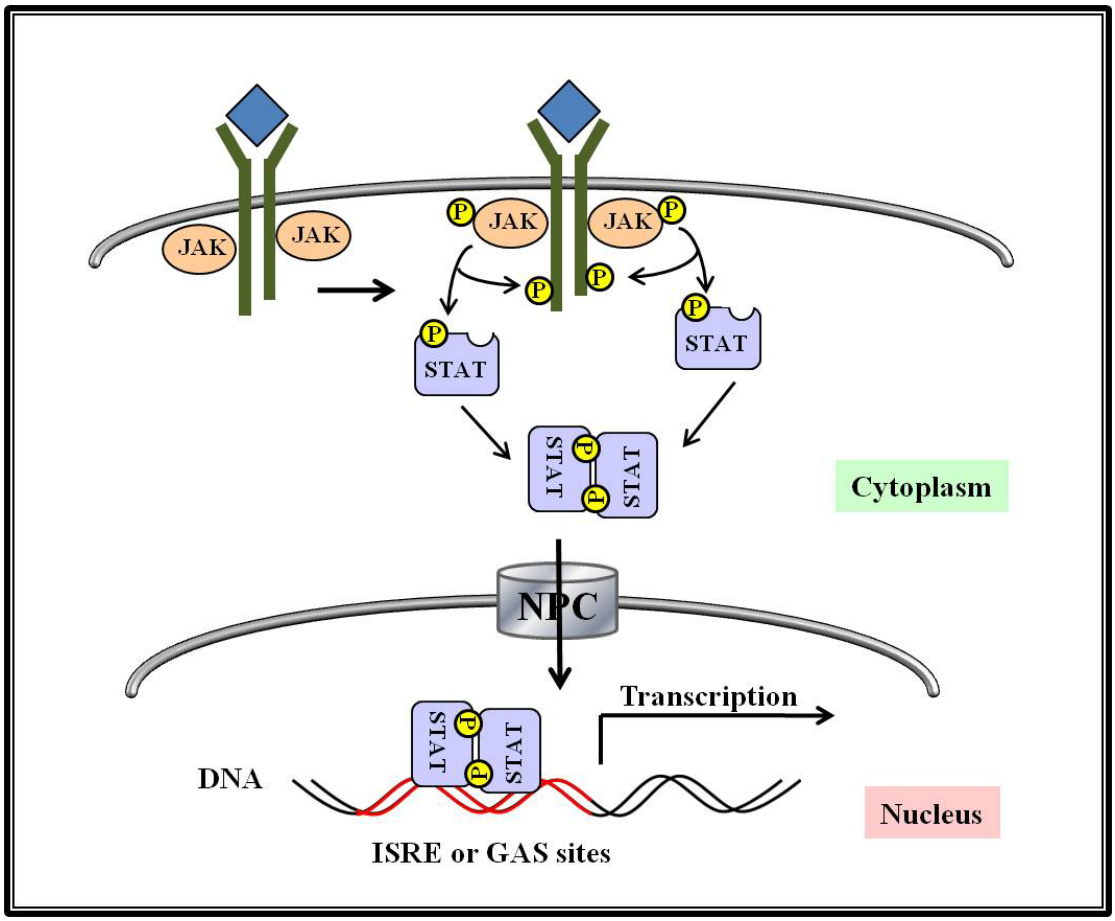

Figure 1: JAK-STAT pathway.

A schematic representation of the JAK-STAT pathway. Cytokine binding to cell surface receptors stimulates activation of JAKs. JAK tyrosine kinases phosphorylate the receptors and STAT factors (P). Tyrosine-phosphorylated STATs form dimers that are able to bind specific gene targets in the nucleus.

organisms, for example *Caenorhabditis. elegans* and *Drosophila melanogaster* (18-20). The *Drosophila* homologue of STAT has been shown to be important for embryonic development (21).

Domain organization and structure of STAT proteins

The seven STAT proteins are structurally and functionally related and about 750-850 in length. STAT2 and STAT6 are approximate 850 amino acids, whereas the other five STATs consist of about 750-800 amino acid residues. Sequence comparisons and mutagenesis studies show that they all share a similar domain structure critical for STAT function (Figure 2) (22). The amino-terminal domain is followed by a coiled-coil domain which contains four α-helices and plays a role in binding with other proteins (23). The central region is a DNA binding domain which contains several β-sheets and has been suggested to regulate DNA binding specificity of different STATs (24). The SH2 domain interacts with phosphorylated tyrosines on receptors or other STATs to form homodimers or heterodimers. Furthermore, the carboxyl-terminus is a transactivation domain which can interact with transcriptional coactivators such as CBP/p300 and facilitates transcriptional activation (25). There is a highly conserved linker domain which might stabilize DNA binding (26). In response to cytokine stimulation, STATs are activated by phosphorylation on a conserved tyrosine residue near amino acid-700 (4).

Although STAT proteins were initially considered to be monomers in a latent state, more biochemical and structural evidence has shown that STAT proteins can form unphosphorylated dimers. In 2005, unphosphorylated STAT1 and STAT5a crystal structures were solved (27, 28). They both showed antiparallel boat-like dimers (Figure 3A). X-ray crystal structures of human STAT1 and mouse STAT3 core fragments (residues ~130-710 lacking the N-terminal domain and the transactivation domain) as phosphorylated dimers bound to DNA have also been reported. Although the structure of each STAT monomer remains the same, the tyrosine phosphorylated STAT dimer is conformationally different from the unphosphorylated STAT dimer. The tyrosine phosphorylated STAT dimer resembles a nutcracker which can stably clamp the DNA (Figure 3B) (29, 30). My research indicates a region in the first coil of coiled-coil domain is required for STAT6 nuclear import. The domain is predicted to be accessible in both

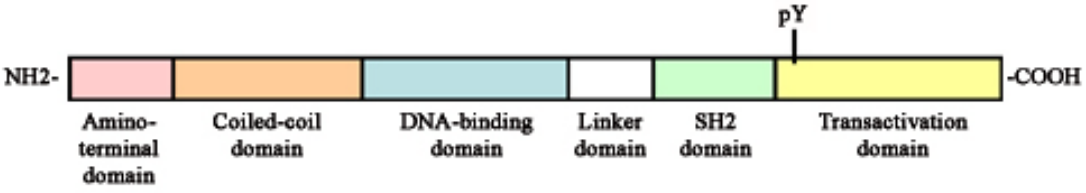

Figure 2: The domain structure of STATs.

STAT proteins are approximately 750-850 amino acids in length and share the same domain arrangement as shown in the linear diagram. pY: phosphorylated tyrosine.

A.

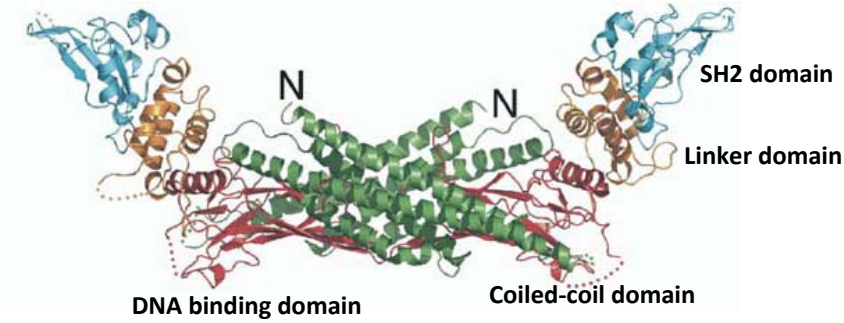

B.

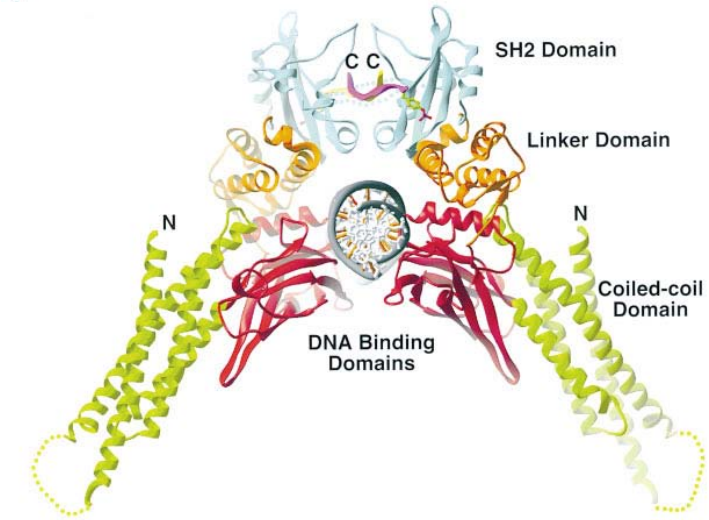

Figure 3: Structures of STAT1 dimers in a ribbon diagram.

A. Structure of unphosphorylated STAT1 dimer (a.a 1-683). (reference 27)
B. Structure of tyrosine phosphorylated STAT1 dimer (a.a 136-710) bound to DNA. (reference 29)

The coiled-coil domain is shown in green, the DNA-binding domain is shown in red, the linker domain is shown in orange, the SH2 domain is shown in blue and the DNA is shown in gray.

unphosphorylated and tyrosine phosphorylated STAT6.

Biological functions of STATs

STATs are activated by cytokines, including interferons and interleukins, as well as hormones and growth factors (31, 32). STATs, STAT1, STAT3, STAT5a and STAT5b are activated by various and even overlapping of cytokines, while other STAT2, STAT4 and STAT6 are only activated by few specific cytokines. STATs activated by different cytokines results in the induction of specific target genes by individual STATs (Table 1).

Table 1: Primary activating ligands and target genes of individual STATs.

Targeted STAT	Primary activating ligands	Main target genes
STAT1	IFN family	T_H1-type immunostimulatory and pro-apoptosis
STAT2	IFN α/β	T_H1-type immunostimulatory and pro-apoptosis
STAT3	IL-6, IL-10, IL-23, IL-21, IL-11, LIF and OSM	T_H17-type, anti-apoptosis, pro-proliferation, angiogenic and metastatic
STAT4	IL-12	T_H1-type, especially IFNγ
STAT5a STAT5b	IL-2, GM-CSF, IL-15, IL-7, IL-3, IL-5, GH and prolactin	anti-apoptosis, pro-proliferation and differentiation
STAT6	IL-4 and IL-13	T_H2-type and anti-apoptosis

(Modified from reference 31)

Because of the specificity of ligands, each STAT plays an important role in different biological functions even though they have the same domain structures. So far all STAT genes have been targeted for disruption in mice to elucidate their *in vivo* function (33, 34). The distinctive phenotypes of these mice as shown in Table 2 demonstrated different functions for each STAT.

Table 2: Phenotype of mice deficient for individual STATs.

Targeted STAT	Phenotype of null mice
STAT1	Impaired response to interferons, susceptibility to viral infection and tumors, impaired growth control
STAT2	Impaired response to interferons
STAT3	Embryonic lethality, defects in adult tissue: impaired responses to pathogens and cell-survival defects
STAT4	Impaired T_H1 cell differentiation owing to impaired IL-12 signaling
STAT5a	Impaired prolactin signaling results in defective in mammary-gland development
STAT5b	Impaired growth-hormone pathway, natural killer (NK) cell-mediated proliferation and cytolytic activity
STAT5a/b	Perinatal death of mice, severe anemia, no NK cells, defective IL-2-induced T-cell proliferation
STAT6	Defects in T_H2 cell differentiation owing to impaired IL-4 and IL-13 signaling

(Modified from reference 34)

STAT1 and STAT2 are predominately activated by the IFN signaling pathways. STAT1- and STAT2- knockout mice both show impaired IFN-dependent immune responses against viruses and microbes (35-37). STAT3 deletion in mice results in a severe defect in development and in embryonic lethality (38). Conditional knockout mice of STAT3 reveal a vital role for STAT3 in IL-2, IL-6 and IL-10 pathways (39). STAT4 is specifically activated by IL-12 which mediates the differentiation of naïve T-cell to T_H1 cells. There is no surprise that STAT4-defective mice are similar to IL-12 or IL-12 receptor knockout mice which are defective in T_H1 cell differentiation (40, 41). The two closely related STAT5 proteins, STAT5a and STAT5b, share more than 90% identity in amino acid sequence. However, knockout of either STAT5a or STAT5b in mice results in different phenotypes. STAT5a-defecient mice show impaired mammary gland development indicating defective prolactin signaling (42) In contrast, STAT5b null mice show loss of sexually dimorphic growth indicating defective growth hormone response (43). Ablation of both STAT5a and STAT5b causes severe anemia and perinatal death.

The mice that survive are sterile and have defects in T-cell proliferation and growth (44-46). The studies of single and double-deficient STAT5 mice suggest both redundant and non-redundant functions for these proteins.

IL-4 and IL-13 are the principal cytokines that activate STAT6. The important role of STAT6 in IL-4 signaling was demonstrated from the STAT6-deficient mice which are defective in T_H2 development. Although the STAT6 deficient lymphocytes are not capable of responding to IL-4 and IL-13, they still can be activated by other cytokines. In addition, these mice are defective in immunoglobulin isotype switching to IgG1 and IgE in B cells, and do not development antigen-induced airway hypersensitivity. The expression of IL-4-induced surface markers on STAT6-deficient B cells, including IL-4R, MHC class II and CD23 are also absent (47-50).

3. Activation of STAT6: signaling through IL-4 receptors

The STAT6 transcription factor was identified as a DNA-binding factor activated in response to IL-4 in B cells (16, 51, 52). Human STAT6 consists of 847 amino acids while murine STAT6 is composed of 837 amino acids. Compared to other STATs, STAT6 has the most similarity to STAT5a and STAT5b (~35%) and only ~22% or less homology to other STATs. The human STAT6 gene is located in chromosome 12 and is 19 kb in length with 23 exons (53). STAT6 expression appears to be ubiquitous and constant in most cell types. It is the only STAT that is specifically activated by IL-4 and required for GATA3 transcription factor expression which is an important regulator for the generation of T_H2 lymphocytes (49, 54). STAT6 is also critical for the normal functions of B lymphocytes, and protection against parasitic nematodes (48, 55, 56).

Classically, STAT6 is activated by tyrosine phosphorylation stimulated in response to T_H2 cytokines IL-4 and IL-13 (Figure 4) (57). IL-4 is a multifunctional cytokine primary produced by T_H2 cells, basophils and mast cells. The major form of the IL-4 receptor is composed of the IL-4 receptor α (IL-4Rα) chain and the common gamma chain (γc). Studies show that IL-4 first binds to IL-4Rα with high affinity followed by dimerization with γc (58). Neither the IL-4Rα chain nor the γc has endogenous kinase activity. The IL-4 receptor is associated with JAK kinases that initiate the signaling pathway. JAK1 and JAK3 are the primary JAKs associated with IL-4Rα

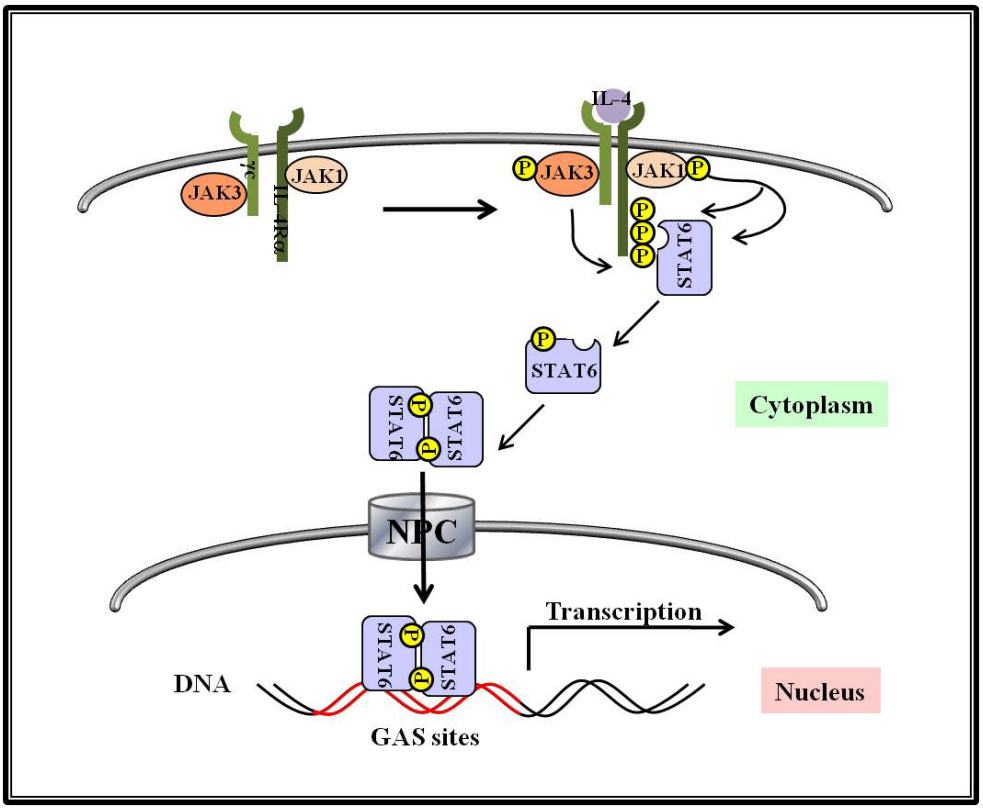

Figure 4: STAT6 signaling pathway.

A schematic represents the STAT6 activation cascade. After IL-4 receptor engagement, JAKs phosphorylate tyrosine residues on the IL-4 receptor which provides docking sites for STAT6. After binding to the receptors, STAT6 is tyrosine phosphorylated, forms dimers and activates gene transcription in the nucleus.

chain and γc individually (59, 60). Following cytokine binding to cell-surface receptors, associated JAKs phosphorylate tyrosine residues on IL-4Rα which provide docking sites for STAT6. Targeted to the receptors, STAT6 is specifically phosphorylated on tyrosine 641 by JAKs. Tyrosine phosphorylation promotes the formation of STAT6 dimers via reciprocal SH2 domain and phosphotyrosine interaction and it gains the ability to bind DNA. In the nucleus, the STAT6 dimer binds to GAS sites of DNA targets leading to gene expression that is responsible for the biological effects of STAT6. STAT6 is the only STAT protein capable of binding to a GAS site spaced by four nucleotides (TTC NNNN GAA, N4 site) and most of the STAT6 binding sites in IL-4 response promoters have the N4 sites (61).

Since STAT6 is activated by tyrosine phosphorylation, dephosphorylation suppresses STAT6 signaliing pathway. The phosphatases, SH2 domain-containing protein tyrosine phosphatase-1 (SHP-1) and T-cell protein tyrosine phosphatases (TCPTP), have been proposed to dephosphorylate STAT6, but this regulation might be cell type-specific manner (62-65). Mice with reduced SHP-1 activity show spontaneous T_H2-like inflammatory responses in the lung indicating that SHP-1 plays a critical role in regulating the IL-4/IL-13 signaling pathway (66). In addition, phosphorylated STAT6 has also been reported to be a cytoplasmic substrate for Protein-Tyrosine Phosphatase 1 B (BPTP1B) (67).

4. STAT6 and diseases

STAT6 plays a fundamental role in the IL-4 signaling pathway which is tightly connected to T_H2 cell-associated immune response. However, collateral damage accompanies unregulated positive effects in the immune response. Hyperactivity of STAT6 predisposes to lymphoproliferative disease and is responsible for diseases associated with T_H2 cell pathologies, like asthma (50, 68, 69). As a factor that can elicit the proliferation of T lymphocytes, STAT6 has been reported to be involved in cell proliferation regulated by a decrease in cyclin-dependent kinase inhibitor p27kip1 levels (70). Also, STAT6 can recognize a subset of E2F target sites and stimulate cell cycle-regulated gene expression which leads to T lymphocyte proliferation (71).

Because STAT proteins regulate diverse cell functions, their aberrant activities usually relate to disease development. Multiple studies have shown that STAT proteins are constitutively active in various types of tumors. Aberrant or constitutive activation of STAT proteins have been found in solid tumors, non-leukemic hematopoietic malignancies, and leukemias (72-77). Constitutive activation or increased DNA binding ability of STAT6 was found in prostate cancer, Hodgkin lymphomas, primary mediastinal large B cell lymphomas, cutaneous T cell lymphomas, and adult T cell leukemia/lymphomas (73, 74, 78, 79). A constitutively activated form of STAT6 (STAT6VT) was identified from an extensive mutational analysis of the STAT6 SH2 domain in which amino acids valine547 and threonine548 are replaced by alanines (80, 81). It undergoes tyrosine phosphorylation, DNA binding, and activation of transcription in the absence of IL-4. Transgenic mice that express STAT6VT in B and T lymphocytes have been generated in which the expression of IL-4/STAT6-regulated cell surface proteins such as MHC class II and IL-4 receptor was increased and IgG1 and IgE level in the serum was also elevated. In addition, about 5% of these mice have a propensity for developing a lymphoproliferative disorder (68, 79, 82). This confirmed that STAT6 mediates many IL-4 stimulated functions and plays a role in cell proliferation and transformation.

5. Nuclear transport

In eukaryotic cells, cytoplasmic and nuclear compartments are separated by the nuclear envelope. The nuclear envelope is a double layer membrane with ~3000 to 5000 nuclear pore complexes (NPCs) as selective filters and movement of proteins in and out of the nucleus occurs by passage through these NPCs (83-86). NPCs are composed of several copies of ~30 proteins, named nucleoporins, and allow proteins smaller than 9 nm or 50 kDa to passively pass through, whereas proteins larger than the diffusion limit need specific carrier proteins for active transport. The most well studied nuclear transport mechanism is mediated by the karyopherin-β protein family, also referred as importins or exportins, based on the direction in which they carry their cargos. The transport directions are controlled by the concentration of a Ras-related GTPase, Ran, which is primarily in a GTP-bound form in the nucleus and a GDP-bound form in the cytoplasm

(87). The nucleotide exchange factors in the nucleus and GTPase activating proteins in the cytoplasm regulate the ratio of Ran-GFP to Ran-GDP in both compartments. Ran-GTP binds to importins causing release of cargo proteins in the nucleus. Ran-GTP binds to exportins with cargo in the nucleus and nucleotide exchange in the cytoplasm causes cargo release. Therefore, the Ran-GTP/Ran-GDP ratio regulates protein nuclear transport direction.

Nuclear import

Typically, nuclear import of a large protein depends on the presence of a nuclear localization signal (NLS). The classical NLS, for example PKKKRK found in Simian virus 40 (SV40) large-T antigen, contains a short stretch of residues (usually 4-8 amino acids) rich in positively-charged amino acids like lysine and arginine. Another type of NLS is bipartite; for example, KRPAATKKAGQAKKKKLD in nucleoplasmin contains two basic stretches separated by ten amino acids (88, 89). The NLS is recognized by a karyopherin-β transport receptor directly or indirectly through an adaptor and facilitates import through the nuclear pore complex (90-93). The nuclear import process is shown in Figure 5; the classical import receptor consists of a dimer with two distinct subunits: an importin-α adapter that binds the NLS and the karyopherin-β , importin-β1, that binds importin-α and interacts with the nucleoporins in the NPC resulting in the transport of complex into the nucleus. In the nucleus, importin-β1 binds Ran-GTP leading to release of the NLS cargo.

Importin-α is distinct from the karyophorin-β family that functions as an adaptor protein to bring the NLS-cargo protein to importin-β1. Importin-α proteins are evolutionarily conserved and can be found in eukaryotes from yeast to humans. In mammalian cells there are six importin-α proteins. The similarity of the six human importin-α proteins is about 56%-89%. The basic structure of importin-α is shown in Figure 6. The amino-terminus is the importin-β1 binding domain (IBB) that interacts either *in trans* with importin-β1 or *in cis* with the NLS binding site on itself (94). Therefore the IBB domain autoinhibits importin-α by occupying the NLS binding grooves while NLS containing cargos are absent. The central region contains ten tandem

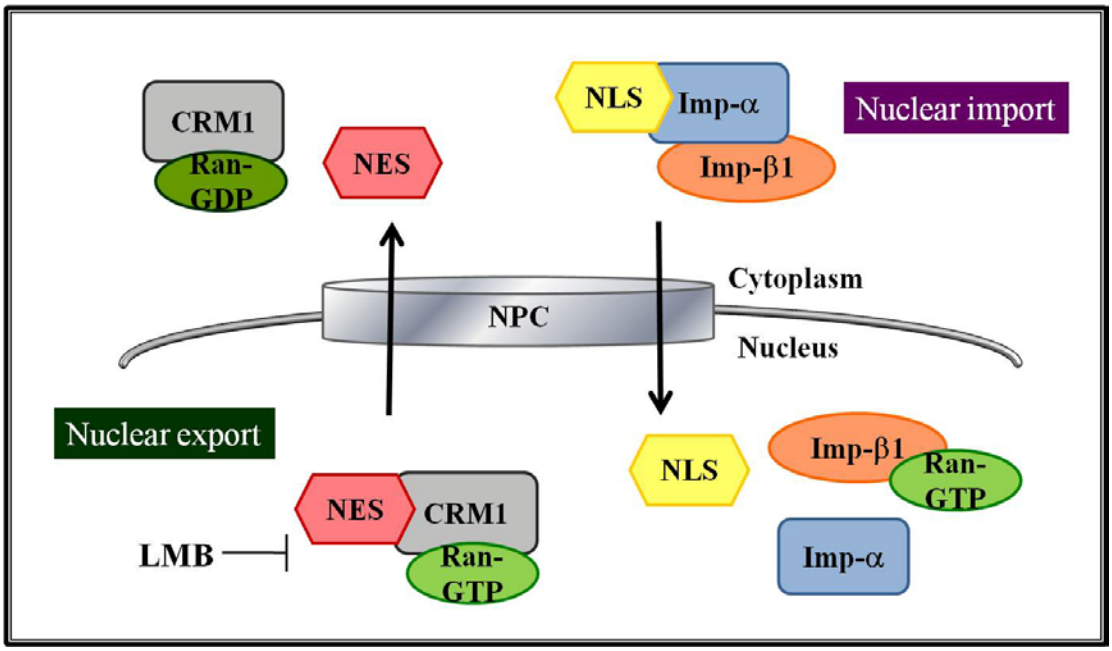

Figure 5: Nuclear trafficking across the nuclear port complexes (NPCs)
Right (nuclear import): NLS-containing cargo is recognized by importin-α that binds to importin-β1. Importin-β1 directly interacts with components of NPC and facilitates the complex transport into the nucleus. After import, the GTP-bound small GTPase Ran in the nucleus binds to importin-β1 and triggers the release of cargo.
Left (nuclear export): Crm1 with GTP-bound Ran binds to NES-bearing cargo and transport this complex out of the nucleus. In the cytoplasm, hydrolysis of GTP to GDP results in the release of cargo.

Figure 6: Domain organization of importin-α molecules.
The amino terminus of importin-α proteins is an importin-β1 binding (IBB) domain which interacts with importin-β1. The central Armadillo (ARM) repeats contain NLS-binding sites. The carboxy-terminal domain can bind to the exportin, cellular apoptosis susceptibility (CAS), which returns importin-α proteins back to the cytoplasm.

armadillo (ARM) repeats which recognize the NLS in cargo proteins. Each ARM repeats is composed of three α-helices and the grooves formed by ARM 2-4 and Arm7-8 can bind to the basic residues of classic NLSs (95). The carboxyl region contains a NES which is recognized by the importin-α-specific exportin, cellular apoptosis susceptibility (CAS), that mediates nuclear export of importin-α. Importin-β1 targets the import complex to the NPCs then translocates the complex into the nucleus. After import, interaction of Ran-GTP with importin-β1 causes disassociation of the complex and release of the cargo in the nucleus. The importin-α is exported to the cytoplasm by CAS, and it can start another cycle of nuclear import.

Recent research showed that some cargos can interact directly with importin-β1 or nucleoporins of NPCs to facilitate nuclear import (96-99), but the cargo binding site for importin-β1 is different from that for importin-αs.

Nuclear export

Protein nuclear export is similar to the import process (Figure 5). The transporter chromosome region maintenance 1 (Crm1) is the best characterized exportin and it can be specifically and irreversibly inhibited by the membrane permeable antifungal agent, leptomycin B (LMB) (100, 101). Therefore, LMB is useful for identifying a Crm1-dependent NES. Crm1 recognizes the nuclear export signals (NESs) in cargo proteins that are hydrophobic and rich in leucine residues, for example, LxxxLxxLxL (x represents any amino acid) (102-104). Crm1 forms a stable ternary complex with NES-cargo and Ran-GTP in the nucleus. This complex can exit the nucleus throungh the NPCs and is dissociated with nucleotide exchange of the Ran-GTP to Ran-GDP in the cytoplasm allowing Crm1 to return to the nucleus.

Proteins should be in the right place at the right time for their proper functions. STATs function as extracellular signal transducers in the cytoplasm and as transcription factors in the nucleus. Since STATs are larger than the diffusion limit, they need to be actively transported into and out of the nucleus. Given the considerable evidence that STAT6 contributes to an effective immune response and plays a dominant role in asthmatic lung pathology, understanding the mechanisms that regulate its nuclear trafficking is essential for therapeutic intervention.

6. Nuclear trafficking of STAT proteins

Current knowledge of the nuclear trafficking of several STAT factors has shown that they have different cellular localization (Figure 7) and their nuclear import is regulated distinctly (105). For example, nuclear import of the STAT1 factor is conditional and dependent on its dimerization mediated by tyrosine phosphorylation (106-109). However, the STAT3 and STAT5a transcription factors are imported continually to the nucleus, independent of tyrosine phosphorylation (110, 111). Nuclear transport of STAT1, STAT3 and STAT5a is briefly summarized in the following sections.

The Founding member, STAT1

Latent STAT1 resides primarily in the cytoplasm. Following tyrosine phosphoylation and dimerization in response to IFN stimulation, STAT1 is recognized by importins and transported into the nucleus. STAT1 mutants which cannot be tyrosine phosphorylated or form dimers do not translocate into the nucleus (112). Phosphorylation of STAT1 induces a conformational change of dimers which creates a functional NLS recognized by importin-α5 to facilitate transport into the nucleus. The STAT1 NLS is located within the DNA binding domain. When Leucine407 in the DNA binding domain is mutated into alanine, STAT1 is retained in the cytoplasm even it is phosphorylated following IFN-γ treatment. Although this STAT1 L407A mutant still has the ability to form dimers and bind DNA, *in vitro* binding assays show it is not able to bind importin-α5. (106). The region of importin-α5 that recognize phosphorylated STAT1 dimers is the carboxyl region of importin-α5 containing ARM repeats 9-10 and CAS-binding site (113). This is distinct from classical NLS recognition. After transport into the nucleus, specific DNA sequences in promoters of target genes have a higher affinity for STAT1 than importin-α5. The results suggest the co-evolution of nuclear import and DNA binding ability of STAT1.

STAT1 is dephosphorylated in the nucleus followed by redistribution of STAT1 to the cytoplasm (114, 115). A Crm1-dependent NES has been identified in the DNA binding domain of STAT1. The crystal structure of STAT1 bound to DNA predicts that the hydrophobic residues in NES are buried and not accessible to Crm1 when STAT1 is bound to DNA (29). In addition, STAT1 DNA binding mutant does not accumulate in the

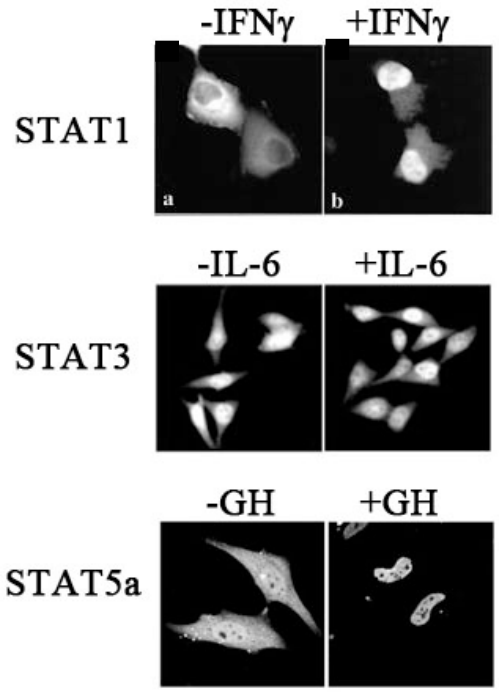

Figure 7: Cellular localization of GFP tagged STAT1, STAT3 and STAT5a.

STATs show different cellular localization. Unphosphorylated STAT1 is primary in the cytoplasm and accumulates in the nucleus following IFN-γ stimulation. STAT3 shows a nuclear presence before and after IL-6 stimulation. However, STAT5a is present both in the nucleus and cytoplasm and is predominately nuclear in response to growth hormone (GH) treatment. (Modified from references 106, 110 and 111)

nucleus following IFN treatment, even though it can be tyrosine phosphorylated, because it is efficiently exported out of the nucleus. Thus STAT1 nuclear trafficking is tightly correlated with tyrosine phosphorylation and DNA binding as a regulatory switch. The tyrosine dephosphorylation results in the dissociation of STAT1 from DNA and NES exposure for Crm1 recognition.

STAT3 and STAT5a

In contrast to STAT1, STAT3 and STAT5a are nuclear even in the absence of cytokines. Immunostaining and live cell imaging assays show that STAT3 and STAT5a constitutively shuttle between the cytoplasm and the nucleus and this process is tyrosine-phosphorylation independent (110, 111). Further studies have shown that the coiled-coil domain contains a region that is required for STAT3 and STAT5a nuclear import. The nuclear import of STAT3 is primary mediated by importin-α3, distinct from the importin-α that mediates STAT1 import.

Nuclear export of STAT3 and STAT5a is not well studied. Three leucine-rich elements in the coil-coiled domain and the DNA binding domain of STAT3 were identified as putative NES sequences of STAT3 (116). However, the STAT3 crystal structure showed that few of these hydrophobic residues are on the surface. Thus it is still not clear that STAT3 nuclear export is mediated by Crm1 or other exportins.

Although translocation mechanisms of several STATs have been investigated, little is known of the mechanisms that regulate STAT6 localization. It was reported that the half-life of STAT6 phosphorylation and DNA binding activity was less than 1 hour and the maintenance of STAT6 activation needed a constant cycle of activation, deactivation, nuclear export and reactivation (117). Since STAT6 is important for IL-4 and IL-13 signaling pathway and plays a role in cell proliferation and transformation, the activity regulation process is tightly controlled. My research goal was to understand the mechanisms that regulate the cellular localization of STAT6 as this may provide a way to control STAT6-mediated diseases such as allergy and leukemia.

Chapter 2

Materials and Methods

Cell cultures and reagents

HeLa, Cos1 and Jurkat cells (ATCC) were cultured in Dulbecco's modified Eagle's medium (DMEM) with 8% fetal bovine serum. Cells were treated with human recombinant human IL-4 (R&D system, Inc.) at 10 ng/ml. DNA transfections were carried out using *Trans*IT-LT1 transfection reagent (Mirus) according to the manufacturer's instructions. Rabbit anti-STAT6 (Santa Cruz Biotechnology), anti-STAT6 phosphotyrosine (Cell Signaling Technology), anti-CBP (Santa Cruz Biotechnology), anti-p300 (Santa Cruz Biotechnology), anti-GST (Santa Cruz Biotechnology), murine anti-GFP (Roche Diagnostics Corp.), anti-V5 (Invitrogen), anti-T7 (Novagen) and anti-Myc antibodies (9E10) (Santa Cruz biotechnology) were used at a 1:1,000 dilution for Western bloting and 1:200 dilution for immunofluorescence. Anti-GFP conjugated to IRDye 88 (Rockland Immunochemicals) was used at a 1:5,000 dilution for Western blotting. Horseradish peroxidase-conjugated anti-rabbit and anti-mouse immunoglobulins (Amersham Biosciences) were used as secondary antibodies for Western blotting (1:5,000). Anti-GFP antibody and MOPC-141 control antibody (Sigma-Aldrich Corp.) were used in electrophoretic mobility shift assay (EMSA) at 1 μg in 40 μl reactions. 2 μg of anti-V5 antibody (Invitrogen) were used for the *in vitro* binding assays. To label the mitochondria, 500 nM MitoTracker orange CMTMRos probe (Invitrogen) was used. Leptomycin B (gift from Barbara Wolff-Winiski, Novartis Research Institute, Vienna, Austria) was used at 10 nM.

Site-directed mutagenesis

The protocol was modified from the manual of the Stratagene QuikChange Site-directed Mutagenesis Kit. Two complementary synthetic oligonucleotides with the

desired mutation at the central region were designed as primers. In a 50 μl reaction, 50 ng of plasmid DNA, 125 ng of each primers, 0.1 mM dNTP, 1 unit of *Pfu Turbo* (Stratagene) and *Pfu Turbo* buffer were mixed and subjected to a thermal cycle of 30-seconds 90°C, 1- minute 55°C and 18-minute 68°C, for 20 cycles. The template DNA was digested with unit of DpnI at 37°C for 6 hours. The reaction was used to transform with RapidTrans™ TAM1 competent *E. coli* (Active Motif) and plasmids were purified from single colonies and sequenced.

Plasmid constructs

Full-length STAT6 cDNA and deletion mutants created by polymerase chain reaction were cloned into mammalian expression vector pEF1/V5-His (Invitrogen) or bacterial expression vector pMAL-c4X (New England Biolabs) to generate V5 or maltose-binding protein (MBP) fusion proteins. A monomeric form of enhanced GFP was produced by mutating A206K, L221K, and F223R in the vector pEGFP-N1 (Clontech) and it was used to generate EGFP tagged STAT6 proteins (118). Site-directed mutagenesis was performed with *Pfu Turbo* DNA polymerase (Stratagene). All mutants were confirmed by DNA sequencing. GST-tagged Importin-α constructs lacking the IBB domain were generated and purified as reported previously (110). MBP-STAT6(1-267) and MBP-STAT6(1-267Δ136-140) proteins were purified following the manufacturer's instructions (New England Biolabs).

Plasmid transformation

25 μl of RapidTrans™ TAM1 competent *E. coli* (Active Motif) or BL21 codon plus *E. coli* (Stratagene) were thawed on ice and 2 μl of plasmid DNA/ligation were added to thawed cells. Transformation reactions were incubated on ice for 30 minutes. After the cells were heat-shocked the tubes by immersing in a 42°C water bath for 30 seconds, the reactions were replaced on ice for 2 minutes. After adding 250 μl of Super optimal broth with catabolite repression (SOC), the reactions were incubated at 37°C with shaking at 225-250 rpm for 1 hour. The transformations were plated out on pre-warmed LB agar plates containing ampicillin or kanamycin at μg/ml and incubated overnight at 37°C.

DNA transfection into mammalian cells

Cells were plated the day before transfection for about 50% confluency at the time of transfection. DNA transfections were performed with *Trans*IT-LT1 transfection reagent (Mirus) according to the manufacturer's instructions. The desired amount of transfection reagent and serum-free Opti-MEM were mixed by gently pipetting. The desired amount of plasmid DNA was added to the diluted *Trans*IT-LT1 reagent. After incubation at room temperature for 20 minutes, the *Trans*IT-LT1 reagent-DNA complex was added dropwise to the cells. Two days after transfection, cells were harvested and assays were performed.

The amount of DNA and transfection reagent used were :

Culture vessel	Total DNA (μg)	*Trans*IT-LT1 reagent (μl)
12-well plate	0.25	0.5
6-well plate	0.5	1.0
35-mm dish	0.5	1.0
60-mm dish	1.0	2.0
100-mm dish	2.5	5.0

Western blot

After transfection, cells were serum-starved for 24 hours and were untreated or treated wih hIL-4 for 30 minutes. Cells were lysed with cold lysis buffer [50 mM Tris (pH8.0), 5 mM EDTA, 0.5% Nonidet P-40, 280 mM NaCl, 1 mM PMSF, 1x protease inhibitor cocktail (Sigma-Aldrich Corp.), 1 mM NaF, and 1 mM sodium vanadate]. Proteins were separated by 8% SDS-PAGE and transferred to nitrocellulose membrane (Pierce Biotechnology). The membranes were incubated in blocking solution (5% non-fat dry milk in TBS-Tween 20: 20 mM Tris pH 7.5, 137 mM NaCl, 0.05% Tween 20) at room temperature for 20 minutes. After blocking, the membranes were incubated with primary antibodies diluted in blocking solution or in TBS-Tween buffer with 5% BSA for anti-STAT6 phosphotyrosine antibody at 4°C overnight. The membranes were washed with TBS-Tween buffer three times and then incubated with appropriate secondary antibodies at room temperature for 1 hour. The membranes were washed and specific

proteins were detected by enhanced chemiluminescence or Odyssey infrared imaging system (Li-COR Biosciences).

Direct imaging of GFP fusion proteins

Cells were plated on glass coverslips, transfected with STAT6-GFP constructs, serum starved twenty-four hours and then evaluated two days after transfection. Cells were treated with or without hIL-4 for 30 minutes and fixed with 4% paraformaldehyde for 10 minutes at room temperature. GFP-tagged protein was observed with a Zeiss LSM 5 laser scanning microscope using a 40x oil objective [Plan-Neofluar, numerical aperture 1.3, differential interference contrast microscopy objective (DIC)]. GFP was excited at 488 nm using an argon laser, and emission was collected using a 505 long pass filter. Images were captured using Zeiss LSM 5 Pascal imaging software.

Immunofluorescence

HeLa cells or transfected HeLa cells seeded on coverslips were serum-starved overnight followed by IL-4 treatment for 30 minutes. After PBS rinses and 4% paraformaldehyde fixation, cells were permeabilized with 0.5% Triton X-100 in PBS for 5 minutes and then blocked with 5% BSA in PBS for 1 hour at room temperature. Subsequently cells were incubated with anti-STAT6, anti-V5 or anti-T7 antibody (1:200) followed by tetramethyl rhodamine isothiocyanate (TRITC)-conjugated secondary antibodies (Jackson Laboratory, 1:200) diluted in blocking buffer for 1 hour at room temperature. Fluorescence was observed with a Zeiss LSM 5 laser scanning microscope using a 40x oil objective [Plan-Neofluar, numerical aperture 1.3, DIC objective]. TRITC was excited at 543 nm, and emission was collected using a 560 long pass filter. Images were captured using Zeiss LSM 5 Pascal imaging software.

Live cell imaging

STAT6-GFP expressing HeLa cells were seeded on glass bottom tissue culture dishes (Mattek Corporation) and transfected. The dishes were mounted on a Zeiss inverted Axiovert 200M microscope using a heating insert coupled with the Incubator S (Zeiss). During imaging the cells were maintained at 37°C and 5% CO2 using the Zeiss

Tempcontrol 37-2 Digital and CTI Controller 3700. The time series images for photobleaching assays were performed with the Zeiss LSA 510 META NLO two-photon laser scanning microscope system (Zeiss) using a 40x oil objective [Plan-Neofluar, numerical aperture 1.3, DIC objective]. The excitation wavelength used for GFP was 488 nm and emission was detected with a 505 nm filter.

For fluorescence recovery after photobleaching (FRAP) analysis, a region in the nucleus was bleached at 100% power of an argon laser at 488 nm for 70 seconds (nuclear FRAP) or 0.3 seconds (nuclear strip FRAP). For fluorescence loss in photobleaching (FLIP) analysis, a region in the nucleus or cytoplasm was bleached every 12 seconds at maximum laser intensity for 5 or 50min. Images were acquired using LSM 510 Meta version 3.2 imaging software. The fluorescence intensity was quantified in the region of interest (ROI) using LSM Imaging software and graphically depicted using Microsoft Excel. Experiments are representative of more than three independent studies.

Electrophoretic mobility shift assay

Cells were lysed with hypotonic lysis buffer [15 mM Hepes (pH7.9), 0.2 mM spermine, 0.5 mM spermidine, 2 mM potassium-EDTA, 80 mM KCl, 1% glycerol, 0.0025% Nonidet P-40, 1 mM dithiothreitol (DTT), 1 mM PMSF, 1 mM sodium vanadate, 1 mM NaF, and 1x protease inhibitor cocktail] for 45 minutes at 4°C followed by passage through a 25 gauge syringe 15 times. One tenth volume of restoration buffer (150 mM HEPES pH 7.9, 2 mM spermine, 5 mM spermidine, 20 mM EDTA, 800 mM KCl, 5% glycerol) was added and the extracts were centrifuged at 2,000 rpm for 10 minutes at 4°C to collect the cytoplasmic extracts. Nuclei were suspended in hypertonic buffer [20 mM Hepes (pH7.9), 0.2 mM spermine, 0.5 mM spermidine, 0.2 mM potassium-EDTA, 0.4 M NaCl, 10% glycerol, 1 mM DTT, 1 mM PMSF, 1 mM sodium vanadate, 1 mM NaF, and 1x protease inhibitor cocktail] for 45 minutes at 4°C and then centrifuged at 10,000 rpm for 10 minutes at 4°C to collect the nuclear extracts. Nuclear and cytoplasmic extracts were combined for the DNA binding reactions.

For DNA binding assays, 10 μg of protein were pre-incubated with 1 μg specific antibodies or 100-fold excess non-radiolabeled probe for 30 minutes at room temperature in reaction buffer (12 mM HEPES pH 7.9, 10% glycerol, 5 mM $MgCl_2$, 0.12 mM EDTA,

0.6 mM EGTA, 0.5 mM DTT, 2 μg poly (dI-dC), 0.5 μg of non-specific plasmid DNA) prior to incubation with radiolabeled oligonucleotide probe for 30 minutes. The dsDNA oligonucleotide corresponding to -407 to -387 of the IL-4R alpha gene (5'-AGCTTCTTCATCTGAAAAGGG-3') was 5' end radiolabeled and used in the binding reactions. Complexes were separated on 4.5% non-denaturing acrylamide gels and exposed to X-ray film for autoradiography.

Human primary lymphocyte purification

Blood was collected in syringes containing 1 ml of 7% EDTA for 60 ml of blood. 15 ml aliquots of blood were mixed with 15 ml of PBS without $Ca2^{+}$ or $Mg2^{+}$ in a 50 ml tube by inverting twice. In another 50 ml tube containing 15 m of Accu-Prep Lymphocytes (Accurate Chemical & Scientific Corporation), the 30 ml of diluted blood was slowly added to form a layer. After centrifugation at 800g for 20 minutes at room temperature, the peripheral blood mononuclear cells (PBMC) are located at the inferface between the top plasma layer and lower reagent layer containing red blood cells. The PBMC was carefully collected from 5 ml above and 5 ml below the interface and washed with an equal volume of cold MACS buffer (PBS with 0,1% BSA and 2 mM EDTA) several times to remove the platelets.

Nuclear extract preparation

Lymphocyte extract was prepared as described previously (119). After washing with PBS, 10^6 of purified lymphocytes were resuspended in 1 ml of 10 mM HEPES pH7.9, 10 mM KCl, 0.1 mM EDTA and 1x protease inhibitor cocktail and incubated on ice for 15 minutes. Nonidet P40 was added to 0.5% and cells were vortexed. Nuclei were collected by centrifugation and then incubated in 20 mM HEPES pH7.9, 0.4 M NaCl 1 mM EDTA and protease inhibitor cocktail at 4°C for 15 minutes. After centrifugation, the nuclear extract was collected and protein concentration was determined by Bio-Rad protein assay (Bio-Rad Laboratories).

Luciferase assay

HeLa cells were seeded in 6-well plates and transfected with 0.5 μg of hIL-4 Receptor-Luciferase (IL-4TKLuc) (120), 10 ng of Renilla Luciferase (pRL-null) (Promega), and 0.5 μg of STAT6-GFP wild type or mutant plasmids. After twenty-four hours, cells were split into 12-well plates. Two days after transfection, cells were untreated or treated with 3 ng/ml of hIL-4 for 8 hours prior to harvest. Dual-luciferase reporter assays were performed according to manufacturer's instructions (Promega). The luciferase results were measured using a Lumat model LB 9507 luminometer and normalized to Renilla luciferase values to compensate for variations in transfection efficiency.

GST and MBP fusion protein purification from bacteria

BL21 condon plus *E. coli* (Stratagene) were transformed with plasmids encoding GST-or MBP-fusing proteins and a single transformant was inoculated into 20 ml LB with ampicillin for overnight culture. The 20 ml culture was added into 800 ml LB with ampicillin and grown at 37°C until the absorbance at 600 reached 0.6. 0.2mM IPTC was subsequently added to induce protein expression for 16-20 hours at room temperature.

For GST-fusion protein purification, cells were harvested, incubated in cold lysis buffer (PBS containing 50 mM EDTA, 1% Triton X-100, 1 mM PMSF) with 1 mg/ml of lysozyme on ice for 30 minutes and French-pressed at 1,000 psi thrice, After centrifugation at 20,000 rpm for 30 minutes, the supernatant was collected and incubated with glutathione beads (Sigma) at 4°C with gentle agitation for 2 hours. The beads were subsequently washed three times with cold lysis buffer. Bound proteins were eluted with 30 mM reduced glutathione in 10 mM TE buffer and then dialyzed twice in 1 liter dialysis buffer (20 mM Hepes pH7.9, 50 mM NaCl, 1 mM EDTA, 10% glycerol, 0.2 mM PMSF and 1 mM DTT).

For MBP-fusion protein purification, cells were harvested, incubated in cold column buffer (20 mM Tris pH7.4, 200 mM NaCl, 1 mM EDTA and 1 mM DTT) with 1 mg/ml of lysozyme on ice for 30 minutes and French-pressed at 1,000 psi thrice, After centrifugation at 20,000 rpm for 30 minutes, the supernatant was collected and incubated with amylose resin at 4°C with gentle agitation for 2 hours. The resin was subsequently

washed with cold column buffer three times. Bound proteins were eluted with 10 mM maltose in column buffer.

In vitro importin binding assay

COSI cells expressing STAT6-V5 were lysed with buffer (280 mM NaCl, 50 mM Tris-HCl pH8.2, 5mM EDTA and 0.5% NP-40), and 500 μg of protein lysate was used for each assay. STAT6-V5 was captured with anti-V5 antibody at 4°C overnight and incubated with protein G beads for 2 hours next day. 15 μg purified GST-importin-αs was added to each reaction and the incubation was continued for additional 2 hours at 4°C with gentle agitation for 2 hours. Bound protein complexes were eluted with SDS sample buffer and analyzed by Western blot with anti-V5 and anti-GST antibodies.

To test importin binding to bacterially expressed STAT6, recombinant GST-importin-αs were incubated with bacterially expressed MBP-tagged STAT6 proteins immobilized on amylase resin in column buffer with 0.05% NP-40 at 4°C with gentle agitation for 2 hours. The resin was washed with column buffer with 0.05% NP-40 four times. Binding was detected by Western blot with anti-GST antibody and the STAT6 protein was quantified by Ponceau S staining.

RNA interference (RNAi)

Short interfering RNA (siRNA) duplexes specific for human importin-β1 (Qiagen) or vimentin (control) were transfected with X-tremeGENE siRNA transfection reagent (Roche). One day prior to tranfection, COSI cells were plated in 6-well plates with coverslips. For siRNA transfection, 160 pmole of siRNA and 10 μl of X-tremeGENE siRNA transfection reagent were mixed in 100 μl of Opti-MEM separately and then combined to form the complex at room temperature for 20 minutes prior to adding to cells. Twenty-four hours after siRNA transfection, cells were transfected with STAT6-GFP. Cellular localization of STAT6-GFP was observed after 24 hours by fluorescence microscopy. Endogenous importin-β1 knockdown was checked by semi-quantitative RT-PCR.

To test the protein silencing efficiency of importin-β1 siRNA, COSI cells were transfected with control or importin-β1 siRNA as described above. The next day, cells

were transfected with a Myc-importin-β1 encoding plasmid. Cells were harvest 24 hours after plasmid transfection and processed for Western blotting with anti-myc antibody.

Semi-quantitative RT-PCR

RNA extraction was performed with Trizol reagent (Invitrogen) according to manufacturer's instruction and cDNA was synthesized with M-MLV reverse transcriptase (Promega). RT-PCR was performed with specific primers for importin-β1 or GAPDH as an internal control for 25 cycles of a 30-seconds 95°C, a 30-seconds 55°C and a 1-minute 72°C. Image J software was used to estimate quantity. Primer sequences for importin-β1 and GAPDH were:

Importin-β1 (forward): 5'-AATCCAGGAAACAGTCAGGTTGC
(reverse): 5'-AGCACTGAGACCCTCAATCAG
GAPDH (forward): 5'-GGAGCCAAAAGGGTCATCATCTC
(reverse): 5'-AGTGGGTGTCGCTGTTGAGTC

Chapter 3

Characterization of STAT6 Nuclear Import

Abstract

The STAT6 transcription factor is essential for the development of protective immunity; however, the consequences of its activity can also contribute to the development of autoimmune disease. As a signal transducer in the cytoplasm and transcription factor in the nucleus, accurate cellular localization of STAT6 is essential for its function. Since STAT6 is about 100 kDa, it needs carrier proteins for active transportation. In addition, tyrosine phosphorylation is known to activate STAT6 in response to cytokine stimulation, but there is a gap in our understanding of the mechanisms by which it enters the nucleus. In this chapter, live cell imaging was used in conjunction with photobleaching techniques to demonstrate the continual nuclear import of STAT6, independent of tyrosine phosphorylation. Although STAT6 is imported to the nucleus continually, it accumulates in the nucleus following tyrosine phosphorylation.

Analysis of a series of STAT6 deletion proteins identifed a protein domain required for nuclear entry. A region that includes amino acids 136-140 in the coiled-coil domain functions similarly before or after cytokine stimulation. This region is essential for importin binding and transcriptional activity of STAT6. *In vitro* binding assays to importins and importin-β1 siRNA experiments demonstrated that the dynamic nuclear shuttling of STAT6 is mediated by the classical importin-α–importin-β1 system. These findings will impact diagnostic approaches and strategies to block the deleterious effects of STAT6 in autoimmunity.

Results

1. STAT6 shows constitutive nuclear presence in resting cells and accumulates in the nucleus after IL-4 treatment

As a founding member, STAT1 nuclear transport was first studied and was thought to be a model for all of other STATs. But more and more reports have shown that, unlike STAT1 which primarily resides in the cytoplasm and is transported into the nucleus upon tyrosine phosphorylation, STAT3 and STAT5 show continuous and tyrosine phosphorylation-independent nuclear import. To understand the process of STAT6 nuclear transport, I first evaluated endogenous STAT6 localization in HeLa cells by immunofluorescent staining. The results in Figure 8A show that STAT6 was both in the cytoplasm and the nucleus in resting cells and, following 30-minute IL-4 treatment, STAT6 showed nuclear accumulation. STAT6 tyrosine phosphorylation was analyzed by Western blotting with anti-STAT6 phosphotyrosine and anti-STAT6 antibodies and the results demonstrated that STAT6 was specifically phosphorylated at tyrosine 641 after IL-4 treatment (Figure 8B). The same result was found with other cell lines such as COSI and HT1080 (data not shown). Because the primary role of STAT6 is to regulate B and T cell functions, I performed cell fractionation with a T lymphocyte cell line (Jurkat) and primary lymphocytes to evaluate localization of endogenous STAT6 in lymphocytes. Nuclear extracts were prepared from Jurkat cells and primary lymphocytes without or with IL-4 treatment and processed for Western blotting (Figure 9). STAT6 was present in the nucleus without IL-4 treatment; however, it showed an increased amount in the nucleus after IL-4 stimulation. P53 was used as a control for a nuclear protein. Although a cytoplasmic protein marker was not used here, the results suggest that STAT6 has constitutive nuclear presence and accumulates in the nucleus after tyrosine phosphorylation.

The fluorescent protein tag enhanced green fluorescent protein (EGFP) is a useful tool to track proteins in fixed cells or live cells. For this reason, I generated GFP-tagged STAT6 protein. To ensure that the GFP tag, which is about 27 kDa, did not influence STAT6 cellular localization and functions, STAT6-GFP was transfected into HeLa cells and characterized. The GFP tag did not influence STAT6 localization as STAT6-GFP

A.

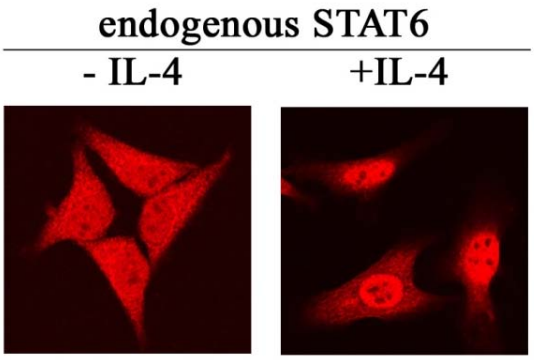

B.

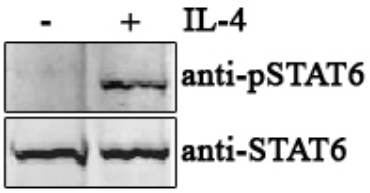

Figure 8: Endogenous STAT6 in HeLa cells.

A. HeLa cells were serum starved, and left untreated (-IL-4) or treated (+IL-4) with IL-4 for 30 minutes. Cells were fixed and stained with anti-STAT6 antibody followed by TRITC-conjugated secondary antibody

B. 10 μg of total cell lysates from HeLa cells treated as for panel A were analyzed by Western blot with anti-phosphotyrosine STAT6 (pSTAT6) or anti-STAT6 antibodies.

A.

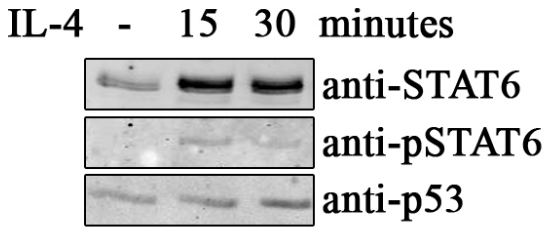

B.

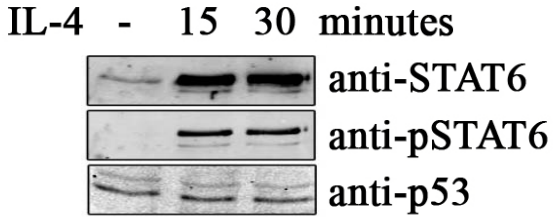

Figure 9: Endogenous STAT6 in Jurkat cells and human primary lymphocytes.

A. Jurkat cells were treated with IL-4 for 15 or 30 minutes and nuclear extracts were prepared. 10 μg of protein was analyzed by Western blot with anti-STAT6, anti-phosphotyrosine STAT6 or anti-p53 as a nuclear marker.

B. Purified human lymphocytes were treated with IL-4 for 15 or 30 minutes and nuclear extracts were prepared. 10 μg of protein was analyzed as in (A).

showed nuclear and cytoplasmic presence and accumulated in the nucleus upon IL-4 stimulation (Figure 10). STAT6 protein with another synthetic peptide V5 tag: (GKPIPNPLLGLDST), showed the same result. In addition, tyrosine phosphorylation and DNA binding ability were evaluated by Western blot and electrophoretic mobility shift assay (EMSA) (Figure 11). STAT6-GFP protein was specifically tyrosine phosphorylated in response to IL-4 treatment. EMSAs were performed with IL-4 receptor GAS site as a probe. The endogenous STAT6-DNA complex was not observed, possibly due to low protein levels relative to exogenous STAT6. However, the STAT6-GFP-DNA complexes were observed and anti-GFP antibody and cold DNA probe specifically abrogated the complex formation demonstrating that STAT6-GFP is in this complex and capable of binding DNA after IL-4 stimulation. Therefore, STAT6-GFP behaves like endogenous STAT6 and can be used as a tool to study STAT6 nuclear transport.

Imaging of fixed cells can provide protein cellular localization at a specific time point but not the spatial and temporal dynamics of protein movement in living cells. In order to characterize STAT6 protein in living cells, I used live cell imaging assays, fluorescent recovery after photobleaching (FRAP) and fluorescent loss in photobleaching (FLIP) with STAT6-GFP-expressing HeLa cells. Because the cells were kept in normal growth conditions, STAT6 nuclear transport can be studied under physiological conditions. With the nuclear FRAP (nFRAP) assay with STAT6-GFP, I can directly evaluate STAT6 import from the cytoplasm into the nucleus (Figure 12). A region in the nucleus of STAT6-GFP-expressing cells was subjected to high-intensity laser to bleach the fluorescent STAT6 in this compartment. Subsequent fluorescence recovery with time in the nucleus was monitored and quantified relative to a site in the cytoplasm. If the fluorescent molecules are imported into the nucleus, the fluorescence intensity in the nucleus will increase with time. Thus the fluorescence recovery rate in the nucleus correlates with the nuclear import rate of the fluorescent protein.

As shown in Figure 13, fluorescence recovery in the nucleus of unphosphorylated STAT6-GFP (STAT6-GFP) was half maximal by 15 minutes and complete by 45 minutes. Thus STAT6 can be constituteively imported into the nucleus and this process is tyrosine phosphorylation independent. Following tyrosine phosphorylation in response to IL-4 (STAT6-GFP, +IL-4), nuclear fluorescence recovery also was half maximal by 15

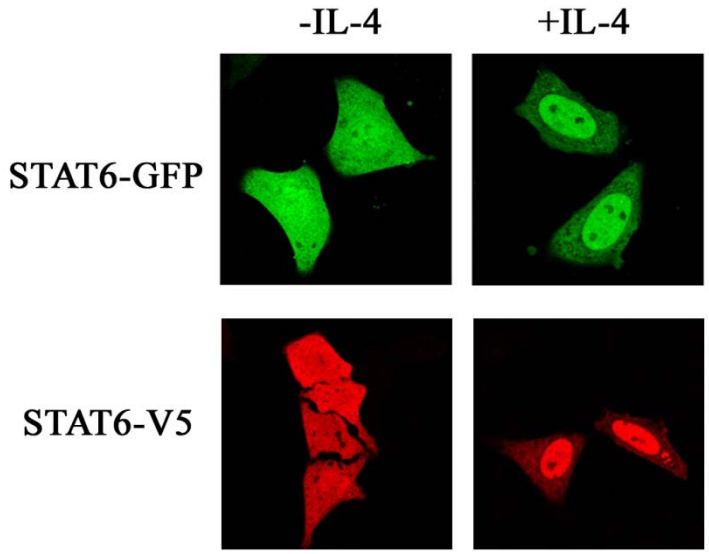

Figure 10: Cellular localization of STAT6-GFP and STAT6-V5 in HeLa cells.

HeLa cells expressing STAT6-GFP (upper) or STAT6-V5 (lower), were untreated (-IL-4) or treated (+IL-4) with IL-4 for 30 minutes. Cellular localization of STAT6-GFP was observed by direct fluorescence microscopy and STAT6-V5 was observed by immunofluorescent staining with anti-V5 antibody.

A.

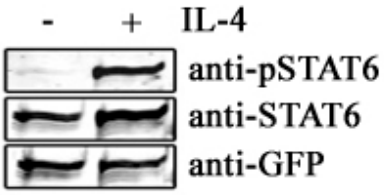

B.

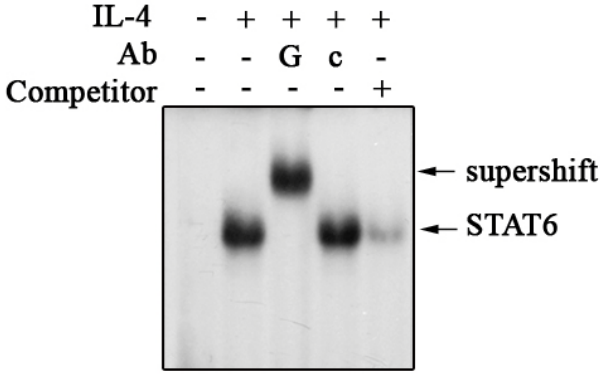

Figure 11: Characterization of STAT6-GFP.

HeLa cells expressing STAT6-GFP were untreated or treated with IL-4 for 30 minutes.

A. Whole cell extracts were prepared and Western blot was performed with anti-phosphotyrosine STAT6, anti-STAT6 or anti-GFP antibodies.
B. EMSAs were performed with the radiolabeled DNA fragment corresponding to the IL-4 receptor alpha gene GAS site and protein lysates from cells as treated in (A). Effects of additions of antibodies (Ab) to the reaction to GFP (G), or control (c), or 100-fold excess unlabeled oligonucleotide (DNA) are shown.

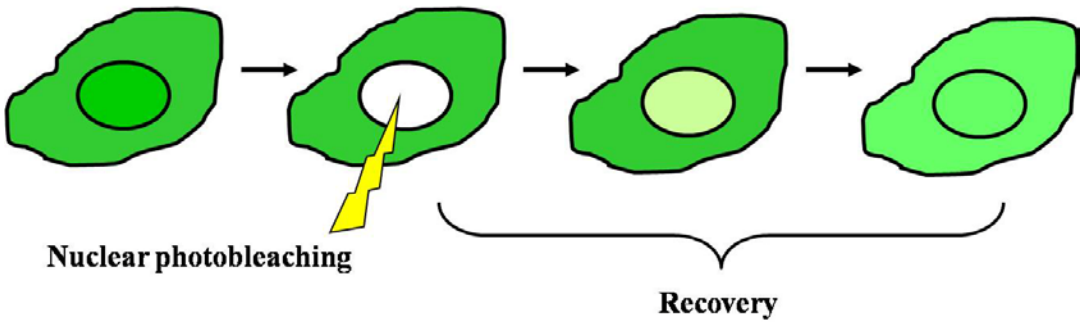

Figure 12: Nuclear fluorescence recovery after photobleaching (nFRAP)

Cells expressing a fluorescently-tagged protein are subjected to a high intensity laser beam in a region of the nucleus. Fluorescence in the nucleus is bleached. If the fluorescent molecules are imported into the nucleus continually, the fluorescence intensity will increase in the nucleus with time. The fluorescence recovery in the nucleus is monitored and the recovery rate correlates to the nuclear import rate of the fluorescent protein.

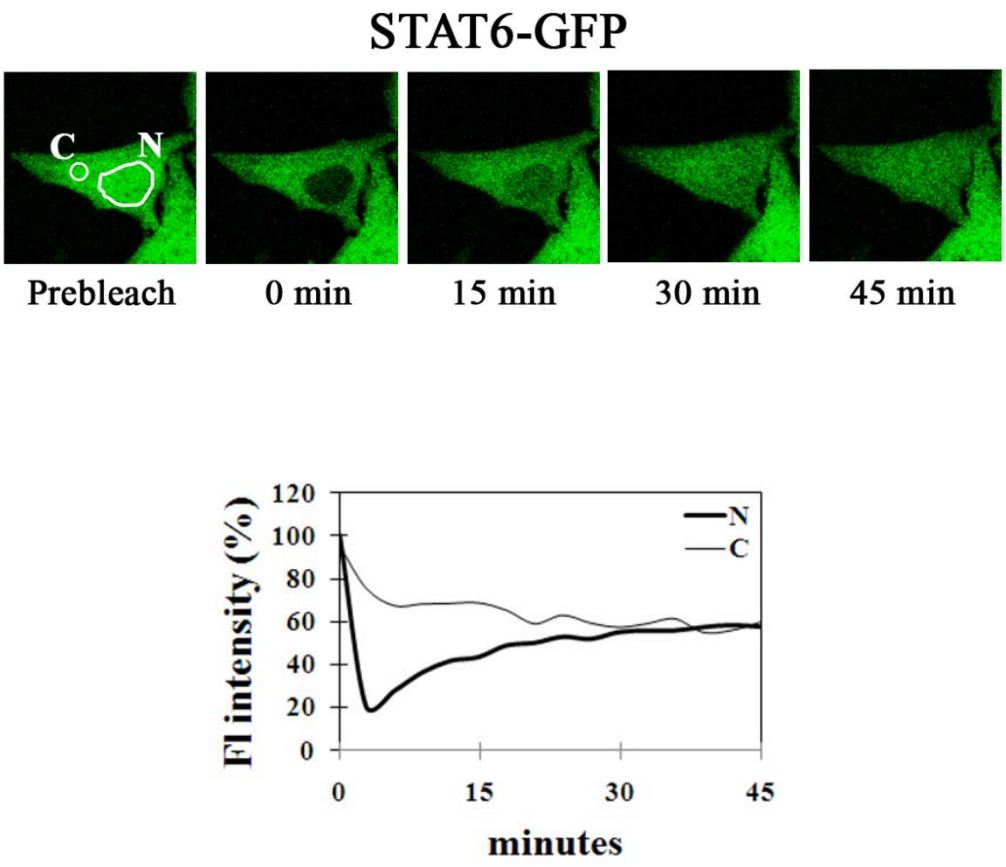

Figure 13: Nuclear FRAP of STAT6-GFP showed constitutive nuclear import.

Nuclear FRAP assays were performed with cells expressing STAT6-GFP without IL-4 stimulation. The nucleus (N) was subjected to high intensity laser to bleach the fluorescent STAT6. Subsequent fluorescence recovery with time in the nucleus was monitored and quantified relative to a site in the cytoplasm (C). The quantitative data of relative fluorescence intensity (Fl) with time in the nucleus (N) and cytoplasm (C) is shown in the lower panel. The data shown are representative of more than three independent studies.

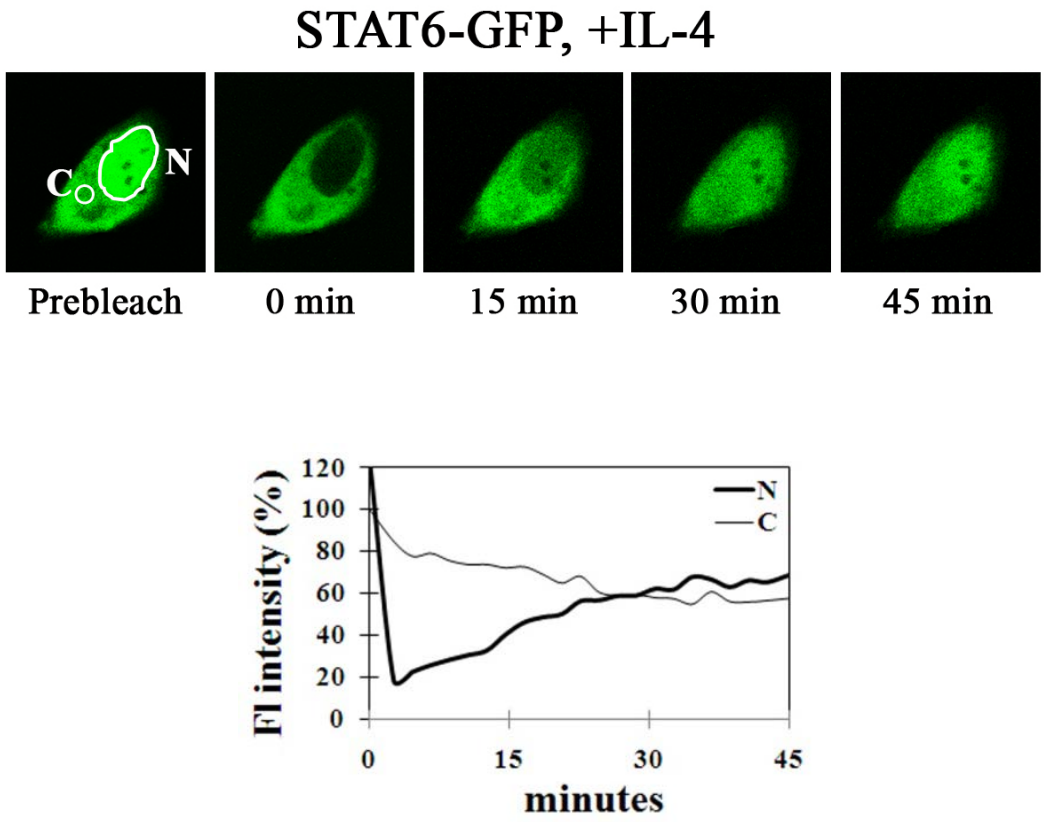

Figure 14: Nuclear FRAP of tyrosine phosphorylated STAT6-GFP.

Nuclear FRAP assays were performed with cells expressing STAT6-GFP with IL-4 stimulation. The nucleus (N) was subjected to high intensity laser to bleach the fluorescent STAT6. Subsequent fluorescence recovery with time in the nucleus was monitored and quantified relative to a site in the cytoplasm (C). The quantitative data of relative fluorescence intensity (Fl) with time in the nucleus (N) and cytoplasm (C) is shown in the lower panel. The data shown are representative of more than three independent studies.

minutes (Figure 14). This indicates the rate of nuclear import is the same for unphosphorylated or phosphorylated STAT6. However, phosphorylated STAT6-GFP accumulated in the nucleus to a greater extent than in the cytoplasm. This result could reflect a decrease in STAT6 nuclear export.

2. STAT6 nuclear import is independent of tyrosine phosphorylation

The nFRAP result of STAT6 in resting cells suggested that STAT6 nuclear import is independent of tyrosine phosphorylation. But it remained possible that unphosphorylated STAT6-GFP could form dimers with phosphorylated endogenous STAT6 bringing STAT6-GFP into the nucleus. To determine if STAT6 nuclear import is independent of tyrosine phosphorylation, the behavior of a STAT6 protein with a double mutation was evaluated. The tyrosine 641 that is specifically phosphorylated in response to cytokine stimulation was substituted with phenylalanine (Y641F), and the critical arginine 562 in the SH2 domain that functions to form dimers capable of specific DNA binding was mutated to alanine (R562A). Therefore, the possibility of forming dimers can be ruled out. Imaging results showed this mutated STAT6 protein, STAT6(RY)-GFP, was imported to the nucleus but did not accumulate following stimulation with IL-4 (Figure 15A). EMSAs and Western blotting were performed to ensure that STAT6(RY)-GFP lacked tyrosine phosphorylation and ability to bind DNA (Figure 15B and C).

In addition, nFRAP assay was performed with STAT6(RY)-GFP expressing HeLa cells with IL-4 treatment. The kinetics of nuclear fluorescence recovery of STAT6(RY)-GFP mutant in the nucleus was similar to that of unphosphorylated STAT6 (Figure 16). The fluorescence recovery in the nucleus was half maximal by 15 minutes and complete by 45 minutes. All these data showed that STAT6 nuclear import is continual and independent of tyrosine phosphorylation; nevertheless, nuclear accumulation requires tyrosine phosphorylation.

A.

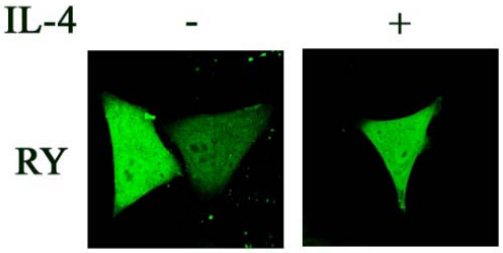

B.

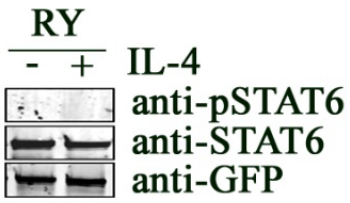

C.

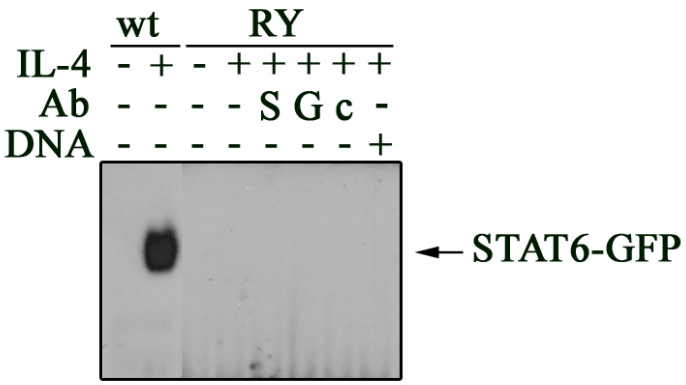

Figure 15: STAT6 nuclear import independent of tyrosine phosphorylation and dimerization.

A. Cellular localization of STAT6(RY)-GFP in HeLa cells without (-) or with (+) IL-4 treatment for 30 minutes.

B. STAT6(RY)-GFP expressing HeLa cells were untreated (-) or treated (+) with IL-4 for 30 minutes. Whole cell extracts were prepared and a Western blot was performed with anti-phosphotyrosine STAT6, anti-STAT6 or anti-GFP antibodies.

C. EMSAs were performed with the radiolabeled DNA fragment corresponding to the IL-4 receptor alpha gene GAS site and protein lysates from STAT6-GFP (wt) or STAT6(RY)-GFP (RY) expressing HeLa cells untreated or treated with IL-4. Effects of additions of antibodies (Ab) to the reaction to STAT6 (S), GFP (G) or control (c), or 100-fold excess unlabeled oligonucleotide (DNA) are shown.

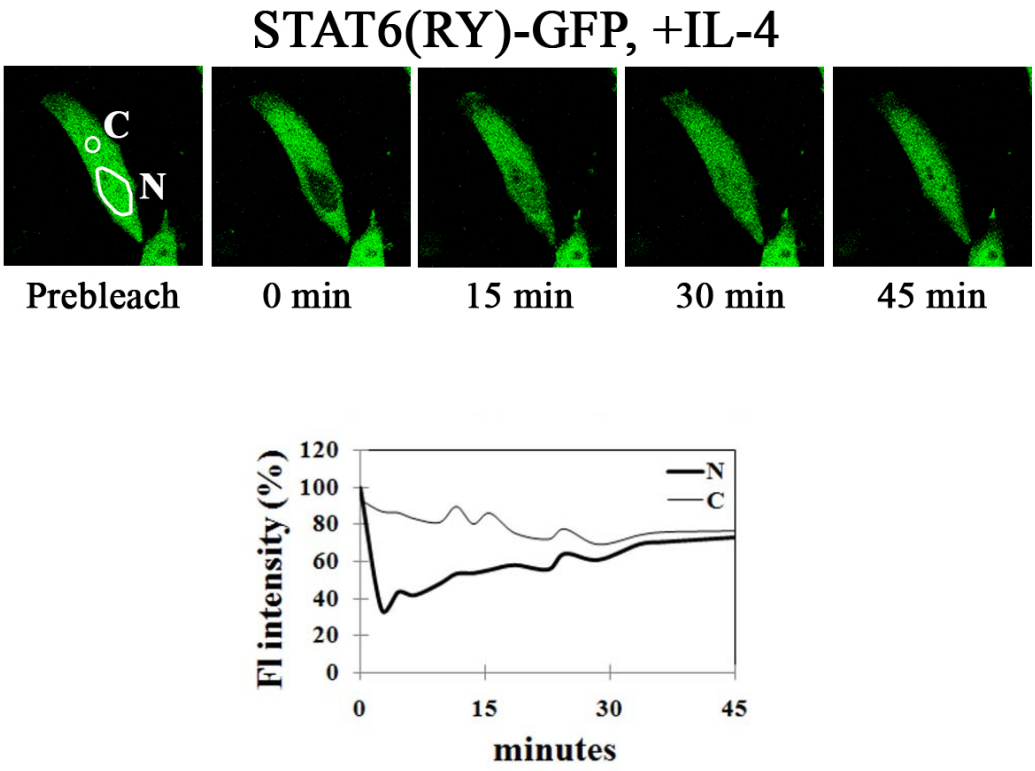

Figure 16: Nuclear FRAP of STAT6(RY)-GFP.

Nuclear FRAP assays were performed with cells expressing STAT6(RY)-GFP with IL-4 stimulation. The nucleus (N) was subjected to high intensity laser to bleach the fluorescent STAT6(RY). Subsequent fluorescence recovery with time in the nucleus was monitored and quantified relative to a site in the cytoplasm (C). The quantitative data of relative fluorescence intensity (Fl) with time are shown in the lower panel. The data shown are representative of more than three independent studies.

3. Identification of sequences required for STAT6 nuclear import

Nuclear import of large molecules such as STAT6 which is about 100 kDa requires an amino acid sequence or structure that serves as a NLS. To identify amino acids that facilitate STAT6 nuclear import, a series of STAT6 deletion proteins were generated and the cellular localization of the truncated proteins was evaluated with or without IL-4 stimulation. Small proteins were tagged with two GFP molecules to ensure they did not passively diffuse into the nucleus, and a diagram of some of the truncations is shown in Figure 17A. The cellular localization of these truncations indicated that a region in the coiled-coil domain is indispensable for nuclear import. STAT6(1-267) containing the amino terminus and the coiled-coil domain of STAT6 was imported to the nucleus. However, STAT6(268-847) containing the DNA binding domain, SH2 domain, and transactivation domain remained in the cytoplasm with or without IL-4 stimulation (Figure 17B). Therefore, the region required for STAT6 nuclear import was present within amino acids 1-267.

To further narrow down the region which is necessary for STAT6 nuclear import, additional deletions within the coiled-coil domain were generated. I identified a region with in amino acids 136-140 that is required for STAT6 nuclear import (Figure 17B). STAT6(136-847) was imported and accumulated in the nucleus following tyrosine phosphorylation, while STAT6(141-847) remained in the cytoplasm with or without tyrosine phosphorylation. Western blotting with antibodies to STAT6 phosphotyrosine 641 confirmed that the deletions were accurately phosphorylated in response to IL-4 (Figure 17C).

The studies with STAT6 truncations identified a sequence between amino acids 136-140 (RLQHR) that is required for nuclear import. To determine the effect of a specific deletion or substitution of these amino acids in otherwise full-length STAT6, I evaluated the localization of two mutated STAT6 proteins linked to GFP. STAT6 lacking 136-140 (dl) or STAT6 containing a substitution of 135-140 amino acids with alanine residues (sub6A) were expressed in cells untreated or stimulated with IL-4 (Figure 18A). The cellular localization of both mutated STAT6 proteins was restricted to the cytoplasm without or with IL-4 treatment. The same mutated STAT6 protein, STAT6(dl136-140), with a V5 tag showed the same cytoplasmic localization (Figure 18B) indicating that the

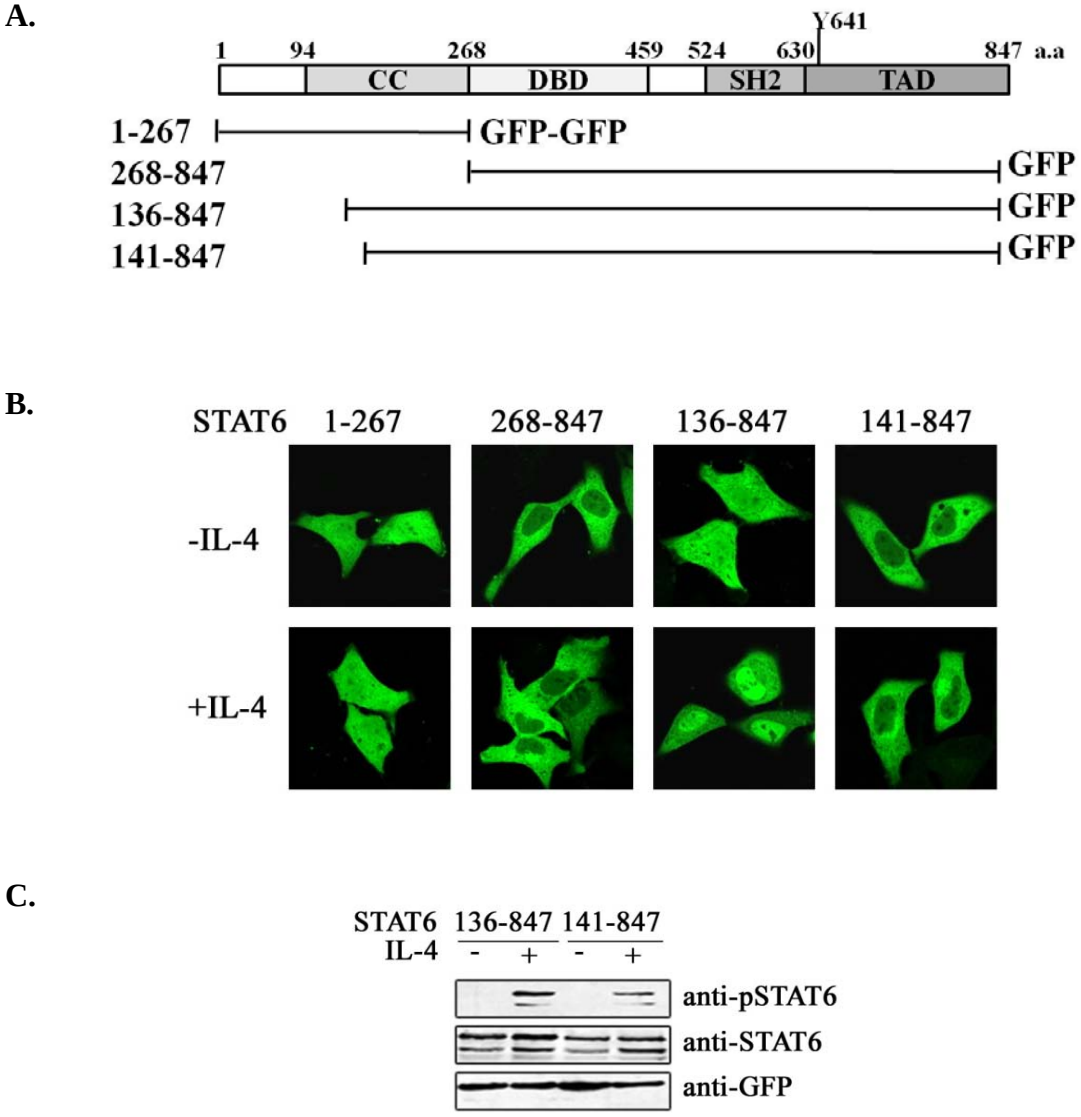

Figure 17: Identification of sequences required for STAT6 nuclear import.

A. Linear diagram of STAT6 functional domains and corresponding deletion mutations. Numbers indicate amino acids. CC: coiled-coil domain, DBD: DNA binding domain, SH2: SH2 domain, TAD: transactivation domain.

B. Fluorescent images of STAT6-GFP deletion mutations expressed in cells serum-starved (-IL-4) or stimulated with IL-4 (+IL-4).

C. Western blot of protein lysates from cells performed with anti-phosphotyrosine 641 STAT6 (anti-pSTAT6), anti-STAT6 or anti-GFP antibodies,

A.

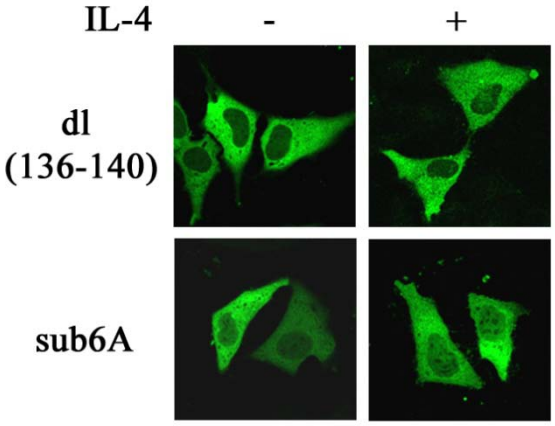

B.

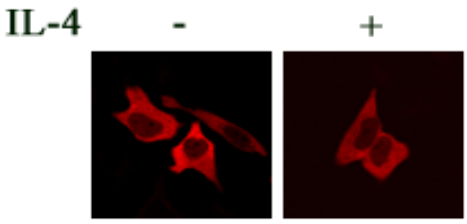

Figure 18: Amino acids 136-140 are required for STAT6 nuclear import.

A. STAT6-GFP with an internal deletion of amino acids 135-140 (dl) or STAT6-GFP with a substitution of six alanine residues for amino acids 135-140 (sub6A) were expressed in cells serum starved (-) or stimulated with IL-4 (+). STAT6 localization was visualized microscopically.

B. HeLa cells expressing STAT6(dl136-140)-V5 were untreated (-IL-4) or treated (+IL-4) with IL-4 for 30 minutes. Cellular localization of STAT6(dl136-140)-V5 was observed by immunofluorescent staining with anti-V5 antibody.

tags do not influence the cellular localization of mutated STAT6 constructs. The cytoplasmic localization indicated a deficiency in nuclear import of both mutanted STAT6 proteins and amino acids 136-140 were important for both unphosphorylated and phosphorylated STAT6 nuclear import. To ensure that the mutants retain the functional characteristics of STAT6, tyrosine phosphorylation and DNA binding ability after IL-4 stimulation were tested with Western blotting and EMSA (Figure 19). Both of these mutanted STAT6 proteins were accurately tyrosine phosphorylated on tyrosine 641 upon IL-4 treatment. Lysates from STAT6(135-140A)-GFP expressing cells and IL-4 receptor GAS site as a probe were used for EMSA. STAT6(135-140A)-GFP formed complexes with the DNA probe in response to IL-4 treatment that migrated at a specific position and was abrogated by the addition of specific antibodies to STAT6, GFP or cold DNA probe. These results show that the internal deletion and substitution mutations did not disrupt STAT6 activation.

Classic NLS sequences, such as the SV40 large-T antigen NLS, are rich in basic residues and the basic amino acids are critical for its function. Although the sequence from amino acid 135 to 140, RRLQHR, of STAT6 does not look like a classical NLS, it contains three arginine residues. To evaluate the importance of specific residues in this region, each amino acid was mutated in the context of full-length STAT6. However, the protein containing individual point mutations behaved as wild-type STAT6 (Figure 20). These results indicated that the amino acids 136-140 are needed for STAT6 nuclear import, but they may function within the context of a larger conformational NLS.

Transcriptional regulation is the primary function of STAT6 in the nucleus. Therefore, the ability to get into the nucleus is critical for STAT6 to induce target gene expression. For this reason I evaluated the ability of mutanted STAT6 proteins to induce gene expression by using luciferase gene reporter assays. The promoter of the IL-4 receptor gene was used to drive expression of a luciferase reporter gene to test STAT6-dependent gene expression (120). Wild type and mutanted STAT6 proteins defective in nuclear localization, STAT6(dl136-140), or DNA binding, STAT6(KR) (see chapter 4-3 for detail), were tested for their competence to induce expression from the IL-4 receptor promoter. Transient transfection experiments clearly demonstrated the ability of wild-type STAT6 to induce the IL-4 receptor reporter in response to IL-4, whereas

A.

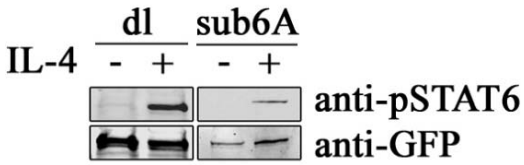

B.

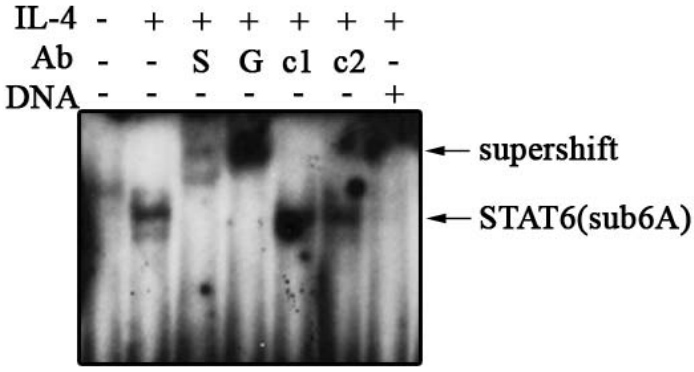

Figure 19: Characterization of STAT6(dl136-140)-GFP and STAT6(135-140A)-GFP.

A. STAT6(dl136-140)-GFP (dl) or STAT6(135-140A)-GFP (sub6A) expressing HeLa cells were untreated (-) or treated (+) with IL-4 for 30 minutes. Whole cell extracts were prepared and Western blot was performed with anti-phosphotyrosine STAT6, anti-STAT6 or anti-GFP antibodies.

B. EMSAs were performed with the radiolabeled DNA fragment corresponding to the IL-4 receptor alpha gene GAS site and protein lysates from STAT6(135-140A)-GFP expressing HeLa cells untreated or treated with IL-4. Effects of additions of antibodies (Ab) to the reaction to STAT6 (S), GFP (G), mouse control (c1) or rabbit control (c2), or 100-fold excess unlabeled oligonucleotide (DNA) are shown.

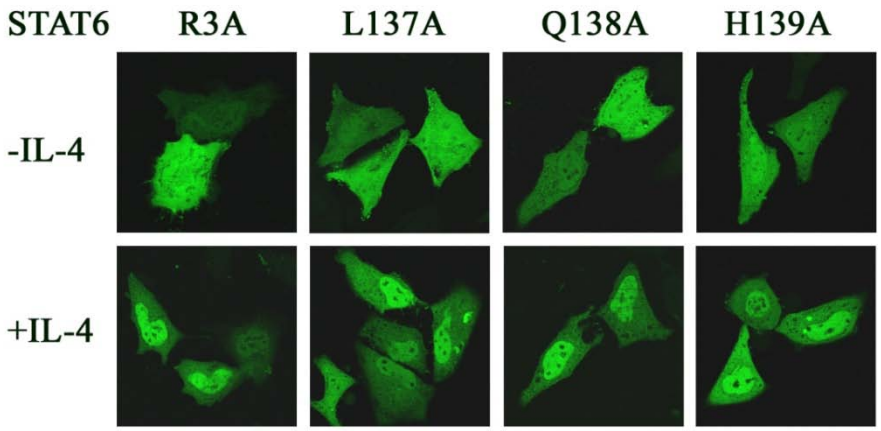

Figure 20: Effect of point mutants within amino acids 135-140 on STAT6 nuclear import.

Each amino acid within 135-160 (RRLQHR) was mutated to alanine separately to generate different mutanted STAT6 proteins, STAT6(R3A)-GFP, STAT6(L137A)-GFP, STAT6(Q138A)-GFP and STAT6(H139A)-GFP. Cellular localization of the mutanted STAT6 proteins was evaluated in HeLa cells that were serum starved (-IL-4) or stimulated with IL-4 (+IL-4) for 30 minutes.

STAT6(dl136-140) and STAT6(KR) did not induce the gene (Figure 21). It confirmed that STAT6(dl136-140) protein can be imported into the nucleus. The inability to be imported into the nucleus resulted in the inability to induce target gene expression by STAT6(dl136-140) even though it was tyrosine phosphorylated and able to bind DNA as demonstrated by Western blot and EMSA. These results demonstrated that both DNA binding ability and nuclear import are necessary for STAT6 to induce target gene expression in response IL-4 treatment.

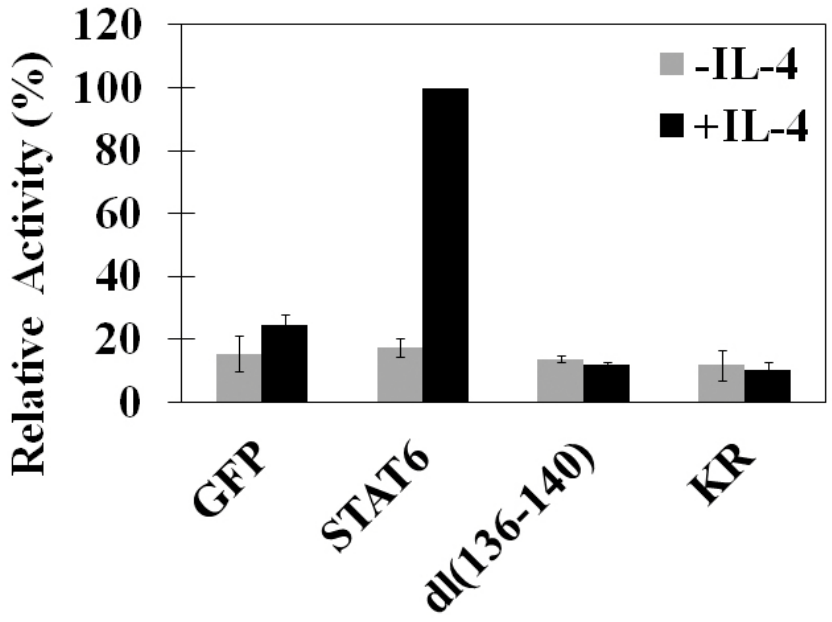

Figure 21: Nuclear import is important for STAT6 to induce gene transcription.

HeLa cells were transfected with IL-4R site-TKLuc reporter construct, pRL-null vector and different STAT6-GFP constructs. Cells were untreated or treated with hIL-4 for 8 hours before the dual-luciferase reporter assay. Luciferase activity was normalized to the Renilla luciferase value. The data shown are representative of more than three independent studies.

4. Evidence supporting a role of importin-α/β1 in STAT6 nuclear import

Active transport of large molecules through the nuclear pore complex is usually facilitated by carrier proteins of the karyopherin-β family. Importin-β1 is a primary karyopherin-β transporter that can bind directly to NLS-containing proteins, or indirectly via the family of importin-α adapters. Importin-α adapters bind directly to the NLS of cargo proteins. There are six characterized mammalian importin-α proteins and it is known that tyrosine-phosphorylated STAT1 binds to importin-α5 and STAT3 binds to importin-α3. To evaluate whether one or more of the importin–α proteins can recognize STAT6, *in vitro* binding assays were performed. Importin-α proteins contain an importin-β1 binding (IBB) domain at amino terminus. The IBB domain contains an NLS-like sequence which can interact with the Armadillo repeats and compete with NLS containing cargo for the same importin-α molecules. To eliminate the auto-inhibitory effect, the IBB domain was removed from full-length importin-α proteins. All importin-α proteins were produced as glutathione-S-transferase (GST) fusions and purified from bacteria.

STAT6 tagged with the V5 epitope (STAT6-V5) was expressed in mammalian cells and immunoprecipitated from cell lysates with V5 antibody and protein G agarose beads. The same amount of purified GST-tagged importin-α proteins was added to the STAT6-V5 immunocomplexes collected on beads. Interaction of importins with STAT6 was detected by Western blot with antibody to GST. As shown in Figure 22, STAT6 is recognized primarily by importin-α3 and importin-α6. Similar results were obtained with STAT6 isolated from untreated cells or IL-4 stimulated cells (data not shown), indicating binding is independent of tyrosine phosphorylation. Since importin-α6 is restricted to the testes, importin-α3 appears to be the primary import adapter (121, 122).

Since amino acids 136-140 in the coiled-coil region of STAT6 are critical for nuclear import, I determined whether this sequence was required for direct interaction with importin-α3. I expressed fragments of STAT6 tagged with maltose binding protein (MBP) in bacteria corresponding to STAT6 1-267a.a. (STAT6(1-267)) or 1-267a.a containing the 136-140a.a deletion (STAT6dl(136-140)). MBP-STAT6(1-267) and MBP-STAT6dl(136-140) were immobilized on amylose resin and incubated with bacterially-

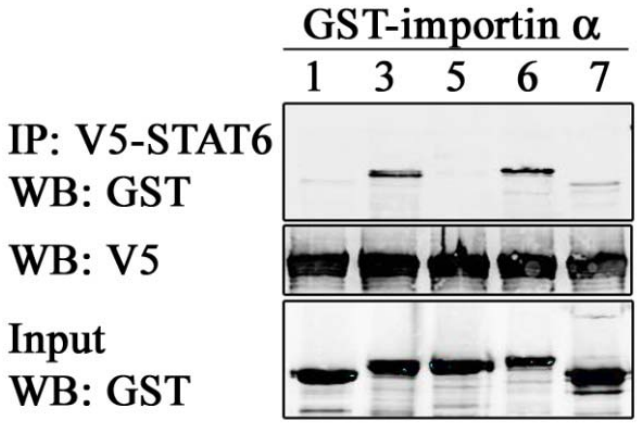

Figure 22: STAT6 binds to importin-α3 and importin-α6 *in vitro*.

Immunoprecipitated (IP) STAT6-V5 expressed in COS1 cells was collected on protein G beads and incubated *in vitro* with bacterially expressed GST-importins. (Numbers correspond to importin-α proteins.) Western blots (WB) identified bound importins (anti-GST), and STAT6-V5 (anti-V5). 10% of importin input is shown in bottom panel (anti-GST).

expressed GST-importin-α3 or GST-importin-α1 as a control. The binding was evaluated by Western blot with antibody to GST (Figure 23). Equal amounts of STAT6 proteins were bound to amylase resin as estimated from Ponceau S staining. The results showed STAT6(1-267) can bind importin-α3 specifically, but STAT6(1-267dl136-140) cannot. These data suggested that amino acids 136-140 are required for STAT6 binding to importin-α3 in *vitro* and nuclear import *in vivo*.

Classical NLSs are known to bind to the shallow grooves formed by ARM repeats 2 to 4 and 7 and 8 of importin-αs for nuclear import (95, 123-125), and the carboxy-terminal domain of importin-αs can be recognized by the export receptor, cellular apoptosis susceptibility protein (CAS). Previous studies showed that STAT3 binds to the central ARM region (ARM repeats 1-8) of importin-α3 (110). However, STAT1 is distinct from classical NLSs and STAT3 as it binds to the carboxyl terminus including ARM repeats 8-10 of importin-α5 (106). To determine whether STAT6 binds to the central ARM region or carboxy-terminal region of importin-α3, *in vitro* binding assays were performed. Bacterially-expressed MBP-STAT6(1-267) was immobilized on amylose resin and incubated with GST-importin-α1 or various GST-importin-α3 deletion proteins (Figure 24A). The result showed that STAT6(1-267) interacted with ARM repeats 1-8 (amino acids 53-366) of importin-α3 but not the amino acids 360-521. Various importin-α3 ARM repeat deletion mutants were evaluated and the data demonstrates that aa 234-305 (ARM repeats 5 and 6) of importin-α3 is required for STAT6 *in vitro* binding (Figure 24B).

Given that the importin-α/β1 system may mediate STAT6 nuclear import, I evaluated the effect of RNAi to inhibit expression of importin-β1 (Figure 25). Small interfering RNA (siRNA) duplexes corresponding to importin-β1 or to vimentin as a control were transfected into cells with STAT6-GFP, and the localization of STAT6-GFP was visualized microscopically. The control siRNA did not show any effect on STAT6-GFP localization. In contrast, the behavior of STAT6-GFP was notably different in the cells treated with importin-β1 siRNA. Approximately 10% of cells showed STAT6 restricted to the cytoplasmic compartment often with punctate cytoplasmic fluorescence. Since the siRNA may not completely inhibit importin-β1 expression in all cells

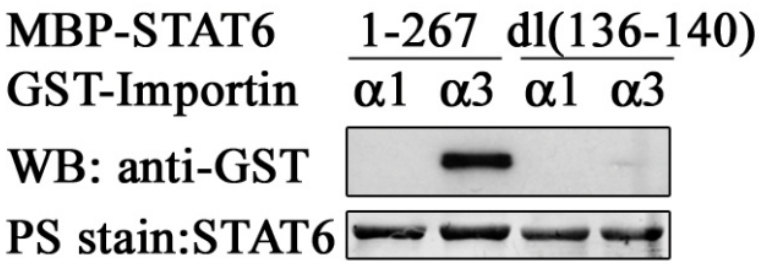

Figure 23: Amino acids 136-140 of STAT6 are required for importin-α3 binding.

Bacterial expressed MBP-STAT6(1-267) and MBP-STAT6(1-267dl136-140) were immobilized on amylase resin and incubated with purified GST-importin-α1 or GST-importin-α3. The binding was evaluated by Western blot with anti-GST antibody. Ponceau S (PS) staining showed the same amount of STAT6 proteins was used.

A.

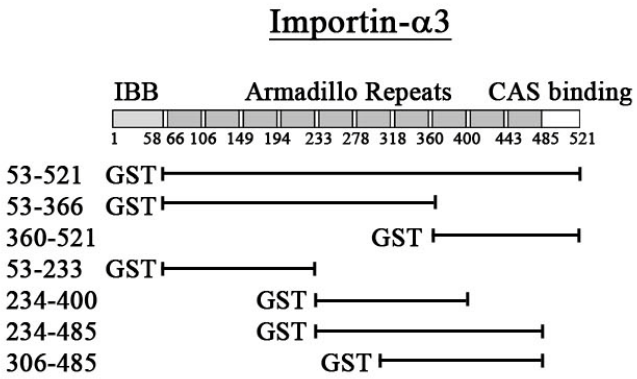

B.

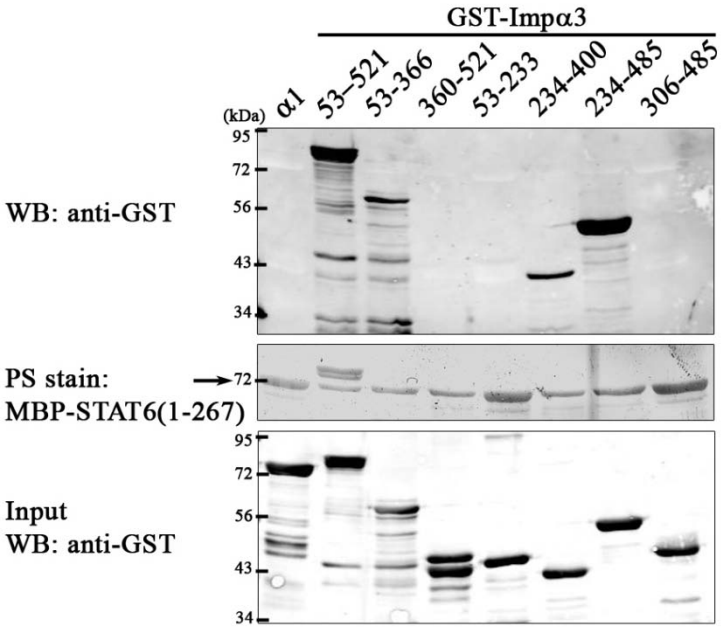

Figure 24: STAT6 interacted with Armadillo repeats 5 and 6 of importin-α3.

A. Linear diagram of importin-α3 functional domains and corresponding deletion mutations. Numbers indicate amino acids.

B. Bacterial expressed MBP-STAT6(1-267) was immobilized on amylase resin and incubated with purified GST-importin-α1 or various GST-importin-α3 truncated proteins. The binding was evaluated by Western blot with anti-GST antibody. Ponceau S (PS) staining showed the same amount of STAT6(1-267) protein was used 10% of importin input is shown in bottom panel (anti-GST).

A.

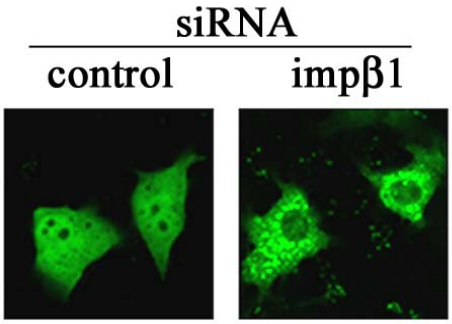

B.

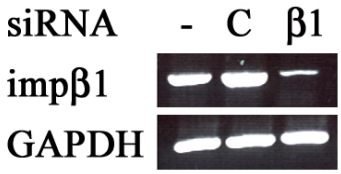

C.

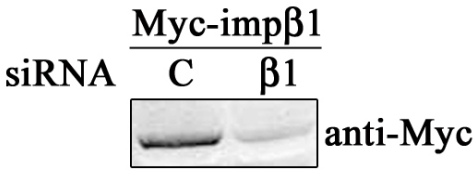

Figure 25: Inhibition of STAT6-GFP nuclear import with siRNA to importin-β1.

A. Fluorescent images of COSI cells transfected with vimentin siRNA (control) or importin-β1 siRNA (impβ1) for 24 hours followed by transfection with STAT6-GFP. Cytoplasmic localization of STAT6-GFP with importin-β1 siRNA transfection was seen in approximately 10% of GFP-positive cells.

B. The effect of control vimentin siRNA or importin-β1 siRNA on endogenous importin-β1 mRNA or GAPDH mRNA evaluated by RT-PCR.

C. The silencing effect of control vimentin siRNA or importin-β1 siRNA on overexpressed Myc-importin-β1 protein expression was evaluated by Western blot with anti-Myc antibody.

expressing STAT6-GFP, the effect appears significant. To evaluate the effectiveness of the importin-β1 siRNA complexes, mRNA levels in cells treated with control or importin-β1 siRNA were assayed by RT-PCR. The siRNA to importin-β1 reduced endogenous importin-β1 mRNA by approximately 70% (Figure 25B). In addition, the effect of knocking down protein expression by the siRNA was evaluated. Cells were transfected with control or importin-β1 siRNA and Myc-importin-β1 then protein expression was checked by Western blot with anti-Myc antibody. As shown in Figure 25C, importin-β1 siRNA but not control siRNA specifically reduced the Myc-importin-β1 protein expression. The results suggested that importin-α/importin-β1 mediated STAT6 nuclear import *in vivo*.

There are several reports that indicate Rac1 and a Rac GTPase-activating protein, MgcRacGAP, are required for tyrosine-phosphorylated STAT3 and STAT5 nuclear import (126-128). They showed that MgcRacGAP contains a nuclear localization signal and chaperones STATs into the nucleus. They reported that a dominant-negative mutant of Rac1, N17 Rac1, can prevent phoshorylated STAT3 and STAT5 from translocating to the nucleus. To test if Rac1 also plays a role in STAT6 nuclear transport, I tested the effect of N17 Rac1. GFP-tagged STAT6 was co-transfected with T7 tagged N17 Rac1 in HeLa cells and STAT6 protein localization was evaluated by fluorescence microscopy. The data showed that the dominant-negative mutant of Rac1, N17 Rac1, did not influence either unphosphorylated or phosphorylated STAT6 nuclear translocation (Figure 26). Results indicated that Rac1 and MgcRacGAP are not involved in STAT6 nuclear import.

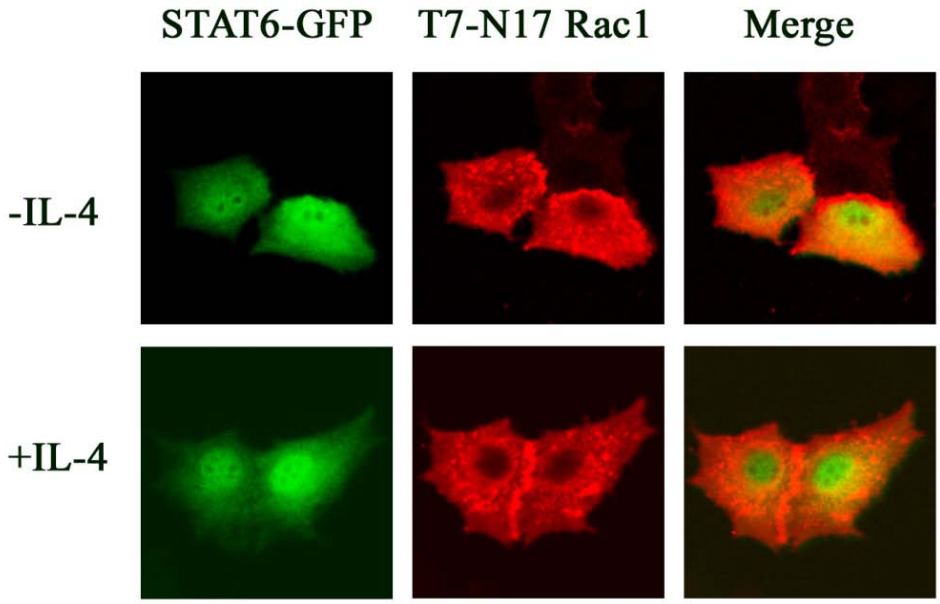

Figure 26: N17 Rac1 does not block nuclear import of STAT6.

HeLa cells were co-transfected with STAT6-GFP and T7 tagged N17 Rac1 and serum starved overnight. Cells were left untreated (-IL-4) or treated (+IL-4) with IL-4 for 30 minutes, fixed and stained by immunofluorescence with T7 primary antibody and TRITC-conjugated secondary antibody. Cellular localization of STAT6-GFP (green) and T7-N17 Rac1 (red) was visualized by microscopy.

Chapter 4

Characterization of STAT6 Nuclear Export

Abstract

Latent STAT6 is present both in the cytoplasm and the nucleus and accumulates in the nucleus after tyrosine phosphorylation. Nuclear localization of STAT6 is a result of a balance between nuclear import and nuclear export. In this chapter, nuclear export of STAT6 before and after tyrosine phosphorylation was studied.

Live cell imaging assays were used to demonstrate that STAT6 nuclear export is constitutive and independent of tyrosine phosphorylation. However, the nuclear export rate and mobility in the nucleus of tyrosine phosphorylated STAT6 were significantly slower than unphosphorylated STAT6. By using a STAT6 DNA binding mutant, it was found that the ability of STAT6 to bind DNA retained it in the nucleus, resulting in a decrease of nuclear export rate and increase in nuclear accumulation.

STAT6 showed nuclear accumulation with the Crm1 specific inhibitor, leptomycin B (LMB), but LMB did not completely block STAT6 nuclear export. Therefore STAT6 appears to have both Crm1-dependent and Crm1-independent export mechanisms.

Results

1. STAT6 nuclear export is constitutive.

After functioning in the nucleus, STAT6 is exported from the nucleus either to shut off signaling or to be reactivated. Cytoplasmic fluorescence loss in photobleaching (cFLIP) was used to address the basis of STAT6 nuclear export (Figure 27). A high-intensity laser beam was continually directed to a small region in the cytoplasm of cells expressing STAT6-GFP. The region was bleached every 12 seconds at maximum laser intensity for 50min. Any STAT6-GFP molecules passing through the laser path of this small region are bleached, and the loss of fluorescence correlates with STAT6 mobility. If STAT6 is mobile in the cytoplasm, the fluorescence in this compartment will decrease with time. Furthermore, if STAT6 can be exported out of the nucleus to the cytoplasm and move into the area of the laser, the fluorescence intensity in the nucleus will also decrease over time.

I tested the nuclear export of unphosphorylated STAT6-GFP in HeLa cells without any cytokine treatment using the cFLIP assay. Images were captured after each bleaching and representative time points were shown in Figure 28. Fluorescence intensity rapidly decreased in the entire cytoplasm within 5 minutes indicating rapid movement of STAT6 through the cytoplasm. For unphosphorylated STAT6-GFP, this loss was followed by a loss of fluorescence in the nucleus that was nearly complete by 50 min. The loss of nuclear fluorescence indicated continual STAT6 export from the nucleus and passage through the laser path in the cytoplasm.

To confirm that STAT6 nuclear export does not require tyrosine phosphorylation, nuclear export of the STAT6(RY)-GFP mutant was evaluated by cFLIP assay (Figure 29). A small region in cytoplasm of STAT6(RY)-GFP expressing HeLa cells was repetitively bleached which leaded to a dramatic loss of fluorescence in the cytoplasm within 5 minutes. In addition, the nuclear fluorescence disappeared within 50 minutes. The fluorescent loss pattern was similar to wild type unphosphorylated STAT6-GFP indicating that STAT6 nuclear export is constitutive and tyrosine-phosphorylation independent.

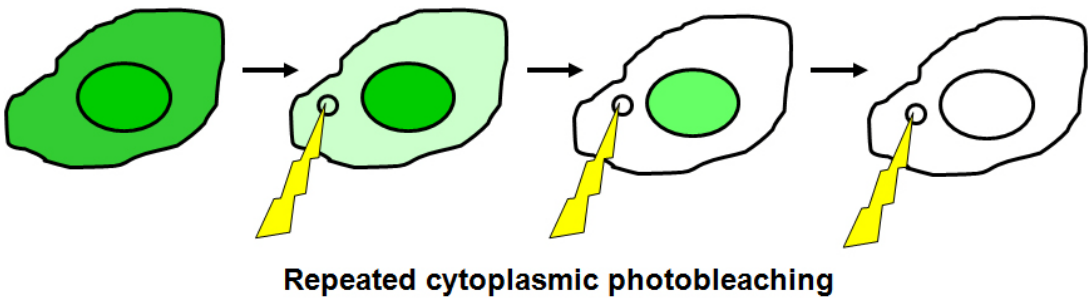

Figure 27: Cytoplasmic fluorescence loss in photobleaching (cFLIP)

In the fluorescently-tagged protein-expressing cells, a region in the cytoplasm is subjected to a continuous high intensity laser beam which bleaches fluorescent molecules passing through it. If the fluorescent molecules can be exported out of the nucleus, the fluorescence intensity will decrease with time. The fluorescence loss in the cytoplasm and nucleus is monitored and the loss correlates to the mobility of the fluorescent protein.

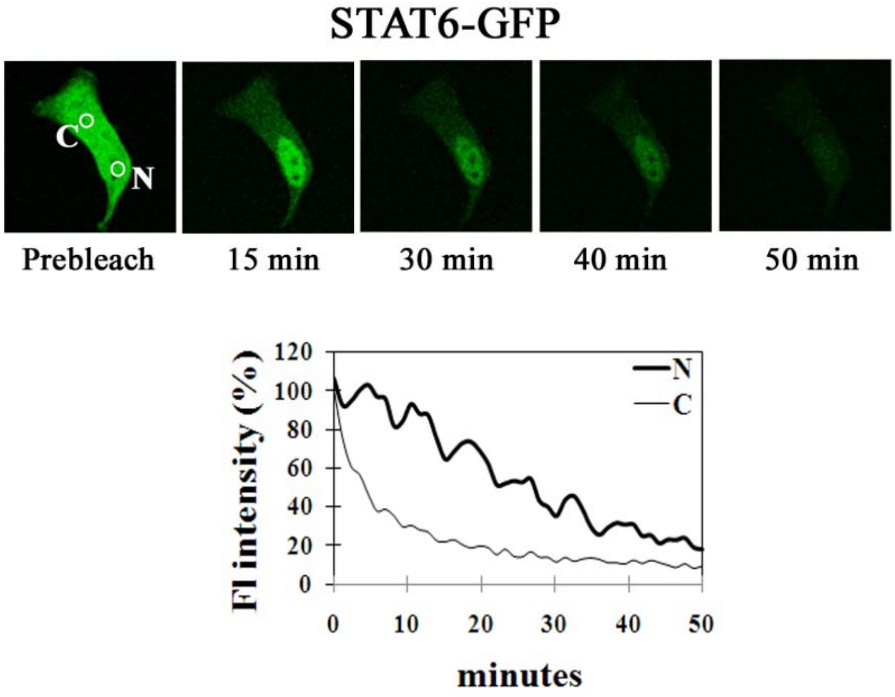

Figure 28: Cytoplasmic FLIP demonstrates constitutive nuclear export of STAT6.

Cytoplasmic FLIP assays were performed with HeLa cells expressing STAT6-GFP. A small region in the cytoplasm (C) was subjected to continuous high intensity laser. Fluorescence loss was monitored with time in the cytoplasm and compared to the fluorescence loss in a region of the nucleus (N). The quantitative data of relative fluorescence intensity (Fl) with time is shown in the lower panel. The results shown are representative of more than three independent studies.

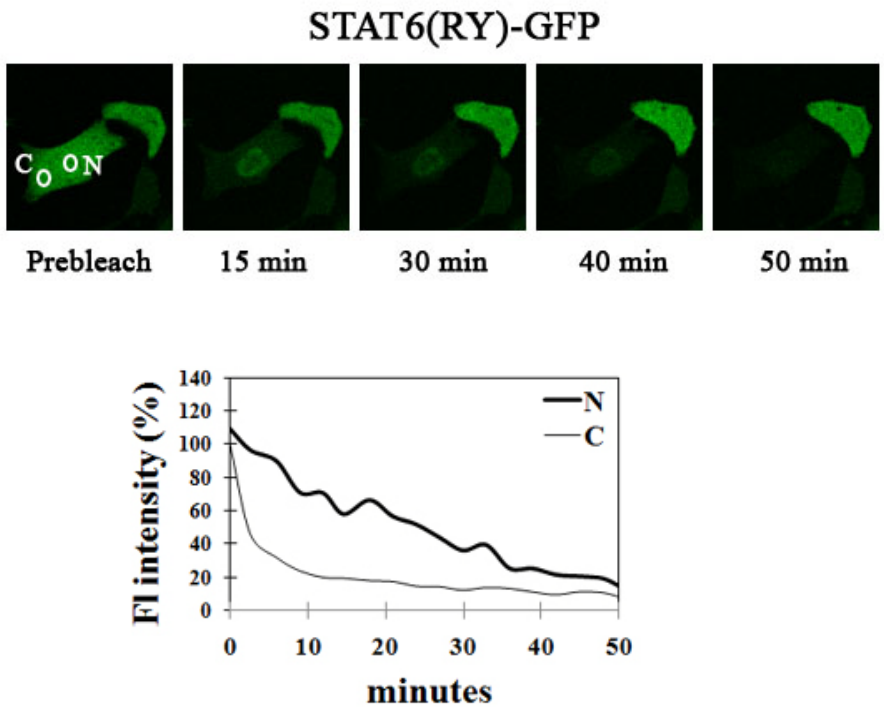

Figure 29: Tyrosine phosphorylation is not required for STAT6 nuclear export.

Cytoplasmic FLIP assay was performed with HeLa cells expressing STAT6(RY)-GFP in the presence of IL-4. A small region in the cytoplasm (C) was subjected to continuous high intensity laser. Fluorescence loss was monitored with time in the bleached area in the cytoplasm and in a region of the nucleus (N). Quantitative data of relative fluorescent intensity (Fl) with time is shown in the lower panel. The results shown are representative of more than three independent studies.

2. Tyrosine phosphorylated STAT6 shows decreased nuclear export and reduced mobility in the nucleus.

As described above in Figure 10 and Figure 11, IL-4 treatment resulted in STAT6 tyrosine phosphorylation and accumulation in the nucleus. The inability of STAT6(RY)-GFP to accumulate in the nucleus upon IL-4 stimulation suggested that tyrosine phosphorylation is required for the nuclear retention. To evaluate the relationship between tyrosine phosphorylation and nuclear accumulation, I treated STAT6-GFP-expressing HeLa cells with IL-4 for various periods of time and checked STAT tyrosine phosphorylation by Western blot and protein localization by fluorescence microscopy (Figure 30). After 15 minutes of IL-4 addition, tyrosine phosphorylation of STAT6 was detected and STAT6 remained phosphorylated for as long as 6 hours. The kinetics of increased STAT6 nuclear accumulation was similar to the kinetics of tyrosine phosphorylation. At 15 minutes, STAT6 started to show increased nuclear localization and this continued for as long as 6 hours after IL-4 treatment. The data confirmed that tyrosine phosphorylation correlates with the nuclear accumulation in response to IL-4 treatment and suggested that nuclear accumulation of STAT6 requires tyrosine phosphorylation.

To evaluate nuclear export of tyrosine-phosphorylated STAT6, cFLIP was performed using STAT6-GFP expressing HeLa cells in the presence of IL-4. Cytoplasmic fluorescence decreased rapidly within 5 minutes indicating rapid movement of STAT6 through the cytoplasm. In contrast to unphosphorylated STAT6, nuclear fluorescence intensity of phosphorylated STAT6 only showed a minor decrease during the 50-minute duration of cytoplasmic photobleaching (Figure 31). The results demonstrate that STAT6 in the presence of IL-4 stimulation is exported much slower. It suggests that the nuclear accumulation that is evident after STAT6 tyrosine phosphorylation is due to a decrease in nuclear export.

By comparing the cFLIP results with unphosphorylated STAT6 and tyrosine phosphorylated STAT6 (Figure 28 and Figure 31), the STAT6 nuclear export rate was dramatically decreased following IL-4 stimulation. The decrease might be due to the slower mobility of phosphorylated STAT6 in the nucleus. If this is the case, the mobility of tyrosine-phosphorylated STAT6 within the nucleus would be expected to be slower

A.

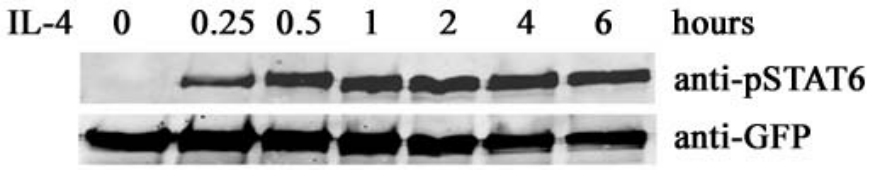

B.

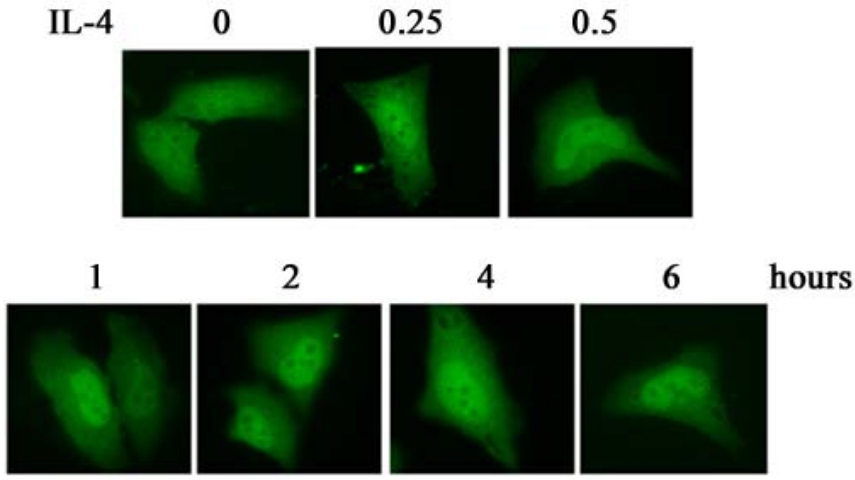

Figure 30: Tyrosine phosphorylation kinetics and cellular localization of STAT6-GFP with IL-4 treatment.

HeLa cells expressing STAT6-GFP were treated with IL-4 for various periods of time.

A. Cell extracts were prepared and a Western blot was performed with anti-phosphotyrosine STAT6 and anti-GFP antibodies.
B. The STAT6-GFP cellular localization imagings were evaluated at indicated time points by confocal microscopy.

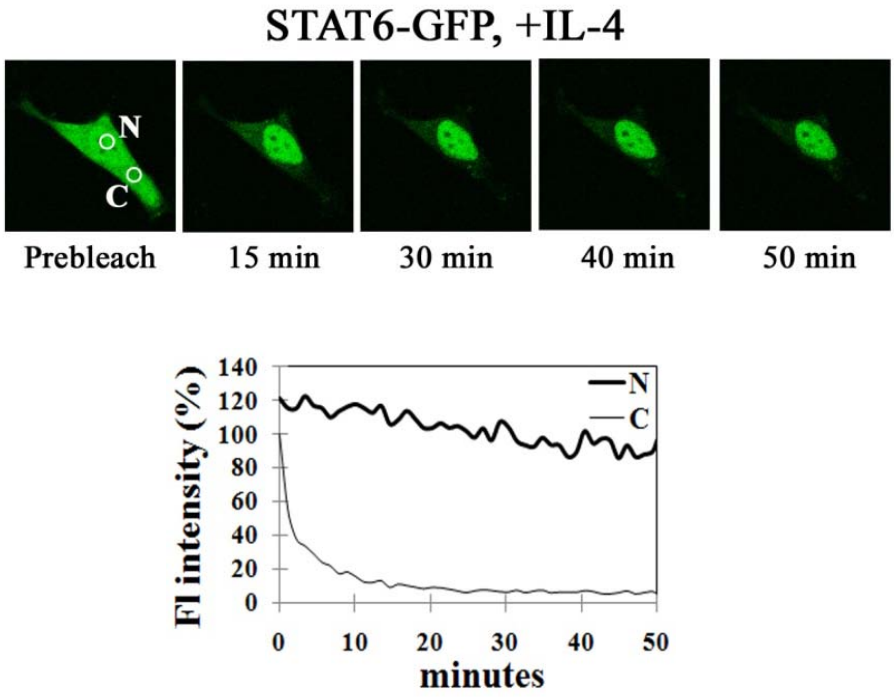

Figure 31: Cytoplasmic FLIP demonstrates decreased STAT6 nuclear export following tyrosine phosphorylation.

Cytoplasmic FLIP assays were performed with HeLa cells expressing STAT6-GFP treated with IL-4. A small region in the cytoplasm (C) was subjected to continuous high intensity laser. Fluorescence loss was monitored with time in the cytoplasm and compared to the fluorescence loss in a region of the nucleus (N). The quantitative data of relative fluorescence intensity (Fl) with time is shown in the lower panel. The results shown are representative of more than three independent studies.

than unphosphorylated STAT6. To evaluate STAT6 mobility in the nucleus, a nuclear FLIP (nFLIP) assay was used (Figure 32). A small region (region 1) in the nucleus of HeLa cells expressing STAT6-GFP, with or without IL-4 stimulation, was subjected to continuous laser bleaching every 12 seconds for total 5 minutes. The fluorescence intensity of region 1 was compared with a distinct region in the nucleus (region 2). If the fluorescent molecules move rapidly through the path of the laser, the fluorescence intensity in region 2 will decrease similarly to region 1, along with the entire nucleus. In contrast, if the fluorescent molecules have a slowed mobility in the nucleus, the fluorescence intensity decrease in region 2 will be slower than it is in region 1.

Without IL-4 treatment, the high mobility of unphosphorylated STAT6 in the nucleus during nFLIP was apparent with a similar decrease in fluorescence intensity in region 1 and region 2 (Figure 33). However, following tyrosine phosphorylation in response to IL-4, STAT6 showed significantly slower movement in the nucleus. The decrease in fluorescence intensity in region 2 and the remainder of the nucleus was delayed considerably compared with region 1 (Figure 34).

In order to compare the mobility rate of unphosphorylated and tyrosine phosphorylated STAT6 in the nucleus, I used a nuclear strip FRAP assay. A strip region in the nucleus of HeLa cells expressing STAT6-GFP without or with IL-4 stimulation was subjected to high intensity laser for 0.25 seconds. The fluorescent molecules in this strip area were photobleached and fluorescence recovery in this area was measured every 0.25 second for 10 seconds (Figure 35). Similar to the nFLIP results, unphosphorylated STAT6 moved fast in the nucleus as the recovery of fluorescence in the strip area was almost complete within 2 seconds, whereas phosphorylated STAT6 mobility was slower as the recovery of fluorescence took nearly twice as long. To quantify and compare the mobility of unphosphorylated and phosphorylated STAT6 in the nucleus, the average half time of fluorescence recovery in the bleached region of nine independent experiments was calculated by curve fitting analyses. A faster fluorescence recovery indicates faster mobility within the nucleus. The recovery half time of phosphorylated STAT6 was about 0.7751 seconds and 0.4659 seconds for unphosphorylated STAT6. Therefore, it can be concluded that STAT6 moves more slowly after tyrosine phosphorylation and the slower mobility results in a decreased nuclear export rate.

A.

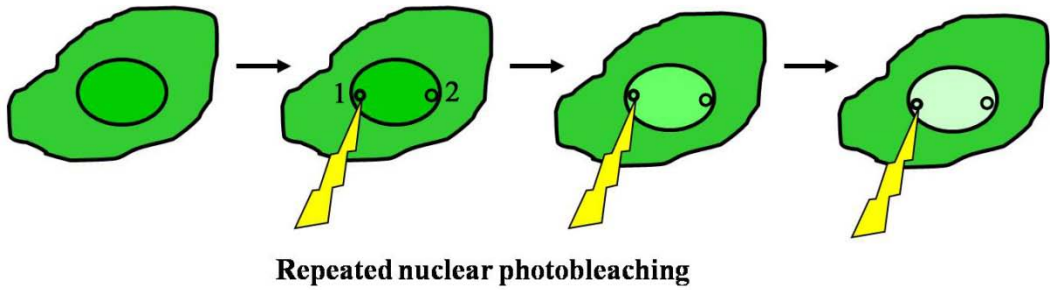

B.

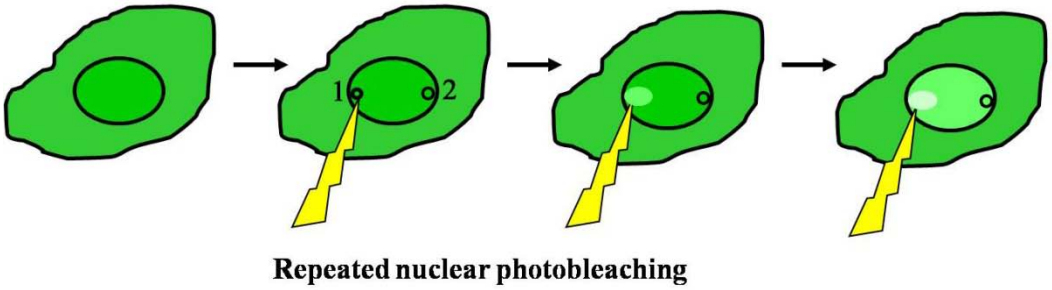

Figure 32: Nuclear fluorescence loss in photobleaching (nFLIP)

Cells expressing a fluorescent tagged protein are subjected to a continuous high intensity laser beam in a region (1) in the nucleus.

A. If the fluorescent molecules have high mobility in the nucleus, the fluorescence intensity will decrease quickly throughout the nucleus. Therefore, the decrease of fluorescence intensity in region1 and 2 will be similar.
B. If the fluorescent molecules have slow mobility in the nucleus, the fluorescence intensity decrease in region 2 will be slower and primarily restricted to the bleached area, region 1.

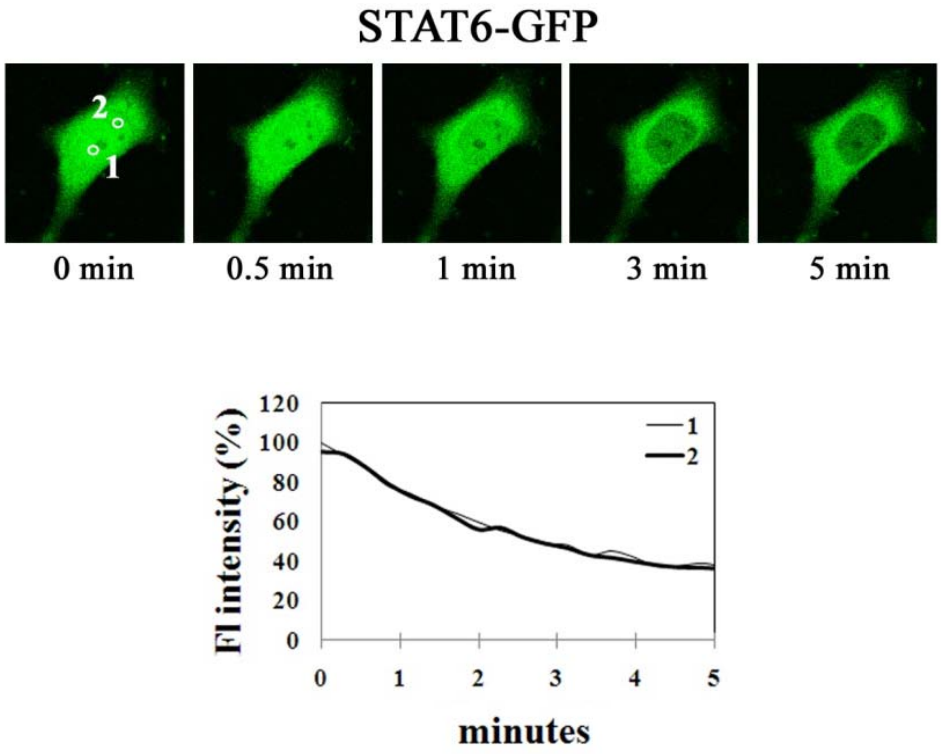

Figure 33: Nuclear FLIP reveals fast STAT6 nuclear mobility in the absence of cytokines.

Live cell imaging was used with nuclear FLIP to evaluate STAT6-GFP mobility within the nucleus. A small region in the nucleus (region 1) of STAT6-GFP expressing HeLa cells in the absence of IL-4 was subjected to continuous high intensity laser. Fluorescence loss was monitored with time in this region and a distinct region in the nucleus (region 2). The quantitative data of relative fluorescent intensity (Fl) with time in the region 1 and region 2 is shown in the lower panel. The results shown are representative of more than three independent studies.

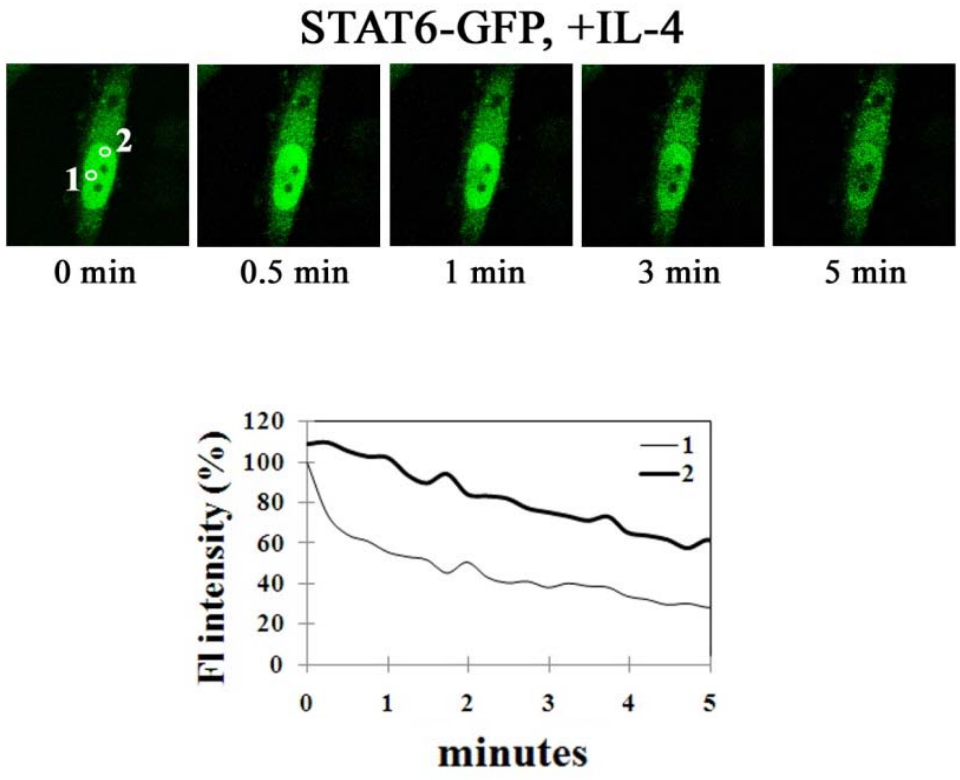

Figure 34: Nuclear FLIP reveals decreased STAT6 nuclear mobility following tyrosine phosphorylation.

Live cell imaging was used with nuclear FLIP to evaluate phosphorylated STAT6-GFP mobility within the nucleus. A small region in the nucleus (region 1) of STAT6-GFP expressing HeLa cells in the presence of IL-4 was subjected to continuous high intensity laser. Fluorescence loss was monitored with time in this region and a distinct region in the nucleus (region 2). The quantitative data of relative fluorescent intensity (Fl) with time in the region 1 and region 2 is shown in the lower panel. The results shown are representative of more than three independent studies.

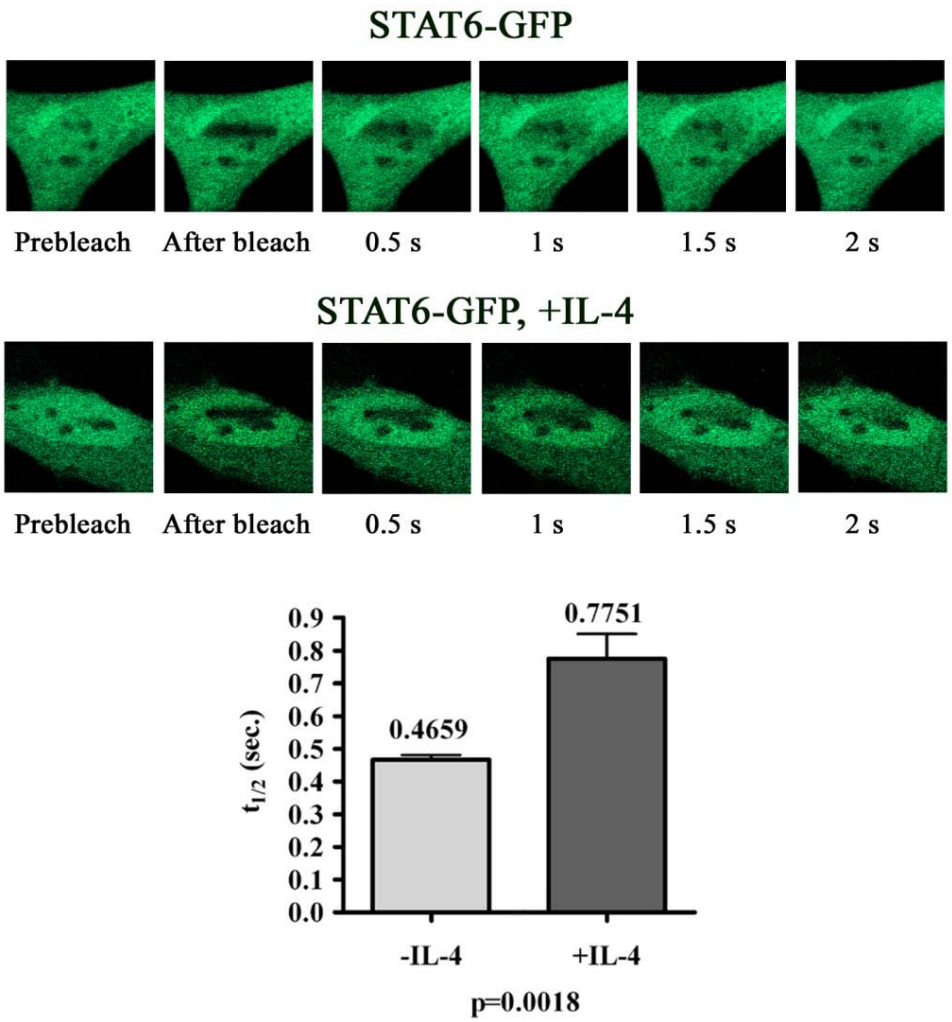

Figure 35: Live cell imaging was used with a nuclear strip FRAP to evaluate STAT6-GFP mobility within the nucleus.

A strip region in the nucleus of untreated HeLa cells (STAT6-GFP) or IL-4 treated cells (STAT6-GFP, +IL-4) expressing STAT6-GFP was subjected to a laser at 488 nm for 0.25 second and subsequent fluorescence recovery was monitored in this region. The fluorescence intensity was quantified and the average half time of fluorescence recovery in the bleached region of nine independent experiments was calculated.

3. DNA binding retains tyrosine phosphorylated STAT6 in the nucleus.

The previous results showed that tyrosine phosphorylation is critical for STAT6 nuclear accumulation in the nucleus following IL-4 treatment. Tyrosine phosphorylation activates STAT proteins by promoting the formation of dimers that have the ability to bind specific DNA target sites. To determine whether the increased nuclear accumulation of STAT6 seen following tyrosine phosphorylation was due to a gain in the ability to bind DNA, the behavior of a DNA binding mutant, STAT6(KR)-GFP, was evaluated. This mutated STAT6 protein was generated based on a STAT5a DNA binding mutant in which a motif rich in basic amino acids in the DNA binding domain was mutated and these basic residues were replaced by alanine residues (111). By comparing the sequence in the DNA binding domain, STAT6 was also found to contain a region rich in basic amino acids. Lysines and arginines within aa 366–374 (366KKIKKRCERK374) were substituted with alanines to generate STAT6(KR). The tyrosine phosphorylation and DNA binding ability of this STAT6(KR) mutant were evaluated by Western blot with antibodies specific to the phosphotyrosine of STAT6 and EMSA. Although the STAT6(KR) mutant was accurately tyrosine phosphorylated in response to IL-4, it did not bind target DNA sequences (Figure 36A and B). Microscopic imaging indicated that STAT6(KR) was imported to the nucleus with and without IL-4 stimulation, but it did not accumulate in the nucleus in response to IL-4 (Figure 36C). This indicated that DNA binding contributes to nuclear accumulation following tyrosine phosphorylation.

Since the STAT6(KR) mutant can not accumulate in the nucleus in response to IL-4 treatment, the nuclear export rate of STAT6(KR) is expected to be similar to unphosphorylated STAT6. To determine if the DNA-binding mutant is not retained in the nucleus following IL-4 stimulation, imaging with cytoplasmic FLIP was used as shown in Figure 37. The export kinetics of tyrosine phosphorylated STAT6(KR) were similar to unphosphorylated wild-type STAT6 (wtSTAT6). The cytoplasmic fluorescence dramatically decreased within 5 minutes and by 50 minutes the fluorescence intensity in the nucleus was also almost undetectable.

In addition, if DNA binding retains STAT6 in the nucleus, the mobility of tyrosine phosphorylated STAT6(KR) within the nucleus would be expected to be similar to unphosphorylated STAT6. A nuclear FLIP assay was used to investigate this

A.

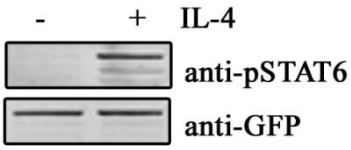

B.

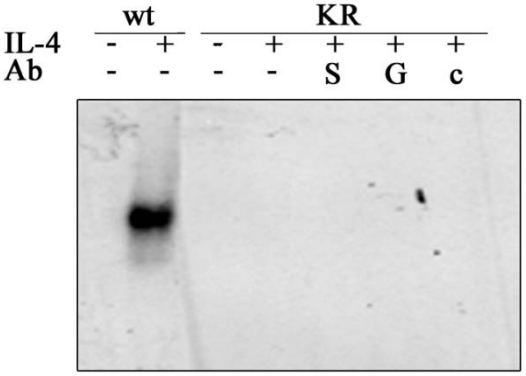

C.

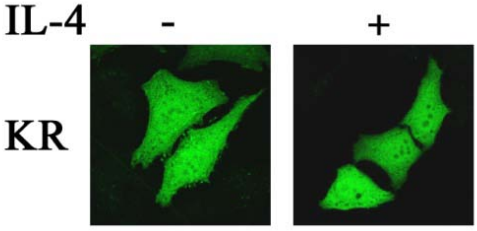

Figure 36: Characterization of STAT6 DNA binding mutant, STAT6(KR)-GFP.

The DNA binding mutant STAT6(KR)-GFP was expressed in cells and untreated (-) or treated (+) with IL-4 for 30 minutes.

A. Western blot of STAT6(KR)-GFP-expressing cell lysate was performed with anti-phosphotyrosine 641 STAT6 (anti-pSTAT6) or anti-GFP antibodies.
B. EMSA was performed with the radiolabeled DNA fragment corresponding to the IL-4 receptor alpha gene GAS site and lysates from cells expressing STAT6-GFP (wt) or STAT6(KR)-GFP (KR) without (-) or with (+) IL-4 treatment. Antibodies to STAT6 (S), GFP (G), or MOPC (c) were added to the binding reactions.
C. Confocal microscopy of cells expressing STAT6(KR)-GFP in the presence and absence of IL-4.

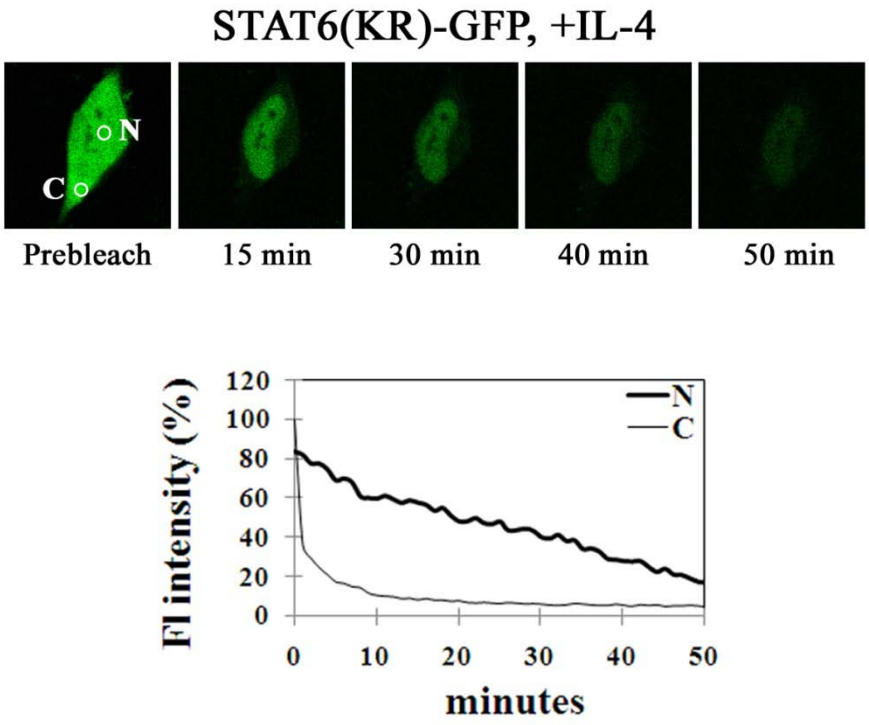

Figure 37: DNA binding ability is required for nuclear accumulation of tyrosine phosphorylated STAT6.

Cytoplasmic FLIP assay was performed with HeLa cells expressing STAT6(KR)-GFP in the presence of IL-4. A small region in the cytoplasm (C) was subjected to continuous high intensity laser. Fluorescence loss was monitored with time in the bleached area in the cytoplasm and in a region of the nucleus (N). Quantitative data of relative fluorescent intensity (Fl) with time is shown in the lower panel. The results shown are representative of more than three independent studies.

possibility. The tyrosine phosphorylated DNA-binding mutant, STAT6(KR), showed the same rapid nuclear movement as unphosphorylated STAT6 in the nucleus (Figure 38). In contrast to phosphorylated wild-type STAT6 which showed slower mobility, STAT6(KR) still showed fast mobility in the nucleus even after tyrosine phosphorylation. Together, the results supported the premise that STAT6 accumulates in the nucleus only if it has a functional DNA-binding domain.

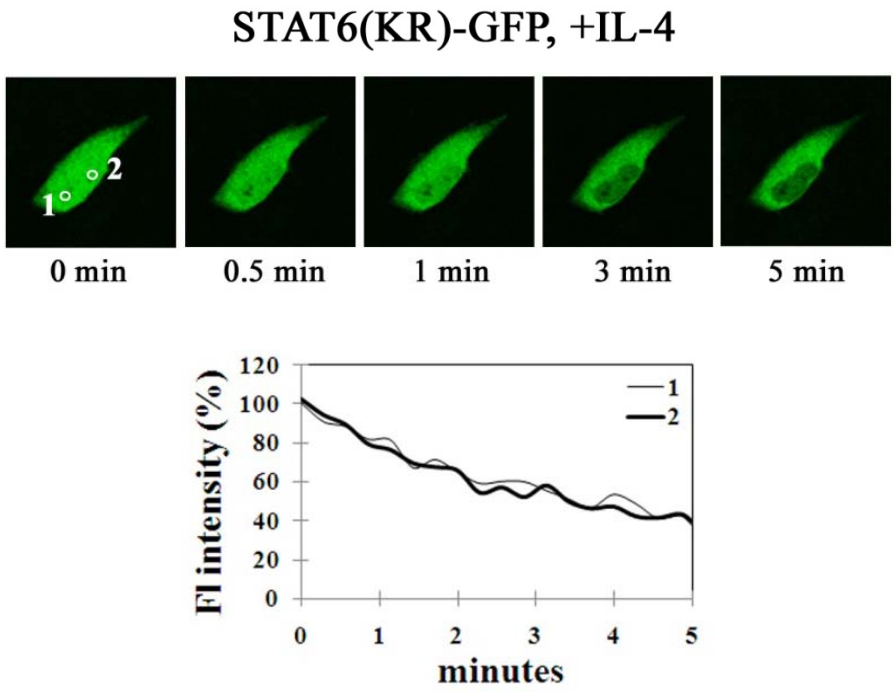

Figure 38: Phosphorylated STAT6 DNA-binding mutant showed the same mobility in the nucleus as unphosphorylated STAT6.

Nuclear FLIP was used to evaluate STAT6(KR)-GFP mobility within the nucleus with IL-4 treatment. A small region in the nucleus (region 1) was subjected to continuous high intensity laser. Fluorescence loss was monitored with time in this region and a distinct region in the nucleus (region 2). Quantitative data of relative fluorescent intensity (Fl) with time is shown in the lower panel. The results shown are representative of more than three independent studies.

4. **STAT6 nuclear export is mediated by both Crm1-dependent and independent pathways.**

Like nuclear import, only molecules smaller than 50 kDa can freely diffuse back to the cytoplasm from the nucleus. Therefore, STAT6 needs carrier proteins for nuclear export. Crm1, also known as exportin 1, is known to mediate nuclear export of many proteins including STAT1 (115). The antibiotic LMB which inhibits Crm1 provides a useful tool to study Crm1-mediated nuclear export. In order to investigate if Crm1 plays a role in unphosphorylated STAT6 nuclear export, STAT6-GFP expressing HeLa cells were treated with LMB and a protein synthesis inhibitor, cycloheximide, for various periods of time. To follow the dynamic distribution of STAT6, STAT6-GFP localization was evaluated by fluorescence microscopy. The data shown in Figure 39 indicated that in the presence of LMB, STAT6 export was partially inhibited. STAT6 showed more nuclear localization by 15 minutes of LMB treatment and significant nuclear accumulation was observed by 30 minutes. The nuclear accumulation after LMB treatment suggested that Crm1 played a role in STAT6 nuclear export. In addition, the redistribution of STAT6 after LMB removal was also evaluated. LMB was added for 30 minutes then removed and STAT6-GFP localization was evaluated with time-lapse after LMB removal (Figure 40). STAT6 accumulated in the nucleus following 30 minutes of LMB treatment. After LMB withdrawal, STAT6 redistributed completely by 4 hours. The results suggested that although LMB is an irreversible Crm1 inhibitor, Crm1 protein still can bind to STAT6 and export it into the cytoplasm after LMB removal.

Studies show that STAT6 can be dephosphorylated by phosphatases in the nucleus (117). In order to evaluate whether Crm1 mediates the export of STAT6, I compared the redistribution of nucler STAT6 to the cytoplasm in STAT6-GFP expressing HeLa cells which were treated with IL-4 for 30 minutes followed by IL-4 removal. Cells were also untreated or treated with LMB. STAT6-GFP protein localization and tyrosine phosphorylation were assayed by fluorescence microscopy and Western blotting. In Figure 41 , IL-4 was removed after 30 minutes of treatment and cell lysates were collected at various time points. With IL-4 treatment, STAT6 accumulated in the nucleus, consistant with previous results. Following IL-4 withdrawal, STAT6 showed significantly less nuclear localization by 2 hours. By 4 hours, the distribution of STAT6

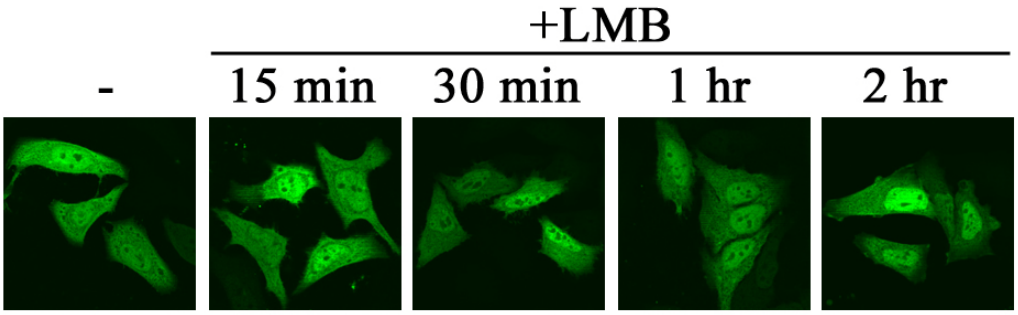

Figure 39: Leptomycin B partially inhibits STAT6 nuclear export.

STAT6-GFP expressing HeLa cells were treated with LMB for various periods of time. The cellular images were evaluated at indicated time points by confocal microscopy.

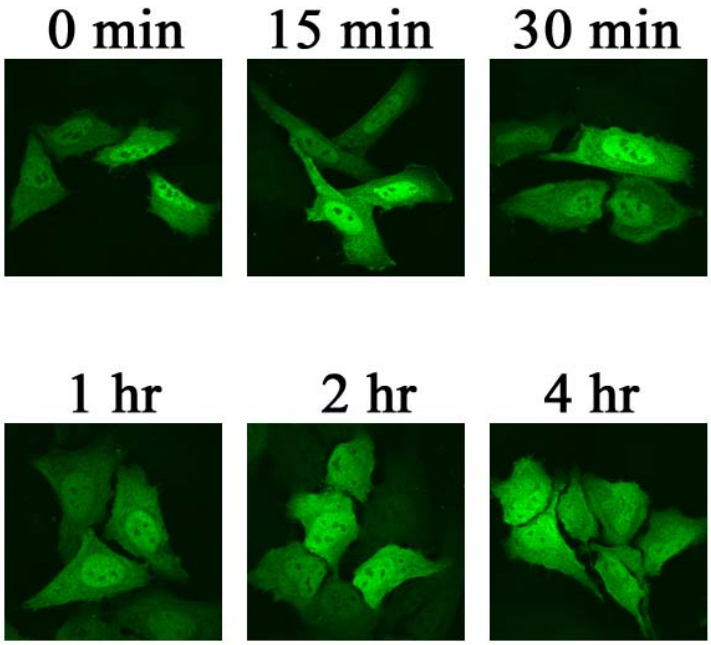

Figure 40: STAT6 redistributes to the cytoplasm after LMB removal.

STAT6-GFP-expressing HeLa cells were treated with LMB for 30 minutes. The LMB was then removed and cellular localization was evaluated after LMB removal at indicated time points by confocal microscopy.

A.

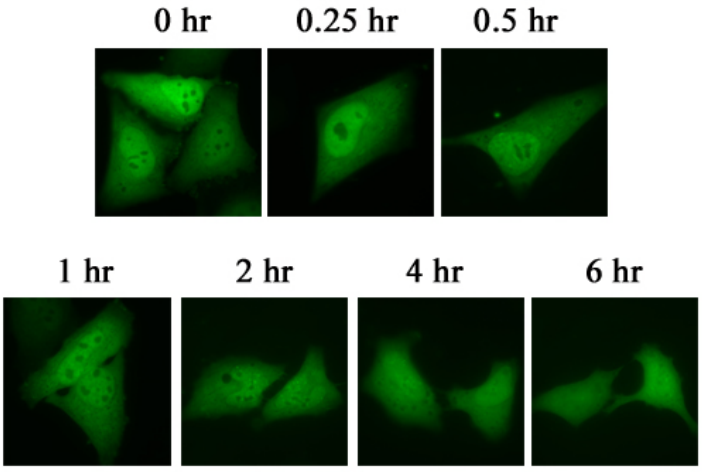

B.

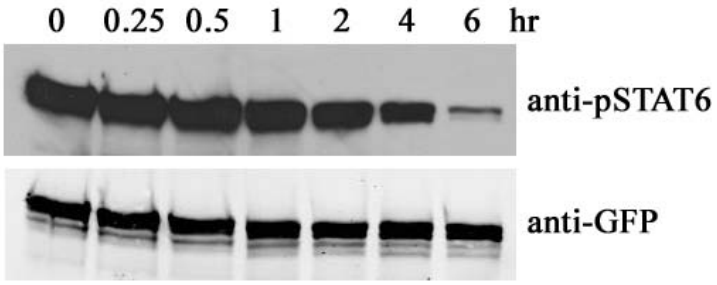

Figure 41: Cellular localization and tyrosine phosphorylation kinetics of STAT6-GFP after IL-4 removal.

HeLa cells expressing STAT6-GFP were treated with IL-4 for 30 minutes then IL-4 was removed.

A. The STAT6-GFP cellular localization images were evaluated at the indicated time points after IL-4 removal by confocal microscopy.
B. Cell extracts were prepared and Western blots were performed with anti-phosphotyrosine STAT6 or anti-GFP antibodies.

was similar to unphosphorylated STAT6. The Western blot result showed that STAT6 remained phosphorylated for 2 hours and then showed a reduction at 4 hours. By 6 hours, the amount of phosphorylated STAT6 was significant decreased. Thus, STAT6 is dephosphorylated after IL-4 withdrawal. This suggested that the relocaliztion of STAT6 back to the cytoplasm was correlated with dephosphorylation.

As shown in Figure 42, cells in the continued presence of LMB after IL-4 removal had more nuclear STAT6 until about 6 hours. This extended time of nuclear accumulation might be caused by either an inhibition of nuclear export or a delay of STAT6 dephosphorylation. To evaluate if dephosphorylation of STAT6 was delayed by LMB treatment, the cell lysates at each time point were collected and assayed by Western bloting. The dephosphorylation pattern was similar to the results in the absence of LMB. By 6 hours, a very low level of phosphorylated STAT6 remained. The results demonstrated that LMB treatment did not influence STAT6 dephosphorylation. Therefore, the retention of STAT6 in the nucleus is due to the inhibition of nuclear export by LMB and Crm1 plays a role in the nuclear export of dephosphorylated STAT6.

To evaluate the role of Crm1 on the nuclear export of STAT6 in living cells, STAT6-GFP expressing HeLa cells were subjected to cFLIP in the presence of LMB for 50 minutes (Figure 43). The fluorescence in the cytoplasm dramatically decreased within 5 minutes. Unexpectedly, LMB did not completely block nuclear export. Significant detectable nuclear fluorescence remained by 50 minutes. Comparing these results to the export rate of STAT6-GFP in cells not treated with LMB (Figure 28), there was only a partial inhibition by 50 minutes. These results suggested that STAT6 nuclear export was only partially blocked by LMB and there might be other exportins that can mediate STAT6 nuclear export.

A.

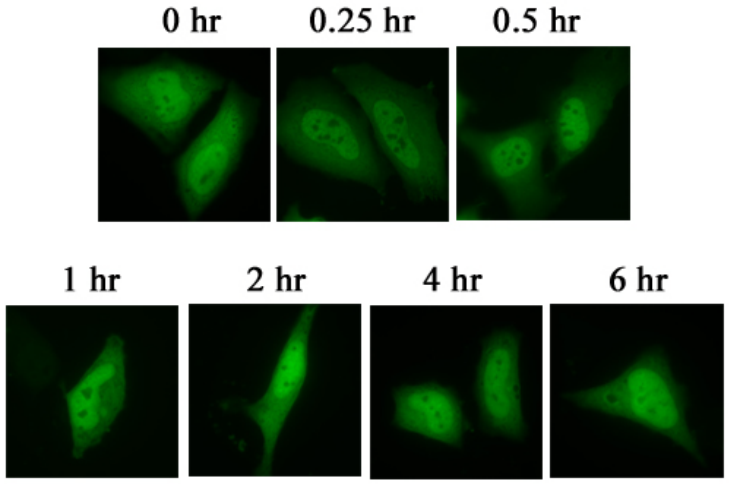

B.

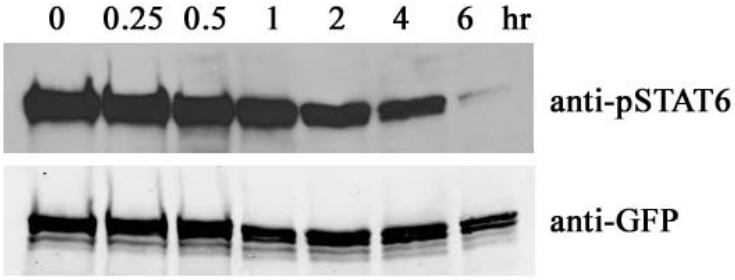

Figure 42: Cellular localization and tyrosine phosphorylation kinetics of STAT6-GFP in the presence of LMB after IL-4 removal.

HeLa cells expressing STAT6-GFP were treated with IL-4 for 30 minutes. Then IL-4 was removed but LMB treatment continued.

A. The STAT6-GFP cellular localization images were evaluated at the indicated time points after IL-4 removal by confocal microscopy.
B. Cell extracts were prepared and Western blots were performed with anti-phosphotyrosine STAT6 or anti-GFP antibodies.

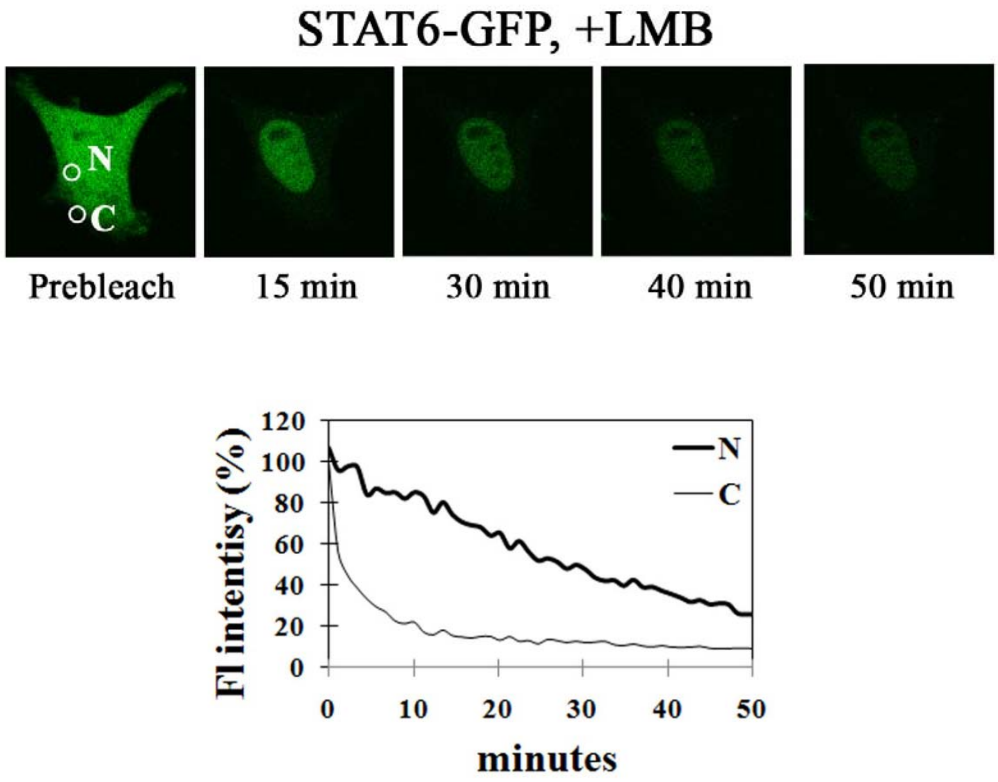

Figure 43: Leptomycin B does not completely inhibit STAT6 nuclear export.

Cytoplasmic FLIP assays were performed with HeLa cells expressing STAT6-GFP treated with LMB. A small region in the cytoplasm (C) was subjected to continuous high intensity laser. Fluorescence loss was monitored with time in the cytoplasm and compared to the fluorescence loss in a region of the nucleus (N). The quantitative data of relative fluorescent intensity (Fl) with time is shown in the lower panel. The results shown are representative of more than three independent studies.

Chapter 5

Discussion

Nuclear trafficking of STAT6 is integral to its function as a signal transducer and activator of transcription. An understanding of how STAT6 is transported into and out of the nucleus may allow the design of small molecules that interrupt STAT6 nucleocytoplasmic transport and STAT6 activity in the nucleus. To study STAT6 intracellular dynamics with microscopy in real time, I attached a fluorescent probe, GFP, to STAT6. The advantage of live cell imaging is that it avoids fixation techniques that can influence cellular architecture. Cell fractionation has been used to evaluate cellular localization; however, the technique is limited in interpreting *in vivo* protein localization, particularly if the protein is actively imported and exported from the nucleus. Live cell imaging with photobleaching techniques provides more quantitative and temporal measure of protein mobility and localization (129-131) Therefore, I used live cell imaging assays, FRAP and FLIP, to study the nuclear import and export behavior of STAT6 in the absence and presence of IL-4.

The steady state localization of endogenous STAT6 was evaluated both in non-lymphocytic and lymphocytic cells. All results showed that STAT6 is both cytoplasmic and nuclear presence in a latent state and following tyrosine phosphorylation induced by IL-4 treatment it accumulates in the nucleus (Figure 8 and Figure 9). STAT6 has important functions in lymphocytes but because they have a low transfection effiency, we evaluated localization of STAT6 primarily in non-lymphocytic cells. GFP-tagged STAT6 showed the same cellular localization, tyrosine phosphorylation and DNA binding ability as endogenous STAT6 which confirmed that the tags did not affect the biological characteristics of STAT6 (Figure 10 and Figure 11).

STAT6 nuclear import is constitutive

Two recent papers showed that STAT3 is detected within mitochondria and that STAT3 regulates a metabolic function in mitochondria supporting Ras-dependent malignant transformation (132, 133). For this reason, I investigated whether STAT6 is also located in the mitochondria. STAT6-GFP expressing HeLa cells were stained with MitoTracker orange CMTMRos probe for 1 hour to label mitochondria. Co-localizaiton of GFP tagged protein with mitochondria was evaluated by microscopy. The results showed that STAT6-GFP was excluded from mitochondria (data not shown). It indicated that STAT6 is not localized in mitochondria.

STAT proteins contain similar domain structures and initially were expected to have the same cellular localization as STAT1. STAT1 is predominantly in the cytoplasm in a latent state and accumulates in the nucleus after tyrosine phosphorylation. But studies have demonstrated that STAT3, STAT5 and now STAT6 can be imported to the nucleus independent of tyrosine phosphorylation. In order to evaluate the nuclear import of unphosphorylated STAT6, a nuclear FRAP assay was performed. I subjected the nucleus with high intensity laser to bleach the fluorescent molecules and monitored the fluorescent recovery in the nucleus with time. Since the bleach is irreversible, the fluorescent recovery in the nucleus comes from the fluorescent molecules imported from the cytoplasm. The fluorescence recovery in the nucleus of unphosphorylated STAT6-GFP (STAT6-GFP) was complete by 45 min (Figure 13) but GFP protein which is small enough to diffuse through the NPC only needed 3 miniutes for the nuclear fluorescence recovery (111). All these result indicated that STAT6 is active transported continually into the nucleus and independent of tyrosine phosphorylation (Figure 13 and Figure 15). The slower import rate suggested that, unlike GFP which can passively diffuse through the NPCs, STAT6 needs carrier proteins for nuclear import.

What does unphosphorylated STAT6 do in the nucleus? The constitutive nuclear import and export of latent STAT6 may provide an advantage for the rapid response to cytokine-stimulated tyrosine phosphorylation, or it may enable an activating response to nuclear kinases. Alternatively, because there is precedence for the function of unphosphorylated STATs contributing to gene expression, unphosphorylated STAT6 may have an undiscovered function in the nucleus. Studies have shown that

unphosphorylated STAT1 with IRF1 mediate constitutive expression of the low molecular mass polypeptide 2 (LMP2) (134). By collaborating with NF-κB, unphosphorylated STAT3 can activate a subset of NF-κB-dependent genes (135, 136) Unphosphorylated STAT6 was also reported to be involved in constitutive expression of the cyclooxygenase-2 (COX-2) which correlates with apoptosis resistance in non-small cell lung cancer (NSCLC) cell lines (137). Therefore, it unphosphorylated STAT6 in the nucleus may induce transcription of certain genes. But this effect might be gene- and cell type-specific since the EMSA performed with the DNA fragment corresponding to the IL-4 receptor alpha gene GAS site did not detect DNA binding ability without IL-4 treatment (Figure 11). To evaluate effects of unphosphorylated STAT6 on gene expression, microarray assays can be performed with STAT6-/- MEF cells and STAT6-/- cells complemented with wild-type STAT6 or STAT6RY mutant without and with IL-4 stimulation. By comparing the results, it will provide information about genes induced not only by phosphorylated STAT6 but also by unphosphorylated STAT6.

Drosophila STAT (STAT92E) controls heterochromatin protein 1 (HP1) distribution and heterochromatin stability (138). The unphosphorylated form of STAT92E associates with HP1 on heterochromatin and is required for stabilizing heterochromatin. In contrast, activation of STAT92E by tyrosine phosphorylation leads to HP1 displacement and heterochromatin destabilization. This result suggests a role for unphosphorylated STAT in heterochromatin stability. Whether mammalian STATs have a similar function needs to be further investigated.

It is known that specific phosphorylation of tyrosine 641 promotes STAT6 dimerization and its ability to bind DNA target sites. In addition to this activating modification, other modifications have been reported that include serine phosphorylation of the carboxy-terminal transactivation domain, which may influence DNA binding (139-141), and acetylation, which may contribute to induction of gene expression (25, 142). Methylation of arginine 27 was reported to be required for STAT6 tyrosine phosphorylation, nuclear translocation, and DNA binding (143). However, our studies indicate that arginine 27 is not necessary for tyrosine phosphorylation, nuclear translocation, or DNA binding. STAT6 that completely lacks 135 aa from the N terminus

is imported to the nucleus, tyrosine-phosphorylated in response to IL-4, and can bind DNA (Figure 17) (data not shown).

STAT6 contains an unconventional NLS

By studying the cellular localization of various STAT6 deletions, we identified a region within the coiled-coil domain required for STAT6 nuclear import (Figure 17). STAT6(136–847) was imported to the nucleus constitutively, whereas STAT6(141–847) was not imported. Deletion or substitution of the small region between amin acids 135–140 eliminated the ability of otherwise full-length STAT6 to be imported to the nucleus, although the proteins were still tyrosine-phosphorylated accurately and have DNA binding ability (Figure 18 and Figure 19). Furthermore, cytokine-regulated gene activation is dependent on the continuous nucleocytoplasmic cycling of STAT proteins. Therefore, I checked the transcriptional activity of different STAT6 constructs by luciferase assay (Figure 21). Only wild-type STAT6 can induce the IL-4 receptor gene but not the import mutant and DNA binding mutant. Thus, nuclear import is critical for transcriptional function of STAT6.

The best-characterized classical NLS sequences contain one or two stretches of basic amino acids, particularly lysines. Although the sequence of amino acids 135–140 (RRLQHR) contains arginine residues, site-directed mutation of individual amino acids within this region was not sufficient to block nuclear import (Figure 20). In addition, classical NLSs can function as an NLS outside the original context. I analyzed the ability of aa 135-140 of STAT6 to import GFP, but did not observe any increase in nuclear localization compared to GFP protein alone (data not shown).This finding suggests that a noncanonical NLS may be functional within 136–267 and the boundary of the real functional NLS for STAT6 nuclear import still needs to be defined. Other STAT molecules seem to use noncanonical NLSs. Leucine407 in the DNA binding domain of STAT1 has been shown important for phosphorylated STAT1 nuclear import (106). Amino acids 150-162 (DVRKRQDLEQKM) of STAT3 and amino acids 142-149 (LQINQTFE) of STAT5 in the coiled-coil domain are required for nuclear transport but neither is sufficient to mediate nuclear import of a heterol protein (110, 111). The results suggest that a larger fragment might be required to mediate STAT6 nuclear import.

To define the function NLS domain in the coiled-coil domain of STAT6, each α-heliex in coiled-coil domain may be tagged with one GST and two GFP proteins (GST-2GFP). The GST-2GFP protein is about 90 kDa and restricted in the cytoplasm. If the region fused with GST-2GFP contains the functional NLS, it should be able to bring the protein into the nucleus and nuclear fluorescence will be observed.

There are many NLSs that do not match the consensus rule but can bind to importins and drive protein nuclear import. By using random peptide library screening, selected peptides were idenfitied that bound to importin-α. Six classes of NLSs were identified including three novel classes (144). For example, the nucleoprotein NP of influenza A virus was shown to have an unconventional NLS (the first 13 amino acids at the amino terminus, MASQGTKRSYEQM) (145, 146). Evidence shows that NLSs are more diverse than previously defined.

Evidence supporting a role of importin-α/β1 in STAT6 nuclear import

Proteins larger than the diffusion limit (50 kDa) are actively transported through the NPCs. Therefore, as proteins with an average molecular mass over 80 kDa STATs need carrier proteins for nuclear transport. Although the STATs do not display classical NLSs, they seem to use the importin-α–importin-β1 receptors. Importin-α5 binds to STAT1 when it is in the conformation of a tyrosine-phosphorylated dimer and facilitates its nuclear import. Importin-α3 and -α6 bind constitutively to STAT3 and mediate its nuclear import. In this study, we found that importin-α3 and -α6 also bind constitutively to STAT6 (Figure 22). In addition, down modulation of importin-β1 by RNA interference notably reduced STAT6 nuclear import (Figure 25). STAT6 isolated from untreated cells or IL-4 stimulated cells (data not shown) bound to importin-α3 and -α6 suggesting that unphosphorylated and phosphorylated STAT6 are imported by importin-α–importin-β1 receptors. It is challenging to determine specific importin-α recognition of a particular NLS outside the framework of the native protein, because recognition depends on the NLS sequence, as well as the protein context. The crystal structure of STAT6 remains to be solved. However, the identity of the importin-α that binds a particular protein may be

significant because the importin-α proteins display specific expression in tissues and during differentiation (122, 147).

Unlike classical NLSs which bind to ARM repeats 2-4 and 7-8 of importin-α, the *in vitro* binding assay showed that ARM repeats 5 and 6 (aa 234-305) of importin-α3 are required for STAT6 binding (Figure 24). This might reflect the unconventional nature of the STAT6 NLS. However, the exact protein interface with importin-α3 needs to be investigated more detail. When six human importin-α proteins are aligned (Figure 44), there are conserved tryptophan and asparagine residues in the helical surface groove of ARM repeats 2-4 and 7-9 that are thought to be critical for NLS binding (95, 123, 148). Although Arm repeats 5 and 6 do not contain the tryptophan-asparagine pair, there are conserved tryptophan and tyrosine residues in Arm 5 and conserved proline and alanine residues in Arm 6 at the corresponding positions. Therefore these critical conserved residues could be mutated to generate various ARM repeat mutated importin-α3 proteins and the *in vitro* binding assays could be performed to investigate the requirement of each ARM repeat and specific residues in the ARM repeats.

Besides importins, it was reported that a Rac GTPase-activating protein, MgcRacGAP, is responsible for nuclear import of activated STAT3 and STAT5 proteins and that the dominant negative N17 Rac1 protein can block nuclear import of the STATs. The MgcRacGAP mutant lacking its NLS was reported to block the STAT3-importin complex formation and limit tyrosine phosphorylation of STAT3 in the cytoplasm. The STAT3 mutant lacking the MgcRacGAP binding site is poorly tyrosine phosphorylated upon cytokine stimulation (126-128). These data suggest that MgcRacGAP is a nuclear localization signal-containing chaperone which mediates tyrosine phosphorylation of STAT3 and phosphorylated STAT3 binding to importins. For this reason, I tested the effect of N17 Rac1 on STAT6 nuclear import but did not detect any effect (Figure 26). The result suggests that MgcRacGAP is not a carrier protein for STAT6 nucler import. It has also proposed that unphosphorylated STAT1 can enter into the nucleus by directly binding to the nucleoporins, Nup153 and Nup214 (149). To understand if it is the case for STAT6, the interacton with nucleoproins (full-length or the phenylalanine/glycine (FG)-rich repeat motifs which provide interaction sites for transport factors) can be evaluated *in vitro* with bacterially-expressed proteins or *in vivo* co-immunoprecipetation assays.

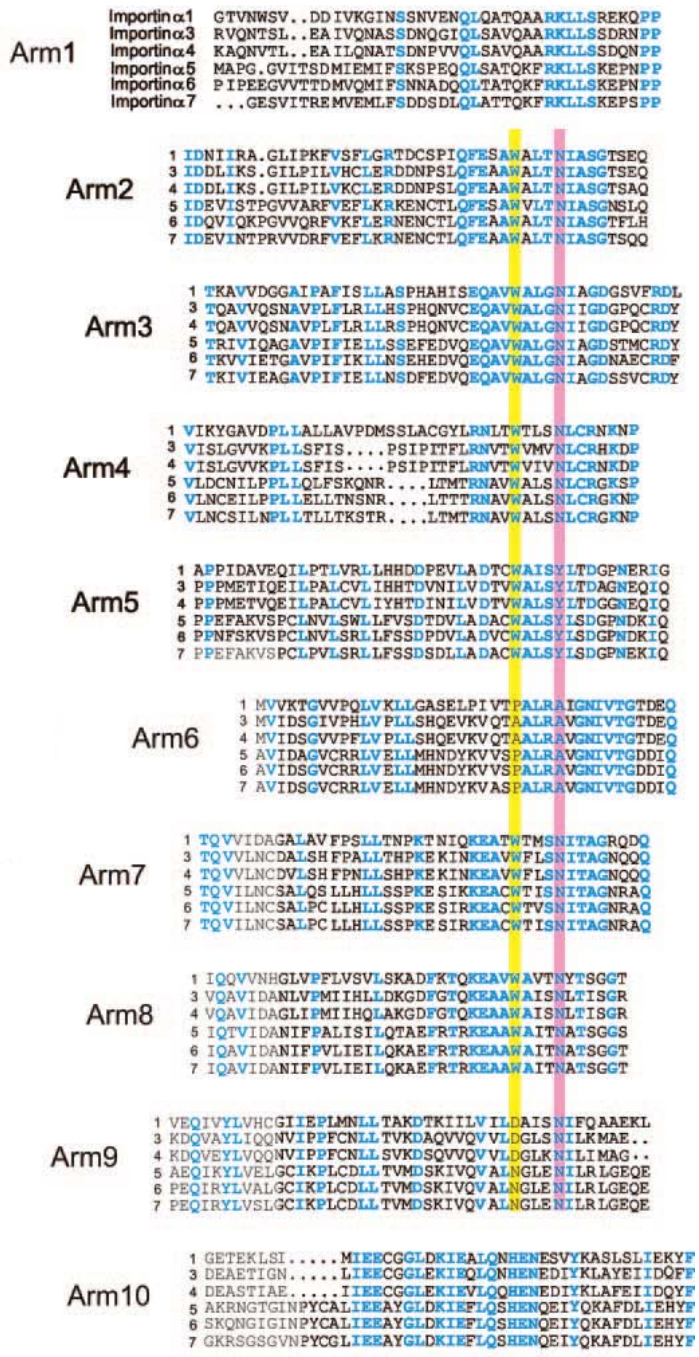

Figure 44: An alignment of ARM domains of six human importin-α proteins. (from reference 148)

All six human importin-α proteins are aligned and identical amino acids are shown in *blue*. Locations of the conserved tryptophan (*W*) and asparagine (*N*) residues in each arm repeat are shown by *yellow* and *pink vertical lines.*

The results presented in Figure 18 showed that amino acids 136-140 are indispensable for nuclear localization of STAT6; therefore, they are expected to be required for importin-α3 binding. The *in vitro* binding assays showed that the wild-type coiled-coil domain of STAT6 can bind to importin-α3 but a derivative lacking amino acids 136-140 cannot bind. The results confirmed the importance of amino acids 136-140 in STAT6 nuclear import and suggest that these amino acids might be part of the importin-α3 binding site. Future structural study of the STAT6-importin-α3 protein complex will provide more critical information in understanding how they interact with each other and designing specific drugs or small molecules to decrease or abolish STAT6 hyper-activation.

Effect of tyrosine phosphorylation and DNA binding on nuclear accumulation of STAT6

Latent-unphosphorylated and tyrosine-phosphorylated STAT6 are both imported to the nucleus. The difference is that STAT6 accumulates in the nucleus when it is tyrosine phosphorylated. The requirement for tyrosine phosphorylation for nuclear accumulation of STAT6 was demonstrated by analysis of the STAT6(RY) mutant protein did not accumulate in the nucleus even with IL-4 treatment (Figure 15). It is possible that the nuclear import rate of STAT6 was increased or the nuclear export rate of STAT6 was decreased. By using the technique of nuclear FRAP, the nuclear import rate of STAT6-GFP was observed to be similar for unphosphorylated and tyrosine-phosphorylated STAT6-GFP (Figure 13 and Figure 14). Therefore, the nuclear accumulation appeared to be the consequence of decreased nuclear export. This was demonstrated with cytoplasmic FLIP (Figure 31). Repeated photobleaching of one small region in the cytoplasm resulted in the loss of total cytoplasmic fluorescence, independent of STAT6 phosphorylation. For unphosphorylated STAT6-GFP, this was followed by a gradual loss of fluorescent signal from the nucleus, indicating continuous export. In contrast, nuclear fluorescence of tyrosine-phosphorylated STAT6-GFP did not decrease during the experiment. Therefore, the increase in STAT6 nuclear accumulation following tyrosine phosphorylation is a result of decreased nuclear export.

Since STAT6 gains DNA binding ability after tyrosine phosphorylation, it is possible that either tyrosine phosphorylation or DNA binding contributes to the slower nuclear export and accumulation. Therefore, a STAT6 DNA-binding mutant (STAT6(KR)) was tested. This STAT6 DNA-binding mutant was shown to behave like unphosphorylated STAT6 and did not accumulate in the nucleus following phosphorylation (Figure 36). Nuclear export rate of phosphorylated STAT6(KR) was the same as unphosphorylated STAT6 evalutated by cFLIP (Figure 37). In addition, nuclear FLIP analyses determined that DNA binding dramatically reduced STAT6 movement within the nucleus. Phosphorylated STAT6 able to bind DNA showed slower nuclear movement compared to unphosphorylated STAT6 or the phosphorylated STAT6(KR) mutant (Figure 33, Figure 34 and Figure 38). These observations indicate that nuclear accumulation of tyrosine phosphorylated STAT6 is due to retention by association with DNA.

Experiments with other STAT proteins indicate DNA binding contributes to nuclear retention. Latent STAT1 is predominantly in the cytoplasm and becomes nuclear after IFNγ treatment. The STAT1 DNA-binding mutant protein in which two glutamic acids (428 and 429) in DNA binding domain are mutated to alanine and serine is still resident in the cytoplasm following stimulation with IFNγ (115). STAT5a accumulates in the nucleus after growth hormone stimulation but without DNA binding ability STAT5a can not accumulate in the nucleus (111). All these evidence shows that DNA binding may be a general cause for observed nuclear accumulation of STAT proteins.

Nuclear export of STAT6

The cFLIP assays with wild-type STAT6 and STAT6(RY) mutant showed loss of nuclear fluorescence indicating that nuclear export of unphosphorylated STAT6 is continuous and tyrosine phosphorylation independent (Figure 28 and Figure 29). However, in IL-4-treated cells nuclear export of STAT6 was much slower than in the untreated cells (Figure 31). Thus, STAT6 nuclear export rate is decreased after tyrosine phosphorylation. My results indicate that STAT6 is continually imported in to and exported out of the nucleus in a latent state, but after tyrosine phosphorylation STAT6 binds to DNA resulting in a slower nuclear export rate and nuclear accumulation.

IL-4 stimulation leads to tyrosine phosphorylation and nuclear accumulation of STAT6 but after IL-4 removal STAT6 is dephosphorylated and redistributes between nuclear and cytoplasmic as latent STAT6 by 4 hours (Figure 41). This result suggests a correlation between dephosphorylation and nuclear export of STAT6. This is the case for STAT1. When bound to DNA, the STAT1 NES is masked and not accessible for Crm1 binding. Only when dephosphorylated and dissociated from DNA, can STAT1 be recognized by Crm1 and return to the cytoplasm. My preliminary data indicates the NES of STAT6 may be in the DNA binding domain (data not shown). Moreover, the redistribution of STAT6 following IL-4 removal was delayed in the presence of LMB without altering the dephosphorylation kinetics (Figure 42). Thus, it is possible that after IL-4 withdrawal STAT6 is dephosphorylated and dissociated from DNA, resulting in binding to exportins and redistribution to the cytoplasm. The exportin might be Crm1 since LMB can block the nuclear export process.

The complete mechanism of STAT6 nuclear export still remains to be determined. Crm1 is a well studied exportin known to mediate nuclear export of many proteins (103, 104) and it has been shown to bind to STAT1 and export STAT1 back to the cytoplasm from the nucleus (115, 150). It is possible that Crm1 plays a role in STAT6 nuclear export. To test this possibility, STAT6-GFP expressing cells were treated with LMB which can specifically inhibit Crm1-mediated nuclear export. Following a 30-minute treatment with LMB, STAT6 showed more nuclear accumulation (Figure 39). Nuclear export of STAT6 in living cells with LMB treatment was also analyzed by cFLIP. The nuclear export rate of STAT6 in LMB treated cells was only slightly decreased comparing to untreated cells (Figure 43). Therefore, nuclear export of STAT6 might be Crm1-dependent and also other export factors might be involved in controlling STAT6 nuclear export. Nuclear trafficking controlled by different proteins and mechanisms has been shown in some proteins; for example, STRADalpha-LKB complexes bind to both Crm1 and exportin 7 for nuclear export (151). These variant mechanisms might provide better and flexible regulation of activity.

Further experiments can be done to analyze the interaction between STAT6 and Crm1 *in vitro* and *in vivo*. Purified proteins from bacteria or mammalian cells can be used for *in vitro* binding assay. *In vivo* interaction can be detected by co-immunoprecipitation

and if the interaction is weak and difficult to detect, the cross-linker, DSP (dithiobis[succinimidylpropionate]), can be added to the cell for protein cross-linking within the cell. DSP is thio-cleavable, primary amine-reactive and has been used in many applications (152-154). To identify the unknown exportins for STAT6, other known mammalian export factors such as importin 13, exportin 4, exportin 6 and exportin 7 can be tested (155, 156). Importin 13 functions in both import and export was known to mediate export of eIF-1A (eukaryotic translation initiation factor 1A) (157). Exportin 4 is involved in nuclear export of eIF-5A (158). It has been reported that nuclear export of profilin-actin complexes was mediated by exportin 6 (159). Exportin 7 accounts for nuclear exclusion of p50RhoGAP and 14-3-3sigma (160). All these export factors appear to be conserved among higher eukaryotes and possibly mediate nuclear export of other cargoes. The interaction between STAT6 and these export factors or the effect of siRNA which specifically target each export protein on STAT6 nuclear localization can be evaluated.

Targeting STATs for cancer therapy

Since aberrant activation of STATs is found in many tumors and diseases, a better understanding of the mechanisms of dysregulation of the STAT pathway may serve as a basis for designing novel therapeutic strategies. Recent studies have tried to inactivate upstream STAT activators (receptors or JAKs) as well as directly target STAT molecules and downstream effectors (161-163). For example, rituximab, an anti-CD20 (a transmembrane B-cell antigen) chimeric antibody, can inhibit constitutive STAT3 activity in non-Hodgkin's lymphomas (164) and SH2 domain–binding phosphotyrosyl peptide can disrupt the STAT3 dimerization (165, 166). However, we have shown that STAT6 constitutively shuttles between the nucleus and the cytoplasm and the process is tyrosine phosphorylation-independent. In addition, unphosphorylated STAT6 might be able to induce expression of certain genes. Therefore, blocking STAT6 tyrosine phosphorylation or dimer formation might not be efficient ways to down-regulate STAT6 activity. Accurate cellular localization is essential for the effective function of transcription factors, such as STAT6. Intracellular trafficking is critical for the proper signal processing of STAT6, hence pharmacological targeting of STAT6

nucleocytoplasmic translocation appears to be an strategy to interfere with dysregulated cytokine signaling (167). Understanding the mechanisms that regulate STAT6 nuclear trafficking will support means to manipulate its activity in health and disease. For example, nuclear import of STAT6 seems to be mediated by importin-α3-importin-β1 therefore blocking STAT6 and importin-α3 interaction could be a strategy for drug design for STAT6 related diseases. However, importin-α3 is also a carrier for many other proteins. Thus, detailed study of how STAT6 and importin-α3 interact with each other will provide information for STAT6 specific drug design.

References

1. Firmbach-Kraft, I., M. Byers, T. Shows, R. Dalla-Favera, and J. J. Krolewski. 1990. tyk2, prototype of a novel class of non-receptor tyrosine kinase genes. *Oncogene* 5:1329-1336.

2. Wilks, A. F. 1989. Two putative protein-tyrosine kinases identified by application of the polymerase chain reaction. *Proc Natl Acad Sci U S A* 86:1603-1607.

3. Leonard, W. J., and J. J. O'Shea. 1998. Jaks and STATs: biological implications. *Annu Rev Immunol* 16:293-322.

4. Greenlund, A. C., M. O. Morales, B. L. Viviano, H. Yan, J. Krolewski, and R. D. Schreiber. 1995. Stat recruitment by tyrosine-phosphorylated cytokine receptors: an ordered reversible affinity-driven process. *Immunity* 2:677-687.

5. Reich, N., B. Evans, D. Levy, D. Fahey, E. Knight, Jr., and J. E. Darnell, Jr. 1987. Interferon-induced transcription of a gene encoding a 15-kDa protein depends on an upstream enhancer element. *Proc Natl Acad Sci U S A* 84:6394-6398.

6. Levy, D. E., D. S. Kessler, R. Pine, N. Reich, and J. E. Darnell, Jr. 1988. Interferon-induced nuclear factors that bind a shared promoter element correlate with positive and negative transcriptional control. *Genes Dev* 2:383-393.

7. Kessler, D. S., D. E. Levy, and J. E. Darnell, Jr. 1988. Two interferon-induced nuclear factors bind a single promoter element in interferon-stimulated genes. *Proc Natl Acad Sci U S A* 85:8521-8525.

8. Levy, D. E., D. S. Kessler, R. Pine, and J. E. Darnell, Jr. 1989. Cytoplasmic activation of ISGF3, the positive regulator of interferon-alpha-stimulated transcription, reconstituted in vitro. *Genes Dev* 3:1362-1371.

9. Dale, T. C., A. M. Imam, I. M. Kerr, and G. R. Stark. 1989. Rapid activation by interferon alpha of a latent DNA-binding protein present in the cytoplasm of untreated cells. *Proc Natl Acad Sci U S A* 86:1203-1207.

10. Fu, X. Y., D. S. Kessler, S. A. Veals, D. E. Levy, and J. E. Darnell, Jr. 1990. ISGF3, the transcriptional activator induced by interferon alpha, consists of multiple interacting polypeptide chains. *Proc Natl Acad Sci U S A* 87:8555-8559.

11. Veals, S. A., C. Schindler, D. Leonard, X. Y. Fu, R. Aebersold, J. E. Darnell, Jr., and D. E. Levy. 1992. Subunit of an alpha-interferon-responsive transcription

factor is related to interferon regulatory factor and Myb families of DNA-binding proteins. *Mol Cell Biol* 12:3315-3324.

12. Schindler, C., X. Y. Fu, T. Improta, R. Aebersold, and J. E. Darnell, Jr. 1992. Proteins of transcription factor ISGF-3: one gene encodes the 91-and 84-kDa ISGF-3 proteins that are activated by interferon alpha. *Proc Natl Acad Sci U S A* 89:7836-7839.

13. Fu, X. Y., C. Schindler, T. Improta, R. Aebersold, and J. E. Darnell, Jr. 1992. The proteins of ISGF-3, the interferon alpha-induced transcriptional activator, define a gene family involved in signal transduction. *Proc Natl Acad Sci U S A* 89:7840-7843.

14. Yamamoto, K., F. W. Quelle, W. E. Thierfelder, B. L. Kreider, D. J. Gilbert, N. A. Jenkins, N. G. Copeland, O. Silvennoinen, and J. N. Ihle. 1994. Stat4, a novel gamma interferon activation site-binding protein expressed in early myeloid differentiation. *Mol Cell Biol* 14:4342-4349.

15. Akira, S., Y. Nishio, M. Inoue, X. J. Wang, S. Wei, T. Matsusaka, K. Yoshida, T. Sudo, M. Naruto, and T. Kishimoto. 1994. Molecular cloning of APRF, a novel IFN-stimulated gene factor 3 p91-related transcription factor involved in the gp130-mediated signaling pathway. *Cell* 77:63-71.

16. Hou, J., U. Schindler, W. J. Henzel, T. C. Ho, M. Brasseur, and S. L. McKnight. 1994. An interleukin-4-induced transcription factor: IL-4 Stat. *Science* 265:1701-1706.

17. Wakao, H., F. Gouilleux, and B. Groner. 1995. Mammary gland factor (MGF) is a novel member of the cytokine regulated transcription factor gene family and confers the prolactin response. *EMBO J* 14:854-855.

18. Wang, Y., and D. E. Levy. 2006. C. elegans STAT: evolution of a regulatory switch. *FASEB J* 20:1641-1652.

19. Wang, Y., and D. E. Levy. 2006. C. elegans STAT cooperates with DAF-7/TGF-beta signaling to repress dauer formation. *Curr Biol* 16:89-94.

20. Hou, X. S., M. B. Melnick, and N. Perrimon. 1996. Marelle acts downstream of the Drosophila HOP/JAK kinase and encodes a protein similar to the mammalian STATs. *Cell* 84:411-419.

21. Yan, R., S. Small, C. Desplan, C. R. Dearolf, and J. E. Darnell, Jr. 1996. Identification of a Stat gene that functions in Drosophila development. *Cell* 84:421-430.

22. Darnell, J. E., Jr. 1997. STATs and gene regulation. *Science* 277:1630-1635.

23. Xu, X., Y. L. Sun, and T. Hoey. 1996. Cooperative DNA binding and sequence-selective recognition conferred by the STAT amino-terminal domain. *Science* 273:794-797.

24. Horvath, C. M., Z. Wen, and J. E. Darnell, Jr. 1995. A STAT protein domain that determines DNA sequence recognition suggests a novel DNA-binding domain. *Genes Dev* 9:984-994.

25. McDonald, C., and N. C. Reich. 1999. Cooperation of the transcriptional coactivators CBP and p300 with Stat6. *J Interferon Cytokine Res* 19:711-722.

26. Yang, E., M. A. Henriksen, O. Schaefer, N. Zakharova, and J. E. Darnell, Jr. 2002. Dissociation time from DNA determines transcriptional function in a STAT1 linker mutant. *J Biol Chem* 277:13455-13462.

27. Mao, X., Z. Ren, G. N. Parker, H. Sondermann, M. A. Pastorello, W. Wang, J. S. McMurray, B. Demeler, J. E. Darnell, Jr., and X. Chen. 2005. Structural bases of unphosphorylated STAT1 association and receptor binding. *Mol Cell* 17:761-771.

28. Neculai, D., A. M. Neculai, S. Verrier, K. Straub, K. Klumpp, E. Pfitzner, and S. Becker. 2005. Structure of the unphosphorylated STAT5a dimer. *J Biol Chem* 280:40782-40787.

29. Chen, X., U. Vinkemeier, Y. Zhao, D. Jeruzalmi, J. E. Darnell, Jr., and J. Kuriyan. 1998. Crystal structure of a tyrosine phosphorylated STAT-1 dimer bound to DNA. *Cell* 93:827-839.

30. Becker, S., B. Groner, and C. W. Muller. 1998. Three-dimensional structure of the Stat3beta homodimer bound to DNA. *Nature* 394:145-151.

31. Yu, H., D. Pardoll, and R. Jove. 2009. STATs in cancer inflammation and immunity: a leading role for STAT3. *Nat Rev Cancer* 9:798-809.

32. Paukku, K., and O. Silvennoinen. 2004. STATs as critical mediators of signal transduction and transcription: lessons learned from STAT5. *Cytokine Growth Factor Rev* 15:435-455.

33. Akira, S. 1999. Functional roles of STAT family proteins: lessons from knockout mice. *Stem Cells* 17:138-146.

34. Levy, D. E., and J. E. Darnell, Jr. 2002. Stats: transcriptional control and biological impact. *Nat Rev Mol Cell Biol* 3:651-662.

35. Durbin, J. E., R. Hackenmiller, M. C. Simon, and D. E. Levy. 1996. Targeted disruption of the mouse Stat1 gene results in compromised innate immunity to viral disease. *Cell* 84:443-450.

36. Meraz, M. A., J. M. White, K. C. Sheehan, E. A. Bach, S. J. Rodig, A. S. Dighe, D. H. Kaplan, J. K. Riley, A. C. Greenlund, D. Campbell, K. Carver-Moore, R. N. DuBois, R. Clark, M. Aguet, and R. D. Schreiber. 1996. Targeted disruption of the Stat1 gene in mice reveals unexpected physiologic specificity in the JAK-STAT signaling pathway. *Cell* 84:431-442.

37. Park, C., S. Li, E. Cha, and C. Schindler. 2000. Immune response in Stat2 knockout mice. *Immunity* 13:795-804.

38. Takeda, K., K. Noguchi, W. Shi, T. Tanaka, M. Matsumoto, N. Yoshida, T. Kishimoto, and S. Akira. 1997. Targeted disruption of the mouse Stat3 gene leads to early embryonic lethality. *Proc Natl Acad Sci U S A* 94:3801-3804.

39. Levy, D. E., and C. K. Lee. 2002. What does Stat3 do? *J Clin Invest* 109:1143-1148.

40. Kaplan, M. H., Y. L. Sun, T. Hoey, and M. J. Grusby. 1996. Impaired IL-12 responses and enhanced development of Th2 cells in Stat4-deficient mice. *Nature* 382:174-177.

41. Thierfelder, W. E., J. M. van Deursen, K. Yamamoto, R. A. Tripp, S. R. Sarawar, R. T. Carson, M. Y. Sangster, D. A. Vignali, P. C. Doherty, G. C. Grosveld, and J. N. Ihle. 1996. Requirement for Stat4 in interleukin-12-mediated responses of natural killer and T cells. *Nature* 382:171-174.

42. Liu, X., G. W. Robinson, K. U. Wagner, L. Garrett, A. Wynshaw-Boris, and L. Hennighausen. 1997. Stat5a is mandatory for adult mammary gland development and lactogenesis. *Genes Dev* 11:179-186.

43. Udy, G. B., R. P. Towers, R. G. Snell, R. J. Wilkins, S. H. Park, P. A. Ram, D. J. Waxman, and H. W. Davey. 1997. Requirement of STAT5b for sexual dimorphism of body growth rates and liver gene expression. *Proc Natl Acad Sci U S A* 94:7239-7244.

44. Teglund, S., C. McKay, E. Schuetz, J. M. van Deursen, D. Stravopodis, D. Wang, M. Brown, S. Bodner, G. Grosveld, and J. N. Ihle. 1998. Stat5a and Stat5b proteins have essential and nonessential, or redundant, roles in cytokine responses. *Cell* 93:841-850.

45. Cui, Y., G. Riedlinger, K. Miyoshi, W. Tang, C. Li, C. X. Deng, G. W. Robinson, and L. Hennighausen. 2004. Inactivation of Stat5 in mouse mammary epithelium during pregnancy reveals distinct functions in cell proliferation, survival, and differentiation. *Mol Cell Biol* 24:8037-8047.

46. Moriggl, R., D. J. Topham, S. Teglund, V. Sexl, C. McKay, D. Wang, A. Hoffmeyer, J. van Deursen, M. Y. Sangster, K. D. Bunting, G. C. Grosveld, and J. N. Ihle. 1999. Stat5 is required for IL-2-induced cell cycle progression of peripheral T cells. *Immunity* 10:249-259.

47. Takeda, K., T. Tanaka, W. Shi, M. Matsumoto, M. Minami, S. Kashiwamura, K. Nakanishi, N. Yoshida, T. Kishimoto, and S. Akira. 1996. Essential role of Stat6 in IL-4 signalling. *Nature* 380:627-630.

48. Shimoda, K., J. van Deursen, M. Y. Sangster, S. R. Sarawar, R. T. Carson, R. A. Tripp, C. Chu, F. W. Quelle, T. Nosaka, D. A. Vignali, P. C. Doherty, G. Grosveld, W. E. Paul, and J. N. Ihle. 1996. Lack of IL-4-induced Th2 response and IgE class switching in mice with disrupted Stat6 gene. *Nature* 380:630-633.

49. Kaplan, M. H., U. Schindler, S. T. Smiley, and M. J. Grusby. 1996. Stat6 is required for mediating responses to IL-4 and for development of Th2 cells. *Immunity* 4:313-319.

50. Kuperman, D., B. Schofield, M. Wills-Karp, and M. J. Grusby. 1998. Signal transducer and activator of transcription factor 6 (Stat6)-deficient mice are protected from antigen-induced airway hyperresponsiveness and mucus production. *J Exp Med* 187:939-948.

51. Kotanides, H., and N. C. Reich. 1993. Requirement of tyrosine phosphorylation for rapid activation of a DNA binding factor by IL-4. *Science* 262:1265-1267.

52. Boothby, M., E. Gravallese, H. C. Liou, and L. H. Glimcher. 1988. A DNA binding protein regulated by IL-4 and by differentiation in B cells. *Science* 242:1559-1562.

53. Patel, B. K., C. L. Keck, R. S. O'Leary, N. C. Popescu, and W. J. LaRochelle. 1998. Localization of the human stat6 gene to chromosome 12q13.3-q14.1, a region implicated in multiple solid tumors. *Genomics* 52:192-200.

54. Onodera, A., M. Yamashita, Y. Endo, M. Kuwahara, S. Tofukuji, H. Hosokawa, A. Kanai, Y. Suzuki, and T. Nakayama. STAT6-mediated displacement of polycomb by trithorax complex establishes long-term maintenance of GATA3 expression in T helper type 2 cells. *J Exp Med*.

55. Finkelman, F. D., T. Shea-Donohue, S. C. Morris, L. Gildea, R. Strait, K. B. Madden, L. Schopf, and J. F. Urban, Jr. 2004. Interleukin-4- and interleukin-13-mediated host protection against intestinal nematode parasites. *Immunol Rev* 201:139-155.

56. Wang, Y., J. T. Evans, F. Rodriguez, P. Fields, C. Mueller, T. Chitnis, S. J. Khoury, and M. S. Bynoe. 2009. A tale of two STAT6 knock out mice in the induction of experimental autoimmune encephalomyelitis. *J Neuroimmunol* 206:76-85.

57. Nelms, K., A. D. Keegan, J. Zamorano, J. J. Ryan, and W. E. Paul. 1999. The IL-4 receptor: signaling mechanisms and biologic functions. *Annu Rev Immunol* 17:701-738.

58. Mueller, T. D., J. L. Zhang, W. Sebald, and A. Duschl. 2002. Structure, binding, and antagonists in the IL-4/IL-13 receptor system. *Biochim Biophys Acta* 1592:237-250.

59. Miyazaki, T., A. Kawahara, H. Fujii, Y. Nakagawa, Y. Minami, Z. J. Liu, I. Oishi, O. Silvennoinen, B. A. Witthuhn, J. N. Ihle, and et al. 1994. Functional activation of Jak1 and Jak3 by selective association with IL-2 receptor subunits. *Science* 266:1045-1047.

60. Russell, S. M., J. A. Johnston, M. Noguchi, M. Kawamura, C. M. Bacon, M. Friedmann, M. Berg, D. W. McVicar, B. A. Witthuhn, O. Silvennoinen, and et al. 1994. Interaction of IL-2R beta and gamma c chains with Jak1 and Jak3: implications for XSCID and XCID. *Science* 266:1042-1045.

61. Mikita, T., D. Campbell, P. Wu, K. Williamson, and U. Schindler. 1996. Requirements for interleukin-4-induced gene expression and functional characterization of Stat6. *Mol Cell Biol* 16:5811-5820.

62. Haque, S. J., P. Harbor, M. Tabrizi, T. Yi, and B. R. Williams. 1998. Protein-tyrosine phosphatase Shp-1 is a negative regulator of IL-4- and IL-13-dependent signal transduction. *J Biol Chem* 273:33893-33896.

63. Hanson, E. M., H. Dickensheets, C. K. Qu, R. P. Donnelly, and A. D. Keegan. 2003. Regulation of the dephosphorylation of Stat6. Participation of Tyr-713 in the interleukin-4 receptor alpha, the tyrosine phosphatase SHP-1, and the proteasome. *J Biol Chem* 278:3903-3911.

64. Huang, Z., J. M. Coleman, Y. Su, M. Mann, J. Ryan, L. D. Shultz, and H. Huang. 2005. SHP-1 regulates STAT6 phosphorylation and IL-4-mediated function in a cell type-specific manner. *Cytokine* 29:118-124.

65. Lu, X., J. Chen, R. T. Sasmono, E. D. Hsi, K. A. Sarosiek, T. Tiganis, and I. S. Lossos. 2007. T-cell protein tyrosine phosphatase, distinctively expressed in activated-B-cell-like diffuse large B-cell lymphomas, is the nuclear phosphatase of STAT6. *Mol Cell Biol* 27:2166-2179.

66. Oh, S. Y., T. Zheng, Y. K. Kim, L. Cohn, R. J. Homer, A. N. McKenzie, and Z. Zhu. 2009. A critical role of SHP-1 in regulation of type 2 inflammation in the lung. *Am J Respir Cell Mol Biol* 40:568-574.

67. Lu, X., R. Malumbres, B. Shields, X. Jiang, K. A. Sarosiek, Y. Natkunam, T. Tiganis, and I. S. Lossos. 2008. PTP1B is a negative regulator of interleukin 4-induced STAT6 signaling. *Blood* 112:4098-4108.

68. Kaplan, M. H., S. Sehra, H. C. Chang, J. T. O'Malley, A. N. Mathur, and H. A. Bruns. 2007. Constitutively active STAT6 predisposes toward a lymphoproliferative disorder. *Blood* 110:4367-4369.

69. Akimoto, T., F. Numata, M. Tamura, Y. Takata, N. Higashida, T. Takashi, K. Takeda, and S. Akira. 1998. Abrogation of bronchial eosinophilic inflammation and airway hyperreactivity in signal transducers and activators of transcription (STAT)6-deficient mice. *J Exp Med* 187:1537-1542.

70. Kaplan, M. H., C. Daniel, U. Schindler, and M. J. Grusby. 1998. Stat proteins control lymphocyte proliferation by regulating p27Kip1 expression. *Mol Cell Biol* 18:1996-2003.

71. McDonald, C., S. Vanscoy, P. Hearing, and N. C. Reich. 2004. Induction of genes involved in cell cycle progression by interleukin-4. *J Interferon Cytokine Res* 24:729-738.

72. Benekli, M., M. R. Baer, H. Baumann, and M. Wetzler. 2003. Signal transducer and activator of transcription proteins in leukemias. *Blood* 101:2940-2954.

73. Ni, Z., W. Lou, S. O. Lee, R. Dhir, F. DeMiguel, J. R. Grandis, and A. C. Gao. 2002. Selective activation of members of the signal transducers and activators of transcription family in prostate carcinoma. *J Urol* 167:1859-1862.

74. Skinnider, B. F., A. J. Elia, R. D. Gascoyne, B. Patterson, L. Trumper, U. Kapp, and T. W. Mak. 2002. Signal transducer and activator of transcription 6 is frequently activated in Hodgkin and Reed-Sternberg cells of Hodgkin lymphoma. *Blood* 99:618-626.

75. Guiter, C., I. Dusanter-Fourt, C. Copie-Bergman, M. L. Boulland, S. Le Gouvello, P. Gaulard, K. Leroy, and F. Castellano. 2004. Constitutive STAT6 activation in primary mediastinal large B-cell lymphoma. *Blood* 104:543-549.

76. Melzner, I., A. J. Bucur, S. Bruderlein, K. Dorsch, C. Hasel, T. F. Barth, F. Leithauser, and P. Moller. 2005. Biallelic mutation of SOCS-1 impairs JAK2 degradation and sustains phospho-JAK2 action in the MedB-1 mediastinal lymphoma line. *Blood* 105:2535-2542.

77. Bromberg, J. F. 2001. Activation of STAT proteins and growth control. *Bioessays* 23:161-169.

78. Qin, J. Z., J. Kamarashev, C. L. Zhang, R. Dummer, G. Burg, and U. Dobbeling. 2001. Constitutive and interleukin-7- and interleukin-15-stimulated DNA binding of STAT and novel factors in cutaneous T cell lymphoma cells. *J Invest Dermatol* 117:583-589.

79. Bruns, H. A., and M. H. Kaplan. 2006. The role of constitutively active Stat6 in leukemia and lymphoma. *Crit Rev Oncol Hematol* 57:245-253.

80. Daniel, C., A. Salvekar, and U. Schindler. 2000. A gain-of-function mutation in STAT6. *J Biol Chem* 275:14255-14259.

81. Mikita, T., C. Daniel, P. Wu, and U. Schindler. 1998. Mutational analysis of the STAT6 SH2 domain. *J Biol Chem* 273:17634-17642.

82. Bruns, H. A., U. Schindler, and M. H. Kaplan. 2003. Expression of a constitutively active Stat6 in vivo alters lymphocyte homeostasis with distinct effects in T and B cells. *J Immunol* 170:3478-3487.

83. Peters, R. 2006. Introduction to nucleocytoplasmic transport: molecules and mechanisms. *Methods Mol Biol* 322:235-258.

84. Davis, L. I. 1995. The nuclear pore complex. *Annu Rev Biochem* 64:865-896.

85. Suntharalingam, M., and S. R. Wente. 2003. Peering through the pore: nuclear pore complex structure, assembly, and function. *Dev Cell* 4:775-789.

86. Strambio-De-Castillia, C., M. Niepel, and M. P. Rout. The nuclear pore complex: bridging nuclear transport and gene regulation. *Nat Rev Mol Cell Biol* 11:490-501.

87. Kuersten, S., M. Ohno, and I. W. Mattaj. 2001. Nucleocytoplasmic transport: Ran, beta and beyond. *Trends Cell Biol* 11:497-503.

88. Gorlich, D. 1997. Nuclear protein import. *Curr Opin Cell Biol* 9:412-419.

89. Lange, A., R. E. Mills, C. J. Lange, M. Stewart, S. E. Devine, and A. H. Corbett. 2007. Classical nuclear localization signals: definition, function, and interaction with importin alpha. *J Biol Chem* 282:5101-5105.

90. Bednenko, J., G. Cingolani, and L. Gerace. 2003. Nucleocytoplasmic transport: navigating the channel. *Traffic* 4:127-135.

91. Terry, L. J., E. B. Shows, and S. R. Wente. 2007. Crossing the nuclear envelope: hierarchical regulation of nucleocytoplasmic transport. *Science* 318:1412-1416.

92. Mattaj, I. W., and L. Englmeier. 1998. Nucleocytoplasmic transport: the soluble phase. *Annu Rev Biochem* 67:265-306.

93. Macara, I. G. 2001. Transport into and out of the nucleus. *Microbiol Mol Biol Rev* 65:570-594, table of contents.

94. Cingolani, G., C. Petosa, K. Weis, and C. W. Muller. 1999. Structure of importin-beta bound to the IBB domain of importin-alpha. *Nature* 399:221-229.

95. Conti, E., M. Uy, L. Leighton, G. Blobel, and J. Kuriyan. 1998. Crystallographic analysis of the recognition of a nuclear localization signal by the nuclear import factor karyopherin alpha. *Cell* 94:193-204.

96. Harel, A., and D. J. Forbes. 2004. Importin beta: conducting a much larger cellular symphony. *Mol Cell* 16:319-330.

97. Okada, M., T. Ishimoto, Y. Naito, H. Hirata, and H. Yagisawa. 2005. Phospholipase Cdelta1 associates with importin beta1 and translocates into the nucleus in a Ca2+-dependent manner. *FEBS Lett* 579:4949-4954.

98. Wagstaff, K. M., and D. A. Jans. 2009. Importins and beyond: non-conventional nuclear transport mechanisms. *Traffic* 10:1188-1198.

99. Fagotto, F., U. Gluck, and B. M. Gumbiner. 1998. Nuclear localization signal-independent and importin/karyopherin-independent nuclear import of beta-catenin. *Curr Biol* 8:181-190.

100. Kudo, N., B. Wolff, T. Sekimoto, E. P. Schreiner, Y. Yoneda, M. Yanagida, S. Horinouchi, and M. Yoshida. 1998. Leptomycin B inhibition of signal-mediated nuclear export by direct binding to CRM1. *Exp Cell Res* 242:540-547.

101. Wolff, B., J. J. Sanglier, and Y. Wang. 1997. Leptomycin B is an inhibitor of nuclear export: inhibition of nucleo-cytoplasmic translocation of the human immunodeficiency virus type 1 (HIV-1) Rev protein and Rev-dependent mRNA. *Chem Biol* 4:139-147.

102. Fornerod, M., M. Ohno, M. Yoshida, and I. W. Mattaj. 1997. CRM1 is an export receptor for leucine-rich nuclear export signals. *Cell* 90:1051-1060.

103. Fukuda, M., S. Asano, T. Nakamura, M. Adachi, M. Yoshida, M. Yanagida, and E. Nishida. 1997. CRM1 is responsible for intracellular transport mediated by the nuclear export signal. *Nature* 390:308-311.

104. Ossareh-Nazari, B., F. Bachelerie, and C. Dargemont. 1997. Evidence for a role of CRM1 in signal-mediated nuclear protein export. *Science* 278:141-144.

105. Reich, N. C., and L. Liu. 2006. Tracking STAT nuclear traffic. *Nat Rev Immunol* 6:602-612.

106. McBride, K. M., G. Banninger, C. McDonald, and N. C. Reich. 2002. Regulated nuclear import of the STAT1 transcription factor by direct binding of importin-alpha. *EMBO J* 21:1754-1763.

107. Sekimoto, T., K. Nakajima, T. Tachibana, T. Hirano, and Y. Yoneda. 1996. Interferon-gamma-dependent nuclear import of Stat1 is mediated by the GTPase activity of Ran/TC4. *J Biol Chem* 271:31017-31020.

108. Reich, N. C. 2007. STAT dynamics. *Cytokine Growth Factor Rev* 18:511-518.

109. McBride, K. M., and N. C. Reich. 2003. The ins and outs of STAT1 nuclear transport. *Sci STKE* 2003:RE13.

110. Liu, L., K. M. McBride, and N. C. Reich. 2005. STAT3 nuclear import is independent of tyrosine phosphorylation and mediated by importin-alpha3. *Proc Natl Acad Sci U S A* 102:8150-8155.

111. Iyer, J., and N. C. Reich. 2008. Constitutive nuclear import of latent and activated STAT5a by its coiled coil domain. *FASEB J* 22:391-400.

112. Shuai, K., C. M. Horvath, L. H. Huang, S. A. Qureshi, D. Cowburn, and J. E. Darnell, Jr. 1994. Interferon activation of the transcription factor Stat91 involves dimerization through SH2-phosphotyrosyl peptide interactions. *Cell* 76:821-828.

113. Sekimoto, T., N. Imamoto, K. Nakajima, T. Hirano, and Y. Yoneda. 1997. Extracellular signal-dependent nuclear import of Stat1 is mediated by nuclear pore-targeting complex formation with NPI-1, but not Rch1. *EMBO J* 16:7067-7077.

114. Haspel, R. L., and J. E. Darnell, Jr. 1999. A nuclear protein tyrosine phosphatase is required for the inactivation of Stat1. *Proc Natl Acad Sci U S A* 96:10188-10193.

115. McBride, K. M., C. McDonald, and N. C. Reich. 2000. Nuclear export signal located within theDNA-binding domain of the STAT1transcription factor. *EMBO J* 19:6196-6206.

116. Bhattacharya, S., and C. Schindler. 2003. Regulation of Stat3 nuclear export. *J Clin Invest* 111:553-559.

117. Andrews, R. P., M. B. Ericksen, C. M. Cunningham, M. O. Daines, and G. K. Hershey. 2002. Analysis of the life cycle of stat6. Continuous cycling of STAT6 is required for IL-4 signaling. *J Biol Chem* 277:36563-36569.

118. Shaner, N. C., P. A. Steinbach, and R. Y. Tsien. 2005. A guide to choosing fluorescent proteins. *Nat Methods* 2:905-909.

119. Sun, Z., C. W. Arendt, W. Ellmeier, E. M. Schaeffer, M. J. Sunshine, L. Gandhi, J. Annes, D. Petrzilka, A. Kupfer, P. L. Schwartzberg, and D. R. Littman. 2000. PKC-theta is required for TCR-induced NF-kappaB activation in mature but not immature T lymphocytes. *Nature* 404:402-407.

120. Kotanides, H., and N. C. Reich. 1996. Interleukin-4-induced STAT6 recognizes and activates a target site in the promoter of the interleukin-4 receptor gene. *J Biol Chem* 271:25555-25561.

121. Kohler, M., C. Speck, M. Christiansen, F. R. Bischoff, S. Prehn, H. Haller, D. Gorlich, and E. Hartmann. 1999. Evidence for distinct substrate specificities of importin alpha family members in nuclear protein import. *Mol Cell Biol* 19:7782-7791.

122. Kohler, M., S. Ansieau, S. Prehn, A. Leutz, H. Haller, and E. Hartmann. 1997. Cloning of two novel human importin-alpha subunits and analysis of the expression pattern of the importin-alpha protein family. *FEBS Lett* 417:104-108.

123. Fontes, M. R., T. Teh, and B. Kobe. 2000. Structural basis of recognition of monopartite and bipartite nuclear localization sequences by mammalian importin-alpha. *J Mol Biol* 297:1183-1194.

124. Conti, E., and J. Kuriyan. 2000. Crystallographic analysis of the specific yet versatile recognition of distinct nuclear localization signals by karyopherin alpha. *Structure* 8:329-338.

125. Fontes, M. R., T. Teh, D. Jans, R. I. Brinkworth, and B. Kobe. 2003. Structural basis for the specificity of bipartite nuclear localization sequence binding by importin-alpha. *J Biol Chem* 278:27981-27987.

126. Kawashima, T., Y. C. Bao, Y. Nomura, Y. Moon, Y. Tonozuka, Y. Minoshima, T. Hatori, A. Tsuchiya, M. Kiyono, T. Nosaka, H. Nakajima, D. A. Williams, and T. Kitamura. 2006. Rac1 and a GTPase-activating protein, MgcRacGAP, are required for nuclear translocation of STAT transcription factors. *J Cell Biol* 175:937-946.

127. Tonozuka, Y., Y. Minoshima, Y. C. Bao, Y. Moon, Y. Tsubono, T. Hatori, H. Nakajima, T. Nosaka, T. Kawashima, and T. Kitamura. 2004. A GTPase-activating protein binds STAT3 and is required for IL-6-induced STAT3 activation and for differentiation of a leukemic cell line. *Blood* 104:3550-3557.

128. Kawashima, T., Y. C. Bao, Y. Minoshima, Y. Nomura, T. Hatori, T. Hori, T. Fukagawa, T. Fukada, N. Takahashi, T. Nosaka, M. Inoue, T. Sato, M. Kukimoto-Niino, M. Shirouzu, S. Yokoyama, and T. Kitamura. 2009. A Rac GTPase-activating protein, MgcRacGAP, is a nuclear localizing signal-containing nuclear chaperone in the activation of STAT transcription factors. *Mol Cell Biol* 29:1796-1813.

129. Koster, M., T. Frahm, and H. Hauser. 2005. Nucleocytoplasmic shuttling revealed by FRAP and FLIP technologies. *Curr Opin Biotechnol* 16:28-34.

130. Pranada, A. L., S. Metz, A. Herrmann, P. C. Heinrich, and G. Muller-Newen. 2004. Real time analysis of STAT3 nucleocytoplasmic shuttling. *J Biol Chem* 279:15114-15123.

131. Lillemeier, B. F., M. Koster, and I. M. Kerr. 2001. STAT1 from the cell membrane to the DNA. *EMBO J* 20:2508-2517.

132. Gough, D. J., A. Corlett, K. Schlessinger, J. Wegrzyn, A. C. Larner, and D. E. Levy. 2009. Mitochondrial STAT3 supports Ras-dependent oncogenic transformation. *Science* 324:1713-1716.

133. Wegrzyn, J., R. Potla, Y. J. Chwae, N. B. Sepuri, Q. Zhang, T. Koeck, M. Derecka, K. Szczepanek, M. Szelag, A. Gornicka, A. Moh, S. Moghaddas, Q. Chen, S. Bobbili, J. Cichy, J. Dulak, D. P. Baker, A. Wolfman, D. Stuehr, M. O. Hassan, X. Y. Fu, N. Avadhani, J. I. Drake, P. Fawcett, E. J. Lesnefsky, and A. C. Larner. 2009. Function of mitochondrial Stat3 in cellular respiration. *Science* 323:793-797.

134. Chatterjee-Kishore, M., R. Kishore, D. J. Hicklin, F. M. Marincola, and S. Ferrone. 1998. Different requirements for signal transducer and activator of transcription 1alpha and interferon regulatory factor 1 in the regulation of low molecular mass polypeptide 2 and transporter associated with antigen processing 1 gene expression. *J Biol Chem* 273:16177-16183.

135. Yang, J., X. Liao, M. K. Agarwal, L. Barnes, P. E. Auron, and G. R. Stark. 2007. Unphosphorylated STAT3 accumulates in response to IL-6 and activates transcription by binding to NFkappaB. *Genes Dev* 21:1396-1408.

136. Yang, J., M. Chatterjee-Kishore, S. M. Staugaitis, H. Nguyen, K. Schlessinger, D. E. Levy, and G. R. Stark. 2005. Novel roles of unphosphorylated STAT3 in oncogenesis and transcriptional regulation. *Cancer Res* 65:939-947.

137. Cui, X., L. Zhang, J. Luo, A. Rajasekaran, S. Hazra, N. Cacalano, and S. M. Dubinett. 2007. Unphosphorylated STAT6 contributes to constitutive cyclooxygenase-2 expression in human non-small cell lung cancer. *Oncogene* 26:4253-4260.

138. Shi, S., K. Larson, D. Guo, S. J. Lim, P. Dutta, S. J. Yan, and W. X. Li. 2008. Drosophila STAT is required for directly maintaining HP1 localization and heterochromatin stability. *Nat Cell Biol* 10:489-496.

139. Wick, K. R., and M. T. Berton. 2000. IL-4 induces serine phosphorylation of the STAT6 transactivation domain in B lymphocytes. *Mol Immunol* 37:641-652.

140. Pesu, M., K. Takaluoma, S. Aittomaki, A. Lagerstedt, K. Saksela, P. E. Kovanen, and O. Silvennoinen. 2000. Interleukin-4-induced transcriptional activation by stat6 involves multiple serine/threonine kinase pathways and serine phosphorylation of stat6. *Blood* 95:494-502.

141. Maiti, N. R., P. Sharma, P. C. Harbor, and S. J. Haque. 2005. Serine phosphorylation of Stat6 negatively controls its DNA-binding function. *J Interferon Cytokine Res* 25:553-563.

142. Shankaranarayanan, P., P. Chaitidis, H. Kuhn, and S. Nigam. 2001. Acetylation by histone acetyltransferase CREB-binding protein/p300 of STAT6 is required for transcriptional activation of the 15-lipoxygenase-1 gene. *J Biol Chem* 276:42753-42760.

143. Chen, W., M. O. Daines, and G. K. Hershey. 2004. Methylation of STAT6 modulates STAT6 phosphorylation, nuclear translocation, and DNA-binding activity. *J Immunol* 172:6744-6750.

144. Kosugi, S., M. Hasebe, N. Matsumura, H. Takashima, E. Miyamoto-Sato, M. Tomita, and H. Yanagawa. 2009. Six classes of nuclear localization signals specific to different binding grooves of importin alpha. *J Biol Chem* 284:478-485.

145. Wang, P., P. Palese, and R. E. O'Neill. 1997. The NPI-1/NPI-3 (karyopherin alpha) binding site on the influenza a virus nucleoprotein NP is a nonconventional nuclear localization signal. *J Virol* 71:1850-1856.

146. Neumann, G., M. R. Castrucci, and Y. Kawaoka. 1997. Nuclear import and export of influenza virus nucleoprotein. *J Virol* 71:9690-9700.

147. Yasuhara, N., N. Shibazaki, S. Tanaka, M. Nagai, Y. Kamikawa, S. Oe, M. Asally, Y. Kamachi, H. Kondoh, and Y. Yoneda. 2007. Triggering neural differentiation of ES cells by subtype switching of importin-alpha. *Nat Cell Biol* 9:72-79.

148. Melen, K., R. Fagerlund, J. Franke, M. Kohler, L. Kinnunen, and I. Julkunen. 2003. Importin alpha nuclear localization signal binding sites for STAT1, STAT2, and influenza A virus nucleoprotein. *J Biol Chem* 278:28193-28200.

149. Marg, A., Y. Shan, T. Meyer, T. Meissner, M. Brandenburg, and U. Vinkemeier. 2004. Nucleocytoplasmic shuttling by nucleoporins Nup153 and Nup214 and CRM1-dependent nuclear export control the subcellular distribution of latent Stat1. *J Cell Biol* 165:823-833.

150. Begitt, A., T. Meyer, M. van Rossum, and U. Vinkemeier. 2000. Nucleocytoplasmic translocation of Stat1 is regulated by a leucine-rich export signal in the coiled-coil domain. *Proc Natl Acad Sci U S A* 97:10418-10423.

151. Dorfman, J., and I. G. Macara. 2008. STRADalpha regulates LKB1 localization by blocking access to importin-alpha, and by association with Crm1 and exportin-7. *Mol Biol Cell* 19:1614-1626.

152. Baskin, L. S., and C. S. Yang. 1982. Cross-linking studies of the protein topography of rat liver microsomes. *Biochim Biophys Acta* 684:263-271.

153. Laburthe, M., B. Breant, and C. Rouyer-Fessard. 1984. Molecular identification of receptors for vasoactive intestinal peptide in rat intestinal epithelium by covalent cross-linking. Evidence for two classes of binding sites with different structural and functional properties. *Eur J Biochem* 139:181-187.

154. Hamada, H., and T. Tsuruo. 1987. Determination of membrane antigens by a covalent crosslinking method with monoclonal antibodies. *Anal Biochem* 160:483-488.

155. Sorokin, A. V., E. R. Kim, and L. P. Ovchinnikov. 2007. Nucleocytoplasmic transport of proteins. *Biochemistry (Mosc)* 72:1439-1457.

156. Pemberton, L. F., and B. M. Paschal. 2005. Mechanisms of receptor-mediated nuclear import and nuclear export. *Traffic* 6:187-198.

157. Mingot, J. M., S. Kostka, R. Kraft, E. Hartmann, and D. Gorlich. 2001. Importin 13: a novel mediator of nuclear import and export. *EMBO J* 20:3685-3694.

158. Lipowsky, G., F. R. Bischoff, P. Schwarzmaier, R. Kraft, S. Kostka, E. Hartmann, U. Kutay, and D. Gorlich. 2000. Exportin 4: a mediator of a novel nuclear export pathway in higher eukaryotes. *EMBO J* 19:4362-4371.

159. Stuven, T., E. Hartmann, and D. Gorlich. 2003. Exportin 6: a novel nuclear export receptor that is specific for profilin.actin complexes. *EMBO J* 22:5928-5940.

160. Mingot, J. M., M. T. Bohnsack, U. Jakle, and D. Gorlich. 2004. Exportin 7 defines a novel general nuclear export pathway. *EMBO J* 23:3227-3236.

161. Benekli, M., H. Baumann, and M. Wetzler. 2009. Targeting signal transducer and activator of transcription signaling pathway in leukemias. *J Clin Oncol* 27:4422-4432.

162. Yue, P., and J. Turkson. 2009. Targeting STAT3 in cancer: how successful are we? *Expert Opin Investig Drugs* 18:45-56.

163. Germain, D., and D. A. Frank. 2007. Targeting the cytoplasmic and nuclear functions of signal transducers and activators of transcription 3 for cancer therapy. *Clin Cancer Res* 13:5665-5669.

164. Alas, S., and B. Bonavida. 2001. Rituximab inactivates signal transducer and activation of transcription 3 (STAT3) activity in B-non-Hodgkin's lymphoma through inhibition of the interleukin 10 autocrine/paracrine loop and results in down-regulation of Bcl-2 and sensitization to cytotoxic drugs. *Cancer Res* 61:5137-5144.

165. Turkson, J., D. Ryan, J. S. Kim, Y. Zhang, Z. Chen, E. Haura, A. Laudano, S. Sebti, A. D. Hamilton, and R. Jove. 2001. Phosphotyrosyl peptides block Stat3-mediated DNA binding activity, gene regulation, and cell transformation. *J Biol Chem* 276:45443-45455.

166. Turkson, J., J. S. Kim, S. Zhang, J. Yuan, M. Huang, M. Glenn, E. Haura, S. Sebti, A. D. Hamilton, and R. Jove. 2004. Novel peptidomimetic inhibitors of signal transducer and activator of transcription 3 dimerization and biological activity. *Mol Cancer Ther* 3:261-269.

167. Meyer, T., and U. Vinkemeier. 2007. STAT nuclear translocation: potential for pharmacological intervention. *Expert Opin Ther Targets* 11:1355-1365.